FIRE ANALYSIS OF AN OPEN CAR PARK BUILDING STRUCTURE

Habbar Ghania

Final report of the thesis presented to the

School of Technology and Management

Polytechnic Institute of Bragança

To the fulfilment of the requirements for the master of science degree in

Industrial Engineering

(Mechanical Engineering branch)

Supervisor at IPB: Prof. Dr. Paulo Piloto

Supervisor at UHBC: Prof. Dr. Abdallah Benarous

July 2017

This page was intentionally left in blank

FIRE ANALYSIS OF AN OPEN CAR PARK BUILDING STRUCTURE

Habbar Ghania

Final report of the thesis presented to the

School of Technology and Management

Polytechnic Institute of Bragança

To the fulfilment of the requirements for the master of science degree in

Industrial Engineering

(Mechanical Engineering branch)

Supervisor at IPB: Prof. Dr. Paulo Piloto

Supervisor at UHBC: Prof. Dr. Abdallah Benarous

July 2017

This page was intentionally left in blank

ACKNOWLEDGEMENT

Initially I would like to thank God, that gave me the opportunity to carry out this outstanding experience, where I grew professionally and personally. Always giving me the strength necessary and accompanying me along the way through the completion of this stage of my studies.

This thesis would not have been possible without the tireless assistance, guidance and motivation provided by the supervisors, Dr. Paulo Alexandre Gonçalves Piloto from the Polytechnic Institute of Bragança (IPB) and Dr. Abdallah Benarous from the University Hassiba Benbouali from Chlef (UHBC). Their patience, encouragement, and on-going support throughout the whole journey were invaluable to me.

My thanks also to the ERASMUS+ ICM program, for awarding the scholarship that allowed me to conduct these master studies. And to the staff of the International Office of the IPB, for the guidance provided whenever necessary. A special thanks to Pr Mahmoudi Hacene and Pr Habbar abderezak from UHBC.

To all the professors who imparted me lessons and constituted a fundamental part of my higher education and professional formation here at the Polytechnic Institute of Bragança (Portugal) specially: Dra. E. Fonseca, Dr. L Mesquita and Dr.J.Ribeiro, or in Algeria since my primary school until my higher education in University Hassiba Benbouali from Chlef specially: M. Djamel-eddine and Z. Hamou.

To my friends and colleagues, in Algeria and in Portugal, who were always aware of my progress and kept me motivated to complete this report, especially to “my second family” for their invaluable support since the first day of our stay in Bragança especially my dear: N.khadouma, A. Soufyane, K. Seddik, and Z. Abdelkader also H. Petra from Czech and H. Mohamed from Tunisia.

I acknowledge the people who mean a lot to me, my parents, Ali and Zohra Zerguerras, for showing faith in me and giving me liberty to choose what I desired. I salute you all for the selfless love, care, pain and sacrifice you did to shape my life. Although you hardly understood what I researched on, you were willing to support any decision I made.

Finally, I express my thanks to my sisters especially my little sister: Khalida and my second mother: Souria, my brothers, sisters in laws and brothers in laws, my nieces and my nephews for their support and valuable prayers. My deepest gratitude goes to them for their unflagging love and unconditional support throughout my life and my studies.

This page was intentionally left in blank

RESUMO

O objetivo deste trabalho é determinar o comportamento térmico de uma estrutura aberta de um parque de estacionamento, usando o evento de incêndio de um carro. A evolução da temperatura de parte do elemento da estrutura também deve ser calculada com o modelo simplificado de EN1991-1-2 (método Heskestad e Hasemi) para determinar o comportamento térmico da estrutura.

O carregamento térmico de uma estrutura mista para estacionamento de carros será analisado, com base em diferentes cenários de incêndio que dependem do número de eventos de incêndio (HRR e tempo). O compartimento vai ser definido e alguns parâmetros devem ser identificados para fazer uma análise paramétrica.

Um método de cálculo avançado (usando a análise FLUENT) será utilizado para determinar curvas temperatura-tempo, com base na análise CFD e no efeito termodinâmico do incêndio localizado.

PALAVRAS CHAVE:

Incêndio localizado; Parque de Estacionamento Aberto; Elefir-EN; Estrutura mistas em Aço e Betão; Ansys fluent; Comportamento térmico.

This page was intentionally left in blank

ABSTRACT

The aim of this work is to determine the thermal behaviour of an open car park building structure, using the fire event of a car. Temperature evolution of part of the element of the structure should also be compared with the simplified model of EN1991-1-2 (Heskestad and Hasemi method) to determine the thermal behaviour of the structure.

The thermal loading of an open car building structure is going to be analysed, based on different fire scenarios that depend on the number of fire events (HRR & time). The compartment is going to be fixed and few parameters should be identified to do a parametric analysis.

An advanced calculation method (using FLUENT analysis) will be used to determine several temperature-time curves, based on the CFD analysis and in the thermal effect of the fluid from the localized fire.

Keywords :

Localized Fire; open car park; Elefir-EN; Composite steel and concrete structure; Ansys fluent; thermal behaviour.

This page was intentionally left in blank

INDEX

INDEX OF FIGURES

INDEX OF TABLES

NOMENCLATURE

Latin lower case letters

$\dot{h}$	The heat flux [kW/m^2].
y	Non dimension parameter [-].
$c_a(\theta)$	Specific heat of steel [kJ/(kg K)] .
$c_p(\theta)$	Specific heat of concrete [kJ/(kg K)].
$\dot{h}_{net}$	Net heat flux[w/m^2]
R	Radial distance from the fire [m]
t	Time [min]

Latin upper case letters

D	Diameter of fire source [m]
H	Distance between the fire and the ceiling [m]
H_f	Vertical distance between the floor and the ceiling [m]
H_s	Distance between the fire source of the car and the floor
L_f	Flame height [m]
L_h	Horizontal flame length
$\dot{Q}$	Total heat release rate (HRR) [kW]
Q_c	Convective part of the rate of heat release [kW], Q_c= 0,8 by default
Q_D^*	Heat release coefficient related to the diameter of the local fire
Q_H^*	Non-dimensional hate release rate [W]
Tgas	Temperature of steel profile [°C].
Z	Height along the flame axis [m]
Z_0	Virtual origin or height of virtual source above burning item [m]
Z'	Vertical position of the virtual heat source [m]

Greek letters

α_c	Coefficient of heat transfer by convection [J/m² K]
ε	Emissivity
ε_f	Emissivity of fire
ε_m	Surface emissivity of the member
λ	Thermal conductivity [kW/(m °C)]
ρ	Density [kg/m^3]

Greek lower case letters

λ_a	Thermal conductivity of steel [W/(m k)].
λ_c	Thermal conductivity of concrete [W/(m k)].
θ_a	Temperature of steel profile [°C].
θ_c	Temperature of concrete [°C].

1- INTRODUCTION

Over recent years, there is considerable interest in the research of vehicle fires in car parking building structures due to the important effect that this kind of accidents have in society. Several accidents were reported with regards to car parking structures, in particular open car parks.

1.1- Fire

Fire is rapid, self-sustaining oxidation accompanied by the evolution of varying intensities of heat and light. This definition indicates that fire is a chemical process of decomposition in which the rapid oxidation of a fuel produces heat and light. This process makes fire the mid-range reaction based on the speed at which the two other common forms of oxidation occur [1]. Rust, or corrosion, is an example of the slower form, and explosion is an example of the more rapid form; see Figure 1.

Figure 1 - Flame example.

Fire need three things to exist; see Figure 2: Fuel - Any combustible material (solid, liquid or gas); Heat - The energy necessary to increase the temperature of fuel to where sufficient vapours are given off for ignition to occur; Oxygen - The air we breathe is about 21% oxygen – fire needs only 16% oxygen [2].

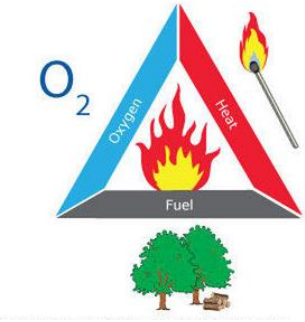

Figure 2 - What fire need [3].

One of the most interesting issues in fire engineering and fire safety is the rapidity of detecting fire using fire detection systems, which operate and depends of the hot gases and smoke. Safety systems need to be able to detect a fire so that any kind of protection system can stop it or alarm people to get out in time. People usually can see smoke and flames, people can smell smoke and can feel heat. Most of the times people need the support from fire brigades for help. When a fire breaks out, people might not be at home, or might be asleep or might not be paying much attention to what is going on around us. Fire detectors have been developed using science knowledge and technology to improve fire protection.

Car fires are usually related to causes associated with fuel, electrical systems, the exhaust system and petroleum based fluids; see Figure 3. By far though, the biggest causes of vehicle fires are fuel related [2].

Figure 3 - A car on fire [4].

The effect of car fires inside parking places can be magnified due to trapped smoke, which limits visibility, and people may not be able to safely attack from the four corner angles of the car due to its location and adjacent cars, columns or walls. Usually the effects of a vehicle fire are: massive amounts of black smoke pouring out of the vehicle due to the materials involved; fuel or other flammable liquids igniting; shocks, struts, bumpers and/or tires

exploding; and the ever-increasing list of unknown contents that people may find use in the vehicle. There are many variables involved in fighting a car fire in a parking garage, including structure type, access, grade or elevation changes, confined spaces or areas trapping heat and smoke, exposures and fire department response [5], see Figure 4.

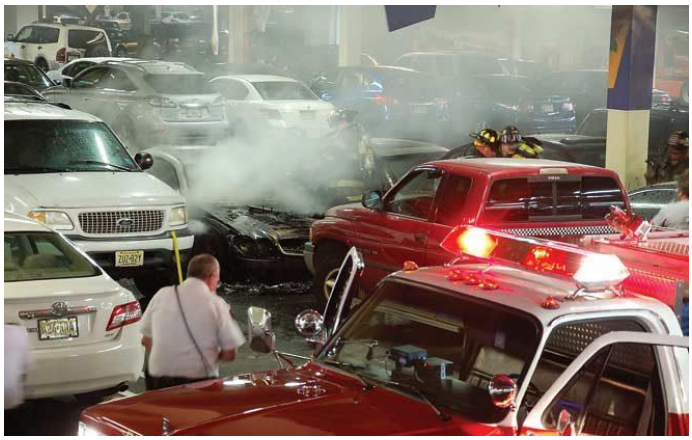

Figure 4 - A car park after fire.

1.2- Defining car park fire scenarios

A fire scenario is a generalized, detailed description of an actual or a hypothetical, but credible, fire incident. Such scenarios identify chains of events leading to deaths and other fire losses.

The fire scenario is mainly just a set of fire conditions. The building fire safety design concept is the solution of more or less well defined predefined variables.

Each fire scenario includes all details relevant to the development of a fire and a subsequent behaviour of people and mechanisms of protection. When properly developed, a fire scenario describes all essential element of fire incident. The components which make up the events and conditions of a fire scenario are not fixed. They may include events such as: ignition, fire spread, extinction, evacuation, smouldering or flaming combustion, smoke production, flashover, back-draft, etc [6].

1.3- State of the art

In 2004, Yuguang Li made his work by collecting historical data, which were filtered from New Zealand Fire Service (NZFS) incident reporting system data. This provided the relevant probabilities for the construction of event tree model that considered the type of

parking buildings and different vehicle fire spread scenarios, and he found that on average, there were 12 vehicle fire incidents each year in New Zealand parking buildings. Multiple vehicle fire incidents accounted for approximately 3% of such fires. Arson is found to be the leading cause of vehicle fires in New Zealand parking buildings (26.7% of all fires). It was also concluded that annual vehicle fire frequencies in New Zealand parking buildings are generally lower than those in buildings of other type. Based on available data collected during this research, it was further found that an economically installed automatic sprinkler system does not justify itself in a parking building situation from the building owner's point of view [7].

In 2005, Noordijk and Lemaire made a study focuses on how to model fire spread between cars in a car parking in which fire was triggered by a fire incident at Schiphol Airport (Netherlands) involving 30 cars where it was believed that the fire spread during the incident was much faster than assumed. The study recognized that fire between cars could occur by emission of radiation, heat transfer through air and absorption of the radiation. As a conclusion, driven by uncertainties, the fire spread model was capable of predicting fire spread between cars [8].

In 2007, X.G. Zhang et al. investigated a large-scale car fire in a specially built car park with a four-storey structure with cars situated at corners on each level of the car park. Their tests mainly tried to investigate the behaviours of car fire and fire spread to adjacent cars and the effect of car fires on the building structure. The researchers decided to put fifty cars in two rows and each parking space had 6 x 3 m, assuring that the space between two cars is 1.2 m. As required by government regulations, ventilation system should be sufficient to provide at least 6 air changes per hour and that all ventilation fans should normally be run continuously. The numerical simulations of fire development in a large underground car park were carried out using the FDS code. The simulated heat release rate was compared well with experimental data. The effect of ventilation on the fire spread and smoke movement in a large underground car park with 50 cars was simulated [9] .

In 2007, De Feijter and Breunese describe the post behaviour of a severe fire in a multi-story car park constructed partially from precast pre-stressed hollow core concrete slabs, which spanned from a central core to a load bearing precast concrete façade. The structure was severely damaged during the fire and the total structural collapse was a serious concern. Excessive crack formation was observed in the hollow core slabs, including horizontal cracks between the individual cores and vertical cracks from the cores to the slabs' bottom surfaces. This resulted in total separation of the bottom half of the hollow core elements (along with the internal pre-stressed reinforcement) over a large portion of the structure. Spalling to a depth of

several centimetres was widespread in both the slab soffit and the concrete façade elements, exposing steel reinforcement in many places. Researchers concluded that thermal cracking took place in all concrete elements that were exposed to fire. It is clear based on the above that it is essential for structures to be considered not as separate parts, but rather as a connected whole [10].

In 2009 , the Building Research Establishment (BRE) made a project titled - Fires In Enclosed Car Parks on behalf of the UK Department of Communities and Local Government. The aim of the research project was to gather information on the nature of fires involving recent model cars for inclusion into existing guidance on fire safety strategies for enclosed car parks. Specifically, " the objectives of this task were to benchmark car fire sizes for a range of vehicle types in a typical car park, determine the spread of fire between cars and the severity (heat release) of car fires and to seek to determine the associated conditions (heat, smoke, toxic gas) to car park occupants exposed to such a fire, under typical conditions". The project involved eleven full-scale tests (fire events) including tests on single cars, several car involvement due to horizontal fire spread and two cars in a multi-tiered vehicle stacking device in a vertical configuration. Ignition factors ranged from 7 cribs on driver's seat with and without ventilation, engine bay fires and subjecting the external car surface to incident radiant heat. Spread of fire was studied in a vertical configuration with an adjacent car and empty spaces, vertically in a multi-tiered vehicle stacking device and from the engine bay to another car in a "nose to nose" configuration. The findings of the research included "The ease with which a car fire in a car park might spread to nearby cars has been demonstrated. Once a very severe fire has developed, fire will spread to other cars separated by an un-filled parking bay". In this situation, where a number of cars are burning simultaneously, the fire is exacerbated by heat-feedback and heat release rates in excess of 16 MW might be achieved from two or three cars. In Test 1 the initial car fire, Car 1, burned at around 2 MW for about 20 minutes and it was only then that Car 2 became involved (although Car 3 then ignited very soon after). However in Test 3, all three cars were burning after around 10 minutes. In Test 4 (Buxton – LPG), Car 2 was in fire after 21 minutes and all four cars were burning after around 23 minutes. In Test 8, an engine fire test with a nearby car "nose to nose" the fire spread to the second car within 5 minutes. The ventilation limitations on such a fire in an enclosed car park result in a very hot ceiling jet, which spreads the fire to nearby cars with the dominant mechanism of heat transfer being radiation from the flames and hot gas layer, but with some direct flame contact. There were only a limited number of cars in each of the tests (a maximum of four); however transmission

to many cars within a specific proximity in an actual car park must be expected under these conditions [11].

In 2010, the Building Research Establishment (BRE) made a project that aimed to gather information on the nature of fires involving the current design of cars and to use this new knowledge as a basis for updating current guidance used in the United Kingdom on fire safety strategies for car park buildings. The project was commissioned by Communities and Local Government Sustainable Buildings Division to carry out a three year project titled Fire Spread in Car Parks. This report was intended to be of value to designers, fire engineers, computer modellers and researchers, involved in the design of car parks and the fire safety provisions that are appropriate. This report includes a world-wide literature review of the related topic of vehicle fires, laboratory tests on car materials, a review of United Kingdom fire statistics, computer modelling of vehicle fires in car park buildings, and a series of eleven full-scale fire tests that included burning a total of sixteen cars [12].

In 2010, Van Der Heijden made a research in open car park. The objective of the research was to know in what extent is there a risk in the safe deployment of the fire brigade during a car fire in a semi-open car park. Researchers began by doing literature reviews of car fires and car park building codes around the world. Then, they looked at general car park dimensions in the Netherlands, the influence of wind in semi-open car parks. The distribution and location of the opening area of the car park building have significant influence on the fire safety level, and the effect of different locations for structural beams. The fire safety levels of semi-open car parking buildings were assessed using Computational Fluid Dynamics (CFD) simulations. The study concludes that the effect of the presence of wind does not make much difference as compared to the same situation without the presence of wind. It was also concluded that from this study, that it is possible to design a semi-open car parking building that complies with current existing Dutch guidelines [13].

In 2011, Collier from Building Research Association New Zealand compiled a report on vehicle fires in car parking buildings. The main objective of his report was to gather information regarding traditional fire design assumptions for car parking building structures to account for modern cars with modern materials. This report also gathers information about vehicle stacking systems in car park buildings that may also have limited natural ventilation and/or mechanical ventilation systems. The research focused on modelling vehicle fire experiments in car park buildings using zone modelling fire software, Fire Dynamics Simulator (FDS). From the research, it was found that fire modelling with the new car fire input parameters indicates that existing New Zealand Building Codes requirements for open natural

ventilation in above-ground car parks remain satisfactory. However, for closed underground car parks and/or car parks that may include stacking systems, the performance of structural steel members may be an issue [14].

1.2.1- Car fire tests

Car fires have been experimentally studied in several countries in the world.

In 1995 Shipp and Spearpoint developed two full-scale calorimetric fire experiments on passenger to obtain information on the consequences of a car fire in a shuttle train in the Channel Tunnel between England and France [15].

In 2000 Stroup et al. made ten full-scale car fire tests at MFPA in Germany. Cars ranging from one to three in each test were put in a closed compartment for measurements. The measurements for each test included temperatures, gas concentrations, heat fluxes, mass loss rate and RHR [16].

In 2001 Stroup et al. made two fire tests in a 1995 with a passenger minivan with some exterior damage. The experiment was conducted under a hood calorimeter at NIST (National Institute of Standards and Technology) in the US [17].

1.2.1.1- Tests of cars in cone calorimeter

Two sources in the literature have reported the results of cone calorimeter tests conducted on component materials found on the exterior of vehicles and these are presented here.

The Motor Vehicle Fire Research Institute (MVFRI) conducted cone calorimeter tests on selected automotive parts used in vehicles. The main objective of the work was to assess possible means for determining the individual flammability characteristics of automotive components, obtain data on the range of flammability behaviour of each component and obtain insights into the fire behaviour observed in related full - scale vehicle fire experiments. However, most of the cone calorimeter test results reported were for the interior components of a vehicle and the only exterior component which is considered appropriate for this analysis is the "windshield" which was made of polyvinyl butyral (PVB) [18].

In 2010 BRE conducted cone calorimeter tests on potential exterior components of vehicles which are likely to ignite first during fire spread between vehicles. The main objective of tests was to investigate the burning characteristics of exterior vehicle components and

determine the likely contribution to fire spread in vehicle fire scenarios. The burning characteristics were identified by determining the critical heat flux for ignition with a pilot source and their heat release rate in accordance with ISO 5660:2002 [19]. Eleven samples from a list of potential components which are likely to burn were chosen for the tests based on their location on a vehicle. The eleven components tested were hubcap, mud flap, rubber tyre, bumper trim, bumper, bumper grill, wheel arch, fuel tank, roof box, mohair soft top, and PVC soft top [12].

1.3- Open car park fire tests

In 1968 Butcher made three car fire tests in a specially built steel scaffolding structure with an insulated ceiling approximately 2.1 m above the floor. During the two firsts tests, the two ends of the structure were left opened. Nine cars in a three by three array were arranged with parallel spacing's ranging from 0.75 m to 1.2 m.

Figure 5 - Fire test in the scaffolding structure – Butcher et al. (1968) [20].

The central car was ignited, but the fire did not spread to any of the adjacent cars. The maximum measured temperature was 840 ºC in the air, 360 ºC in the steel column, 275 ºC in the steel beam. The main Conclusions were: A fire single parked vehicle is unlikely to cause uncontrollable fire spread within a car park. The damage to the car park building is not critical. The wood equivalent fire load density for a car park was found to be 17 kg/ m^2 [20].

In 1973 in Gewain – USA, Pennsylvania, A full-scale car fire test was developed in the multi-storey open car park showed, see Figure 6, with unprotected steel frames and concrete decks. Three cars were arranged, and the central one was ignited.

Figure 6 - Open car park in Pennsylvania – Gewain (1973 [20].

The main thermal and structural results were: The maximum temperature of the air was 432 ºC (above windscreen, after 11 minutes). The air temperatures for most parts in the building was smaller than 204 °C and the maximum temperature of the steel was 226 ºC. The deflection and elongation of elements was null after cooling.

The main conclusions were: The fire did not spread to any of the adjacent cars during the 50 minutes of test. There is a low fire hazard in an open air parking structure. The steel provide adequate safety against the structural collapse under a car fire. This test confirmed results of Butcher et al. (1968). The wood equivalent fire load density for a car park was found to be 9.8 kg/ m^2 [21].

In 1985 Bennetts et al. in Australia developed two fire in the two-level open-deck car park showed in Figure 7, using unprotected steel and concentred loads on the first floor. Five cars were arranged. In the first test the fire did not spread to any of the adjacent vehicles. Maximum temperature in the steel was 285 ºC. For the second test, 3 cars were involved. The fire spread from the first car ignited to two neighbouring cars at 14 and 35 minutes. The maximum temperatures were: 340 ºC in a beam and 320 ºC in a column.

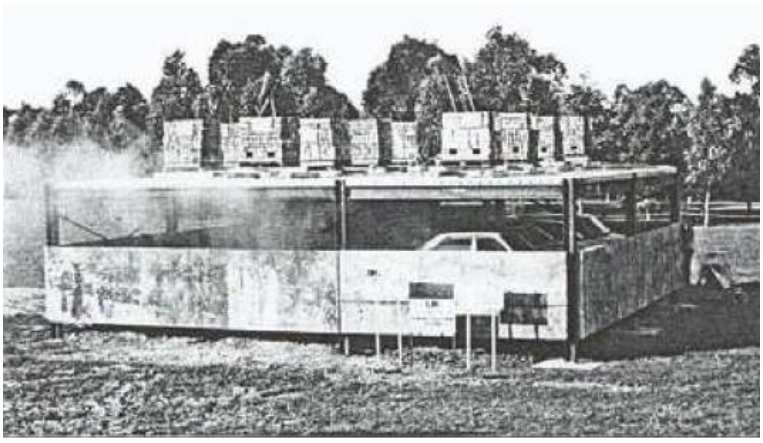

Figure 7 - Open-deck car park – Bennetts et al. (1985) [20].

The main conclusions were: The probability to involve more than 2 cars is very small (fire brigades arrive before); The safety was assured with unprotected steel.

1.4- Objective of the thesis

The main objective of the thesis is to find the thermal effect of the structure from a localized fire from a car. Different models were used to determine the temperature of the structure and a comparison is made between them.

1.5- Outline of the thesis

The thesis contains 6 chapters divided with the following information.

Chapter 1 presents the state of the art, an overview of the unprotected steel in open car park under fire (car fire tests and cone calorimeter tests.). This chapter also includes an introduction about fire modelling and fire events.

Chapter 2 provides a general idea about some fire events in open car park buildings around the world and the fire requirements in different European countries under localised fire. Fire statics in open car park is also presented.

Chapter 3 discusses fire events and Heat release rate HRR of cars. Also includes the information about fire compartment and presents the method (Heskestad and Hasemi) usually used to define the effect of the fire in specific parts of the structure.

Chapter 4 describes the simple calculation method, and temperature calculation using a mix of Heskestad and Hasemi method during the fire event. A parametric analysis is also presented.

Chapter 5 is dedicated to the numerical simulation using ANSYS FLUENT and the ELEFIR_EN software. A brief definition of both will be presented followed by a discussion of the results about the temperature of the gas and the temperature of the steel. The velocity is also analysed, taking in consideration different car classes, different radial position, and different section factors for secondary beams.

Chapter 6 presents the conclusions and the future research about the effect of fire in open car parks.

2- FIRES IN OPEN CAR PARKS

2.1- Historic events

A short list is given of reported damages in real car park fire accidents that occurred mostly in the Netherlands and Switzerland during the period 2002–2007 [22].

2.1.1- Schiphol Airport (Netherlands)

On October 13, 2002, a fire occurred in an aboveground car park for rental cars at Schiphol Airport. Approximately 51 cars were burned, due to which a partial collapse of the structure occurred, see Figure 8. The structure consisted of massive pre-tensioned concrete slabs which were supported by concrete T-girders. It was a very large fire, because the car park was fully booked, with only 40 cm spacing between the cars. Furthermore, the cars were relatively new (with high amounts of synthetic materials) and had a full fuel tank (as is often the case for rental cars) [22], [23].

Figure 8 - Fire in car park of Schiphol airport [24].

2.1.2- Apartment building Geleen (Netherlands)

In the apartment building Geleen (The Netherlands), during the night of 23–24 June 2004 a fire happened in a car park beneath. Twelve vehicles burned in total. The concrete was heavily damaged with complete cover loss for the slabs, walls and some columns, see Figure 9. The structure was repaired with shotcrete and supplementary reinforcement [22], [23].

Figure 9 - The Apartment building Geleen after fire [24].

2.1.3- Car park Gretzenbach (Switzerland)

A fire took place on November 11, 2004, in a car park in Gretzenbach, see Figure 10. After approximately 90 min, the roof of the underground car park collapsed due to punching effect and 7 firemen died during their intervention. Fire investigation revealed design and execution mistakes resulting in an overload of soil and a decreased of punching shear capacity. Because of a clear punching failure and the typical car park geometry, this example is often used as the basis for the geometry of a case study [22], [23].


Figure 10 - The Apartment building Geleen after fire [25].

2.1.4- Apartment building Harbour Edge (Netherlands)

A fire occurred on October the 1st of 2007, in the open car park of an apartment building (Harbour Edge) in Rotterdam, see Figure 11. During the fire, 7 cars were parked at the level where the fire took place. The fire started near the middle of the first six cars parked side by side. The fire spread to both sides in this row of cars. According to Feijter and Breunese [23], it is most likely that the initial fire spread to the second car started after 10 min and to the third car after 12 min. After 22 min of fire also the 4th car got involved. The moments of ignition of

the 5th and the 6th car are somewhat uncertain. Finally, the 7th car, which was separated from the group of 6 by an empty space, was only partially involved in the fire, was not considered to contribute to the fire in terms of HRR in the fire scenario analyses, because it was only partially damaged, not burnt out [23].

Figure 11 - The open car parking of building Harbour Edge after fire [26].

2.2- Fire requirements in different countries

A car park as part of a building can be classified as open or closed depending on the ventilation condition. In accordance with ECCS, it may be considered as "open" if, for every parking level, the ventilation areas in the walls are: i) located in at least two opposite façades, ii) equal at least 1/3 of the total surface area of all the walls and iii) correspond to at least 5% of the floor area of one parking bay [27]. The main advantages of open car parks are: i) lower energy consumption, ii) natural light that contributes to the human comfort and safety of users, iii) natural ventilation, and iv) attractive architectural design. In addition, open car parks present specific characteristics that must be considered in the fire design.

Table 1 presents the limitations, the general requirements for fire protection and the indication of acceptance or not of alternative design conditions in different European countries. It is showed that in some countries, this type of building does not require (or very few) any time of fire resistance (ex.: R0 in Italy or R15 in U.K.). Portugal is one of the countries with the highest requirements for fire resistance of structural elements (from R60 to R180). However, the use of Natural Fire as an alternative to ISO fire is accepted and it is also allowed limiting or avoiding any fire protection on steel elements. This table also shows that, actually, still some of European countries prescribe long fire resistance time under ISO fire, and do not indicate anything about the use of Natural Fire (Hungary, Spain and Poland). In France and Finland, the use of bare steel is allowed if the fire safety is proved by tests or scientific studies.

According to the ECCS report (1993) [27], steel structures in open car parks do not require fire protection, and therefore have economic advantages. The fire safety of these structures is ensured by the following conditions: i) the design at room temperature (or "cold design"), according to the current rules, is the basic condition for the stability of the structure in the fire situation; no additional measures for fire neither a special "hot" design are required; ii) beams with composite steel concrete section including shear studs should be used. For economic reasons, it is recommended to use light weight sections (IPE, HEAA and UB); iii) large flange sections (HEA, HEB, UC) should be considered for the columns; and iv) horizontal forces must be supported by frames or bracings (protected against fire).

In 2004 Fraud et al. indicates: i) use the same cross sections for all columns in the same floor; these columns must be filled with concrete between the flanges, ii) use of concrete stairs to increase the horizontal stability and to be used as emergency stairs; iii) use a minimum steel grade of S355, and minimum concrete class of C30/37; iv) steel beams connected to the concrete slab by shear studs with a minimum degree of connection of 80%; v) concrete slabs built in situ or precast concrete; the essential point is the static and structural integration of the slab in the load-bearing system [28].

Table 1 - Resistance requirements of car parking, according to INERIS [29] ,ECCS [27].

Country	Limitations						General requirement for fire ISO 834	Alternative design conditions	
	Minimum percentage of opening (%)		Maximum						
	Openings /floor	Openings /walls and facades (*1)	Dist. between opposites facades (m)	n° of stories	Building height (m)	Floor area per story (m^2)		No fire protection	Natural fire (*3)
Germany [30]	-	33	70	-	22	-	R0(*5)	/	/
Austria [31]	-	33	70	-	22	-	Up to R90	Yes	Yes
Belgium [32]	-	17	60	-	-	-	R0 (*5)	/	yes
Denmark	5	-	24	-	-	-	R0 (*5) to R60	Yes	Yes
Spain	-	-	-	-	-	-	R60 to R120(*2)	-	-
Finland [33]	10	30	-	8	-	9000	R60	No (*4)	Yes
France [34]	5	-	75	-	-	-	Up to R60	No (*4)	Yes
Netherlands	-	30	54	-	20	-	R0 (*5) to R30	/	/
Hungary	-	-	-	-	-	-	R30 (*2) to R90	No	No
Italy [35] ,	15	60	-	-	-	-	R0	-	-
Luxemburg [36]	-	50	-	-	-	-	R0 (*5) to R30	/	/
Norway	-	-	-	-	16	5400	R10 to R60	Yes	-
Poland	-	-	-	-	25	4000	R60	No	-
Portugal [37] [38].							R60 to R180	-	Yes
U. K.	5	-	90	-	15.2	-	R15	Yes	Yes
Sweden [27]	-	-	-	-	-	-	Up to R90 (*4)	Yes	Yes
Switzerland	-	25	70	-	-	-	R0 (*5)	/	/

(*1): Total area of openings / total area of walls and facades surrounding one parking level.
(*2): General requirements of National Building Code.
(*3): Use of Natural Fire as an alternative to ISO fire to prove the fire resistance.
(*4): Bare steel is allowed if this can be proved by tests or scientific studies.
(*5): If specific structural conditions defined in National code are met.

2.3- Fire Statistics in open car parks

Some statistics of fires occurred in car parks have been realized, in order to define the car park structure and the scenario we will use for testing in Open car parks. The existing statistics in literature concerning fires in car parks are poor. The technical note n° 75 from ECSC and the final report ECCS research on Closed Car Parks of the gives a general view of the statistics of the 80's, mainly from United States. Therefore, it was necessary to get new statistics of fires in car parks.

The information about fires comes mainly from fire brigades, and particularly from the Fire Brigade of Paris (BSPP) which usually writes a report for each intervention. The statistic study is based on: 327 intervention reports from BSPP in 1997 concerning fires in underground car parks, 78 intervention reports from BSPP, concerning fires in upper-structure car parks during three years: 1995 (18 reports), 1996 (26 reports) and 1997 (34 reports).

The underground car parks are generally closed car parks and upper-structure parks are usually open car parks. Even if some upper-structure car parks are closed, the statistics will be considered representative of open car parks. Some statistics from the towns of Marseille, Toulouse, Brussels and Berlin were also included.

The intervention reports usually give the following information: date, call time, Intervention duration, injured people, type of building, ignition of fire, propagation of fire, time to extinction, description of fire and damage.

The time to extinction is usually classified by period: 1 and 5 minutes, 6 and 15 minutes, 16 and 30 minutes, 31 and 59 minutes, 60 and 89 minutes, 90 and 119 minutes, 120 and 179 minutes, 180 and 239 minutes.

The propagation is generally never described and known, and the ignition source is usually unknown. Only two or three cases are recognised. The description concerns the combustible, the problems for extinction, and description of the injured people.

The "damage" part gives the number of burning cars and some information about them: electrical problems, smoke propagation. The statistics resulting from the analysis of these reports are given in terms of time to extinction, number of cars involved in the fire, classifications of cars, injuries, daytime of fire occurrence [22].

2.3.1- Open car park

The design method presented in this document applies, as indicated from the very beginning, to the open steel car parks. According to the Building Regulations the car park is considered open if it satisfies the conditions presented here in.

These conditions ensure the natural ventilation as it is shown in Figure 12, which helps to avoid accumulation of smoke and additional increase of temperature [39].

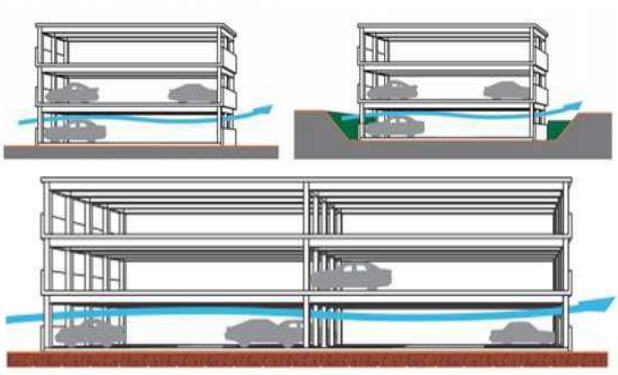

Figure 12 - Natural ventilation in open car parks [39].

3- FIRE EVENTS AND SCENARIOS

A “fire event” shall be defined as: “An occurrence in which extinguishing media was used to suppress fire” . This may mean a portable fire extinguisher, water from fire department efforts, the activation of a kitchen vent hood, a building’s sprinkler system, or any other fire suppression system within a building can be used to reduce the fire event. On the rare occasion when evidence of fire is present, and the fire has self-extinguished, this will also be identified as a fire event.

The best characterization of the structural fire response of open car parks, Figure 13, is the real evidence or experimental tests that reproduce closely the reality, such as the study performed in 2000 by CTICM. The maximum gas temperature near the ceiling reached 1040 °C above the vehicle. However, the average gas temperature during the 15 minutes of higher temperatures was 510 °C, which means that a peak temperature was reached only during a very short time. The maximum temperature in the beam lower flange at a distance of 2.5 m from the column was 700 °C with a gradient of 250 °C in the cross-section [40].

For steel structures, the application of the global structural analysis needs to pay attention to following points: Regarding the material models, the designer must think of the transient heating regime of structures during fire, which requires the use of a step by step incremental and iterative solution procedure rather than a steady state analysis. The existing boundary conditions should be rightly represented, in particular the type of fire; and the material models used in the numerical modelling should be representative of real material behaviour at elevated temperatures. When performing advanced simulations for fire design of steel structures, designers must be careful with certain other specific features, which in general are not taken into account in the direct modelling, such as the joint resistance [41].

Figure 13 - Application of steel framed for different open car parks [40].

3.1- Heat release rate of cars

The heat release rate is a key parameter which can be used as an input to a wide range of fire assessment tools, ranging from zone models to computational fluid dynamics models. The heat release rate is usually obtained from experimental data through the use of oxygen consumption calorimetric, although other approaches such as measurement of temperature rise, mass loss, or species production can also be used. However the natural variability of fire means that even if the same item is burned using the same procedure for repeated experiments, the heat release rate curves obtained will not be exactly the same. The results of the HRR that were consider in this thesis are represented in Table 2 and plotted in Figure 14.

Table 2 - The HRR of different car categories.

	Vehicles categories				
	Class 1	Class 2	Class 3	Class 4	Class 5
Time	HRR	HRR	HRR	HRR	HRR
min	kW	kW	kW	kW	kW
0	0	0	0	0	0
4	884	1105	1400	1768	1768
16	884	1105	1400	1768	1768
24	3474	4342	5500	6947	6947
25	5242	6553	8300	10448	10448
27	2842	3553	4500	5684	5684
38	632	789	1000	1263	1263
70	0	0	0	0	0

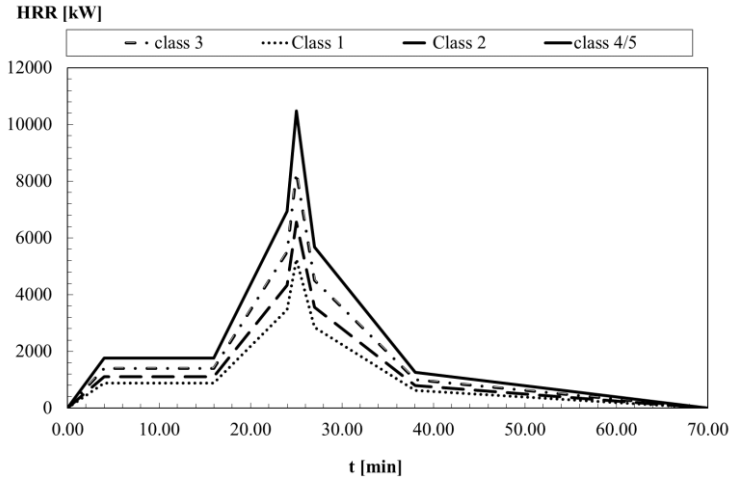

Figure 14 - Hate release rate for 5 car classes.

axes of the fire plumes are assumed to be 2 m apart according to the dimensions of ordinary passenger cars [27]. This is shown in Figure 15.

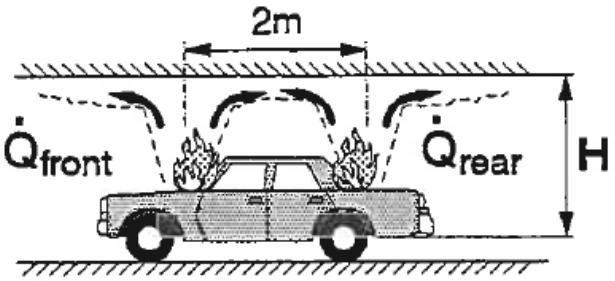

Figure 15 - the fire plume [27]

3.2-Fire scenarios

3.2.1- Fire scenarios in car park

The fire scenario (position and number of the vehicles) should represent the most unfavourable situation for the elements in the compartment (or substructure). The vehicles' type mostly used in fire scenarios are cars, classified according their calorific potential or combustion energy (E). There are basically two approaches available when determining the fire design for a given scenario. One is based on knowledge of the amount and type of combustible materials in the compartment of fire origin [39].

In order to define some fire scenarios, this car park structure was chosen (see Figure 17). In this work, one fire scenario was identified to be representative of their effect of the steel structure. The fire event of a class 3 vehicle was considered to define all these possible scenarios: Fire scenario 1 with one car burning below the secondary beam (IPEA 600) at mid-span (most severe case); Fire scenario 2 with two cars burning below the main beam (HEAA 650) and; Fire scenario 3 with three cars burning near the columns (HEM 300).

3.2.2- Parameters with significance in a fire scenario

All of the parameters in a fire scenario have, more or less impact in how a fire is going to develop. The material properties in the compartment, i.e. the thermal inertia, have a significant influence in fire scenarios within semi-infinite surrounding structures. For the final temperature in a compartment, it seems like the combustion efficiency and the specific heat capacity of the hot gases in the compartment have most importance. However, for the fire development with time, the compartment geometry and the thermal properties of the surrounding structure have most importance. More research is needed to make sure how all the depending parameters should be taken care of [42].

3.2.3- Classification of cars

The cars are classified according to the Table 2. Not all reports give the type of each car, so only 91 % of cars (175 cars) have been used to determine the distribution in category. The distribution is given in Figure 16. The categories 4 and 5 represent 13 % of cars [43].

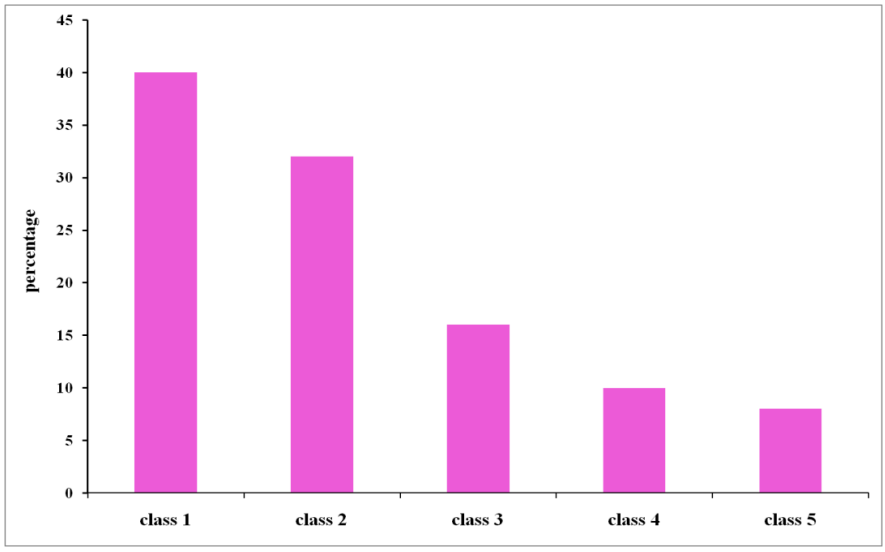

Figure 16 - Classification of cars involved in car fires in underground car park [43].

Table 3 presents a few examples of car manufacturers for each car class.

Table 3 - Definition of car classes (categories).

Type	Category1	Category 2	Category 3	Category 4	Category 5
Peugeot	106	306	406	605	806
Renault	Twingo-Clio	Mégane	Laguna	Safrane	Espace
Citroën	Saxo	ZX	Xantia	XM	Evasion
Ford	Fiesta	Escort	Mondeo	Scorpion	Galaxy
Opel	Corsa	Astra	Vectra	Omega	Frontera
Fiat	Punto	Bravo	Tempra	Croma	Ulysse
Volkswagen	Polo	Golf	Passat	//	Sharan

3.2.4- Fire scenarios

A few scenarios have been studied by other researchers, see Figure 17**.** Scenario 1 considers one car burning at mid-span under the beam (corresponding to the maximum bending moment position). Scenario 2 involves two burning cars, one on each side of the element of the column. This fire event was considered being the most dangerous for the columns. The Scenario 3 considers seven class 3-cars, having the possibility of a commercial vehicle in a special

position of each fire event. Scenario 4 involves four class 3-cars parked face to face, with the possibility to have a commercial vehicle in each place.

For all scenarios, the fire spread time from a vehicle to another can be considered equal to 12 minutes, but the initial document by ECCS recommended a time delay equal to 15 minutes [44].

Scenario 5 involves three cars - class 3, parked side by side. The scenario of three cars class 3 involved in a fire is an envelope scenario of around 98.7% of all possible scenarios [40].

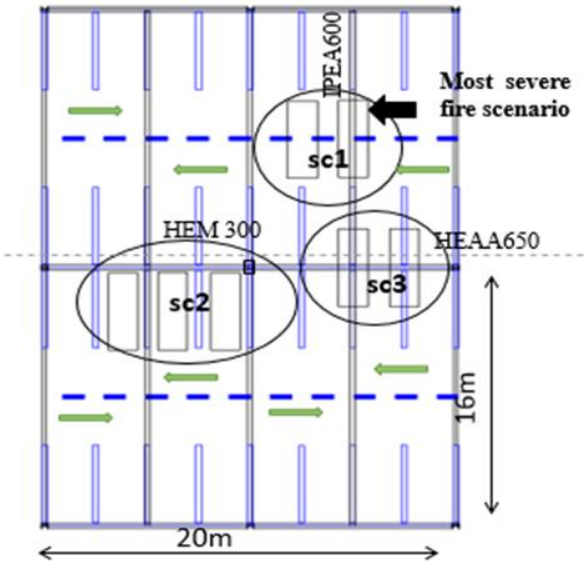

Figure 17 - Fire scenarios in open car park [44].

Figure 18 represents the simulation of the fire scenario 1 and is going to be analysed considering different positions for the car with respect to position of the secondary beam. Figure 19 represents an example of the main elements of a case study for the thermal analysis of the structure.

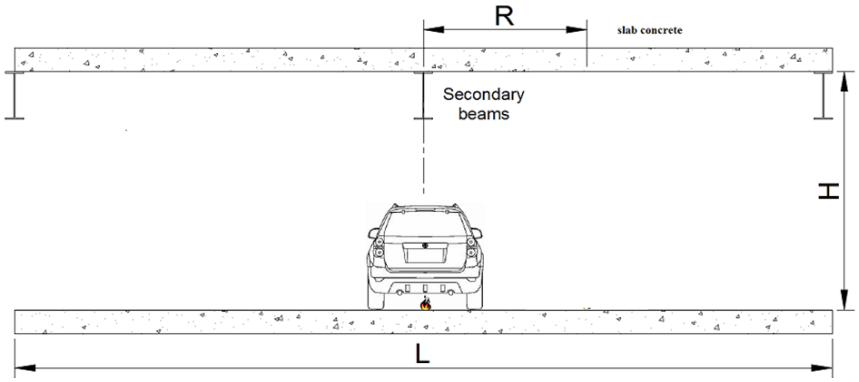

Figure 18 - The lateral view of fire scenario 1.

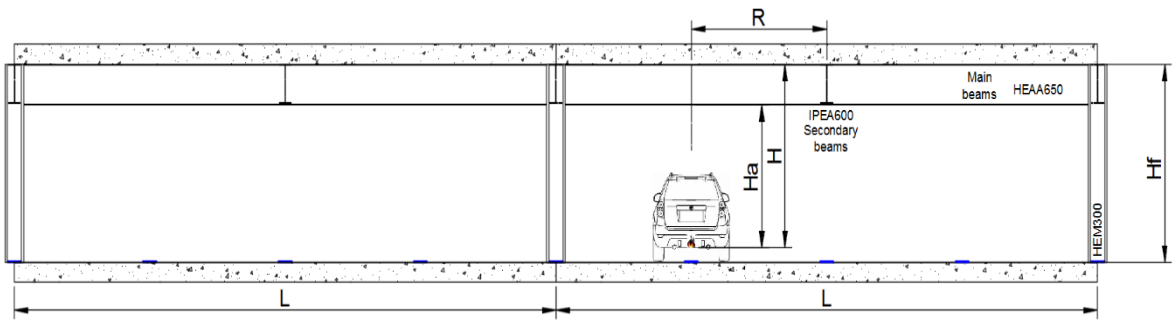

Figure 19 - The front view of the fire scenario 1

3.3- Fire compartment

3.3.1- Definition of fire compartment

Space within a building, extending over one or several floors, which is enclosed by separating elements such that fire spread beyond the compartment is prevented during the relevant fire exposure [45]. A fire compartment is an area within a building which is completely surrounded with fire-resistant construction, usually with features such as automated fire-resistant doors which close when a fire is detected. Fire compartments are required by law in some types of buildings, and strongly recommended in others as a basic safety measure. Some insurance companies may also demand that fire compartments be installed before they will write policies for certain types of businesses, in the interests of reducing their liability.

In new construction, a fire compartment can be integrated right into the structure of the building. In addition to compartments, it is also possible to install barriers which are designed to slow a fire if it starts. The fire compartments can consist of rooms or groups of rooms. When a fire starts inside a compartment, the sealed nature of the area can compartmentalize the fire, preventing it from spreading to other areas. When a fire occurs outside the compartment, it can remain sealed off, and may potentially protect objects inside from the fire. Fire compartments are not fire proof. Fire can work its way into or out of a fire compartment if it is intense enough, poorly managed, or not addressed quickly enough. However, fire compartments can still be valuable tools. Anything which slows the speed at which a fire can spread can contribute to fire safety, creating more time for people to evacuate, and potentially reducing fire damage. Valuable or important materials can be stored inside a compartment so that in the event a fire occurs, they may make it through the fire.

3.3.2- Phases of fires in compartment

Fire in enclosures may be characterized in three phases. The first phase is fire development as the fire grows in size from a small incipient fire. If no action is taken to suppress the fire, it will eventually grow to a maximum size that is controlled by the amount of fuel present (fuel controlled) or the amount of air available through ventilation openings (ventilation limited), see Figure 20.

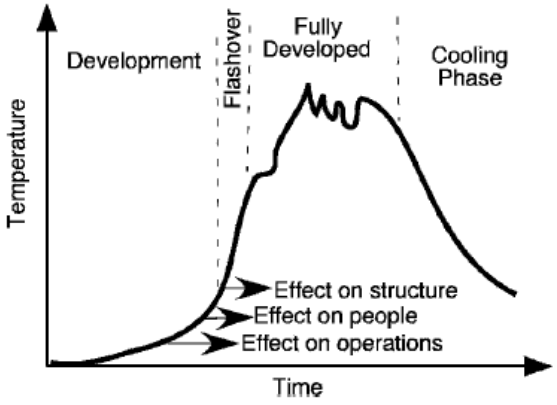

Figure 20 - Phases of fire development [46].

If all of the fuel is consumed, the fire will decrease in size (decay).

These stages of fire development can be seen in the fully developed fire and are affected by: (a) the size and shape of the enclosure; (b) the amount, distribution and type of fuel in the enclosure; (c) the amount, distribution and form of ventilation of the enclosure and (d) the form and type of construction materials comprising the roof (or ceiling), walls and floor of the enclosure.

The significance of each phase of an enclosure fire depends on the fire safety system component under consideration. For components such as detectors or sprinklers, the fire development phase will have a great influence on the time at which they activate. The fully developed fire and its decay phase are very important for the verification of the integrity of the structural elements.

Flashover is a term demanding more attention. It is a phenomenon that is usually obvious to the observer of fire growth. However, it has a beginning and an end. The former is the connotation for flashover onset time given herein. In general, flashover is the transition between the developing fire that is still relatively at the beginning and the fully developed fire. It usually also marks the difference between the fuel-controlled or well-ventilated fire and the

ventilation-limited fire. Flashover normally occurs at 500 °C or 590 °C for ordinary combustibles, and with an incident heat flux at floor level of 20 kW/m^2.

Flashover can be initiated by several mechanisms, while this fire eruption to the casual observer would appear to be the same. The observer would see that the fire would 'suddenly' change in its growth and progress to involving all of the fuel in the compartment. If the compartment does not get sufficient stoichiometric air, the fire can produce large flames outside the compartment. A ventilation-limited fire can have burning mostly at the vents, and significant toxicity issues arise due to the incomplete combustion process [46].

3.4- Localized fires

In a localized fire, there is an accumulation of combustion products in a layer beneath the ceiling (upper layer), with a horizontal interface between this hot layer and the lower layer where the temperature of the gases remains much colder. This situation is well represented by a two-zone model, useful for all pre-flashover conditions. Besides allowing for the calculation of the evolution of gas temperature, these models are used in order to know the smoke propagation in buildings and to estimate the life safety as a function of smoke layer height, toxic gases concentration, radiative flux and optical density.

The thermal action on horizontal elements located above the fire also depends on their distance from the fire location. The temperature and the heat flux can be assessed by specific models for the evaluation of the local effect on adjacent elements, such as Heskestad' s or Hasemi's method [45].

3.4.1- Heskestad model

Thermal action of a localised fire can be assessed by using the Heskestad method. Differences have to be made regarding the relative height of the flame to the ceiling. The flame lengths L_f of a localised fire is given by Eq 1. If the length is smaller than the height of the compartment, this method should be applied. Due to the size of the fire the virtual origin Z_0 should be calculated according to Eq 2. Figure 21 represents the relative position of the fire and the element of the structure under analysis.

$$L_f = -1.02D + 0.00524\,Q^{2/5} \qquad \text{Eq 1}$$

$$Z_0 = -1.02D + 0.083\left(\frac{Q}{1000}\right)$$ Eq 2

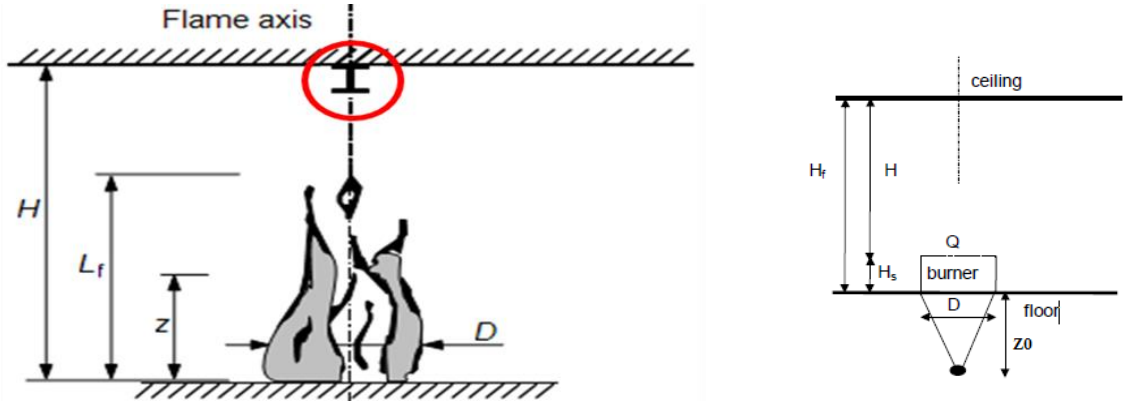

Figure 21 - Localised fire model for flames not touching the ceiling (Heskestad) [47].

When the flame is not touching the ceiling of a compartment (L_f < H) or in case of fire in open air, the temperature Θ(z) in the plume along the symmetrical vertical flame axis is given by:

$$\Theta_{(z)} = 20 + 0.25 Qc^{2/5} (Z - Z_0)^{-5/3}$$ Eq 3

Where: D represents the diameter of the fire [m], Q is the Heat Release Rate [W] of the fire, Q_c is the convective part of the rate of heat release [W], with $Q_c = 0{,}8\,Q$, Z is the height [m] along the flame axis, H is the distance [m] between the fire source and the ceiling and Z_0 represents the virtual origin [13].

This model is applied to calculation of the effect to any steel member locate above the flame position.

3.4.2- Hasemi model

Hasemi's method is a simple tool for the evaluation of the localised effect on horizontal elements located above the fire, but not only in the flame axis but also in radial position. This method is based on the results of tests made at the Building Research Institute in Tsukuba, Japan. The Hasemi method considers that the flame is touching the ceiling ($L_f \geq H$) and rotates in radial direction to create a ceiling jet motion of smoke, particles an flames, see Figure 22. This method does not give information about the surrounding gas temperature. This method provides information about the heat flux arriving to the element of the structure.

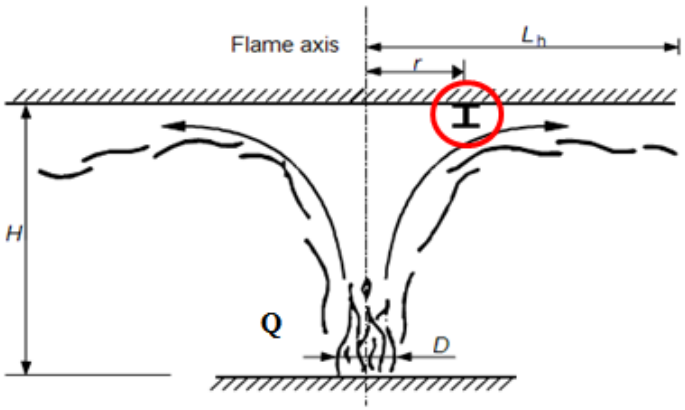

Figure 22 - Localized fire model for flames touching the ceiling (Hasemi).

The parameters for the application of the method are: Q representing the Rate of the Heat Release of the fire [W], D represents the diameter (or characteristic length) of the fire [m], H is the distance between the fire source and the ceiling [m], Lh represents the horizontal length of the flame on the ceiling [m] and r the horizontal distance, at the ceiling, from the flame axis [m].

The heat flux that arrives to a beam depends on the following parameters: Rate of heat release of cars: Q, Height of the lower flange of the beam from the floor: H_a, Diameter of the fire: D (2 m is used), Distance from the beam section to the car center: r, Height of the fire source from the floor: H_s (0.3 m is used).

The heat flux $\dot{h}$ is calculated with the Hasemi method by the following equations:

$$\begin{cases} y < 0.30 & \dot{h} = 100 \\ 0.30 < y < 1.00 & \dot{h} = 136.30 - 121.00\,y \\ 1.00 < y & \dot{h} = 15\,y^{-3.7} \end{cases} \qquad \text{Eq 4}$$

where y is the non-dimensional parameter [-] calculated by:

$$y = \frac{r + H + Z'}{L_H + H + Z'} \qquad \text{Eq 5}$$

With L_H is the horizontal length of the flame [m] determined by [6]:

$$L_H = 2.90.H.Q_H^{*\,0.33} - H \qquad \text{Eq 6}$$

And

$$H = H_a - H_s \quad \text{Eq 7}$$

$$Q_H^* = \frac{Q}{1.11.10^6.H^{2.5}} \quad \text{Eq 8}$$

$$Q_D^* = \frac{Q}{1.11.10^6.D^{2.5}} \quad \text{Eq 9}$$

Where : Q_H^* and Q_D^* are the non-dimensional heat release rates [6].

This method does not provide the temperature of the surrounding gas. This temperature can be determined using the equilibrium of the heat flux arriving to the steel element and the heat flux lost by this profile for the cold layer by convection and radiation.

$$\begin{array}{ll} Q_D^* < 1.00 & Z' = 2.4..D.(Q_D^{*\,2/5} - Q_D^{*\,2/3}) \\ Q_D^* \geq 1.00 & Z' = 2.4.D.(1.0 - Q_D^{*\,2/5}) \end{array} \quad \text{Eq 10}$$

3.4.2.1- The Newton Raphson method

Newton's Method is traditionally used to find the roots of a non-linear equation. This procedure is required to determine the temperature of the surrounding gas. The Newton Raphson method is going to be used for solving non-linear equation.

This solution method is illustrated in Figure 23 and is going to provide the gas temperature near the surrounding of the steel element, see Eq 11.

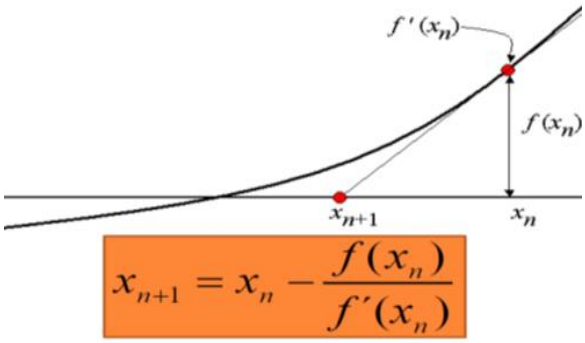

Figure 23 - Newton Raphson method.

The iterative procedure uses a trial value of gas temperature. The solution method is applied with 5 iterations maximum to get the solution value of the new gas temperature. Usually three or four iterations are sufficient.

The nonlinear equation to be solved is represented in Eq 12. This equation results from the hypothetical possibility to have material with very high conductivity and a profile with high

section factor. This means that the gas temperature should be equal to the temperature of that material (steel), establishing a thermal equilibrium between the heat flux received and the heat flux that this material can send the cold layer.

$$T_{gas}^{\,n+1} = T_{gas}^{\,n} - \frac{f(T_{gas})}{f'(T_{gas})} \qquad \text{Eq 11}$$

$$\dot{h} - \alpha_c.((T_{steel} + 273) - 293) - \Phi \varepsilon_f \varepsilon_m .5.67.10^8 [(T_{steel} + 273)^4 - 293^4] = 0 \qquad \text{Eq 12}$$

Taking in consideration the hypothesis, Eq 12 can be rewritten, assuming the Tgas equal to Tsteel, see Eq 13.

$$\dot{h} - \alpha_c.((T_{gas} + 273) - 293) - \Phi \varepsilon_f \varepsilon_m .5.67.10^8 [(T_{gas} + 273)^4 - 293^4] = 0$$
$$\Leftrightarrow \qquad \text{Eq 13}$$
$$f(T_{gas}) = 0$$

To solve this equation by the newton Raphson method, the derivative should be calculated, see Eq 14.

$$f'(T_{gas}) \Rightarrow -\alpha_c . - \Phi \varepsilon_f \varepsilon_m .5.67.10^8 \times 4 \times [(T_{gas} + 273)^3] \times 1 \qquad \text{Eq 14}$$

Because the Eq 12 is non-linear we can start the iterative process with any temperature having Tgas or Tsteel, and for the time in analysis. The first time to apply this process corresponds to 19 min. The starting value can be 500 ºC and the solution is Tgas=683.6 ºC.

Table 4 - Example of calculation with the solver using the Newton Raphson method.

time	19 min				
	ITER	[ºC] Tgas	F(X)	F'(X)	[ºC] Tgas new
	1	500	23653	-98	740.5
	2	740.5	-10075	-190	687.6
	3	687.6	-662	-166	683.6
	4	683.6	-3	-164	683.6
	5	683.6	0	-164	683.6

After getting Tgas that corresponds to the heat flux of the localized fire, this value can be used for the calculation of the increment of the temperature of the steel beam. This procedure is included in Eurocode 1 part 1-2.

4- THERMAL ANALYSIS - SIMPLE CALCULATION METHOD

4.1- Material properties

4.1.1- Thermal properties of steel

The specific heat is the quantity of heat required to raise the temperature of one gram of material one degree Celsius (or one Kelvin). The specific heat of steel c_a is defined in accordance to Eurocode EN 1993-1-2 [47] as the following :

$20 \leq \theta_a < 600[℃]$ $\quad c_a = 425 + 7{,}73\times10^{-1}\theta_a - 1{,}69\times10^{-3}\theta_a^2 + 2{,}22\times10^{-6}\theta_a^3 [J/kg.K]$ Eq 15

$600 \leq \theta_a < 735[℃]$ $\quad c_a = 666 + \frac{13002}{738-\theta_a}[J/kg.K]$ Eq 16

$735 \leq \theta_a < 900[℃]$ $\quad c_a = 545 + \frac{17820}{\theta_a - 731}[J/kg.K]$ Eq 17

$900 \leq \theta_a < 1200[℃]$ $\quad c_a = 650[J/kg.K]$ Eq 18

where : θ_a is the steel temperature [℃]. Figure 24 represents the variation of specific heat with temperature.

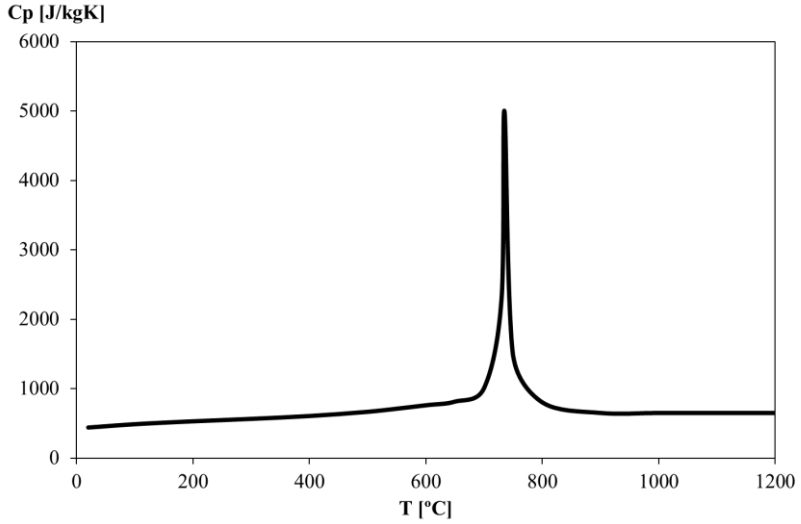

Figure 24 - Specific heat of carbon steel as a function of the temperature.

The thermal conductivity is the ability of a material to transport heat energy through it from high temperature region to low temperature region.

The thermal conductivity of steel λ_a should be determined according to the following equations:

$$20 \leq \theta_a < 800[℃] \qquad \lambda_a = 54 - 3{,}33 \times 10^{-2}\,\theta_a \quad [W/m.K] \qquad \text{Eq 19}$$

$$800 \leq \theta_a < 1200[℃] \qquad \lambda_a = 27{,}3 \quad [W/m.K] \qquad \text{Eq 20}$$

Where: θ_a is the steel temperature [℃]. According to Eurocode EN 1993-1-2 [47] the variation of thermal conductivity with temperature is represented in Figure 25.

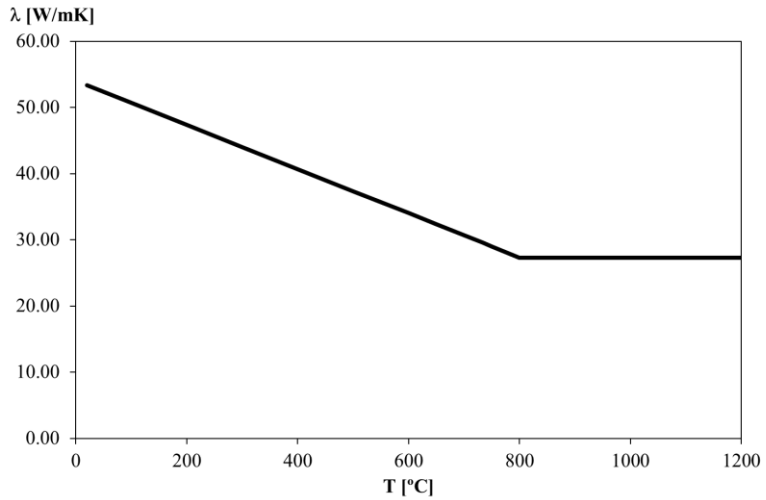

Figure 25 - Thermal conductivity of carbon steel as a function of the temperature.

The density of steel is constant $\rho = 7850$ kg/m^3, even when the temperature is modified. According to Eurocode EN 1993-1-2 [47]. The variation of the density with temperature can be illustrated in Figure 26.

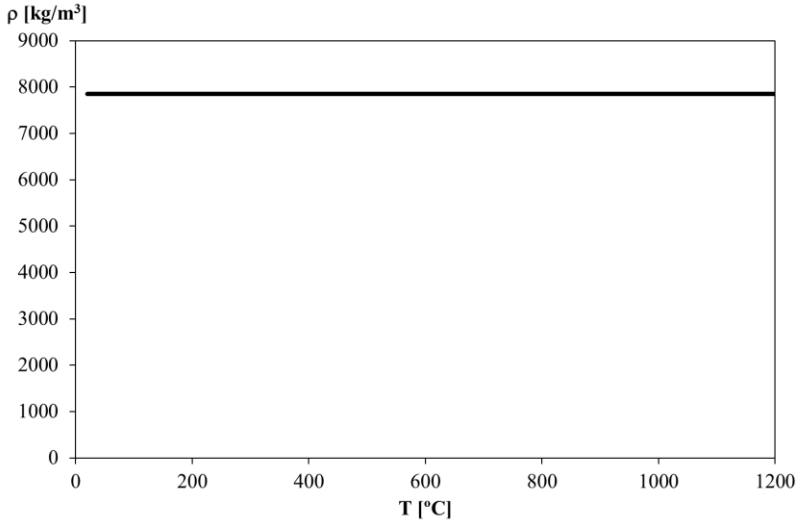

Figure 26 - The density of steel as a function of the temperature.

4.1.2- Thermal properties of concrete

The Specific heat represents the heat capacity of concrete. It increases with the moisture content of concrete and is affected by the mineralogical characteristics of the aggregate. The specific heat increases with an increase in temperature and also increases with a decrease in the density of concrete [48].

The moisture within the concrete causes a peak between 100 [ºC] and 200 [ºC] due to the water being driven off. Figure 27 depicts the variation of this property with temperature. The peak value depends on the amount of moisture, in this case $\mu = 3\ \%$ was assumed.

The specific heat of concrete should be determined from the following equations according to the Eurocode EN 1992-1-2 [49].

$20 \leq \theta_c \leq 100$[℃]	$c_P = 900[J/kg.K]$	Eq 21
$100 < \theta_c \leq 115$ [℃]	$c_P = 2020[J/kg.K]$	Eq 22
$115 < \theta_c \leq 200$ [℃]	$c_P = 2020 - \frac{\theta_a - 115}{12}[J/kg.K]$	Eq 23
$200 < \theta_c \leq 440$ [℃]	$c_P = 1000 - \frac{\theta_a - 200}{2}[J/kg.K]$	Eq 24
$440 < \theta_c \leq 1200$ [℃]	$c_P = 1100\,[J/kg.K]$	Eq 25

Figure 27 represents the variation of specific heat with temperature for the specified moisture content.

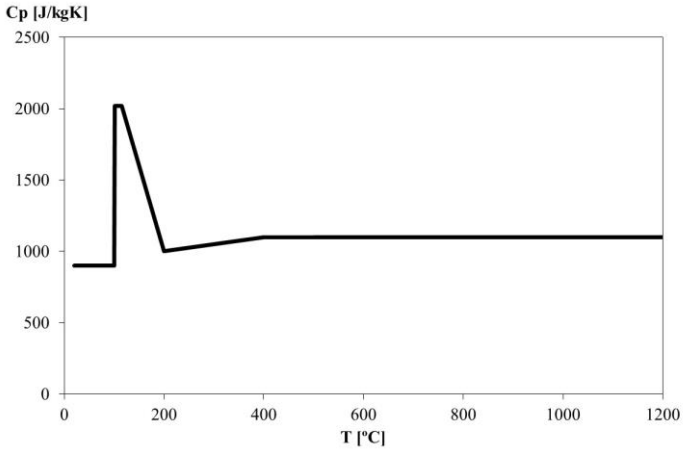

Figure 27 - Specific heat of concrete as a function of the temperature [49].

Concrete has moderate thermal conductivity, much lower than metals, but significantly higher than other building materials such as wood, and is considered a poor insulator. The thermal conductivity λ_c of concrete may be determined between the lower and upper limit, as defined in Eurocode EN 1992-1-2 [49].

The upper limit of thermal conductivity λ_c of normal weight concrete may be determined from the equation below:

$20 \leq \theta_c \leq 1200$ [℃] $\lambda_C = 2 - 0{,}2451 \times (\theta_c/100) + 0{,}0107(\theta_c/100)^2 [W/m.K]$ Eq 26

The lower limit of thermal conductivity λ_c of normal weight concrete may be determined from the equation below:

$20 \leq \theta_c \leq 1200$ [℃] $\lambda_c = 1{,}36 - 0{,}136 \times (\theta_c/100) + 0{,}0057(\theta_c/100)^2 [W/m.K]$ Eq 27

where: θ_c is the concrete temperature [℃].The variation of thermal conductivity with temperature is represented in Figure 28.

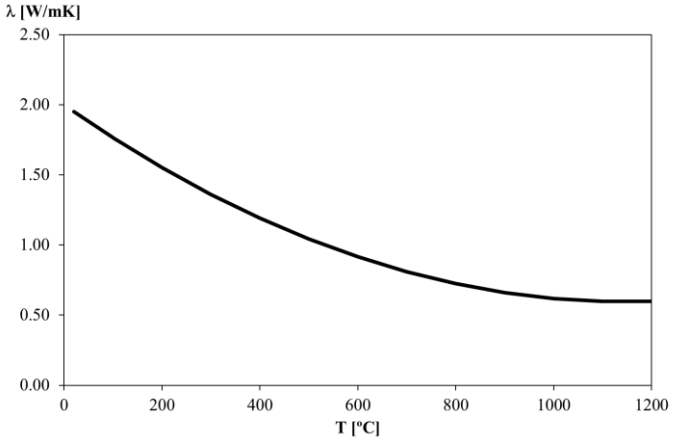

Figure 28 - Thermal conductivity of concrete as a function of the temperature [49].

The variation of density of concrete with temperature is influenced by water loss and is defined in Eurocode EN 1992-1-2 [49] as follows :

$100 < \theta_c \leq 115$ [℃] $\rho(\theta_c) = \rho(20°C) kg/m^3$ Eq 28

$115 < \theta_c \leq 200$ [℃] $\rho(\theta_c) = \rho(20°C) \times \left(1 - \frac{0{,}02(\theta_c - 115)}{85}\right) kg/m^3$ Eq 29

$200 < \theta_c \leq 440$ [℃] $\rho(\theta_c) = \rho(20°C) \times \left(0{,}98 - \frac{0{,}03(\theta_c - 200)}{200}\right) kg/m^3$ Eq 30

$440 < \theta_c \leq 1200$ [℃] $\rho(\theta_c) = \rho(20°C) \times \left(0{,}95 - \frac{0{,}07(\theta_c - 400)}{800}\right) kg/m^3$ Eq 31

The variation of the density with temperature can be illustrated in Figure 29.

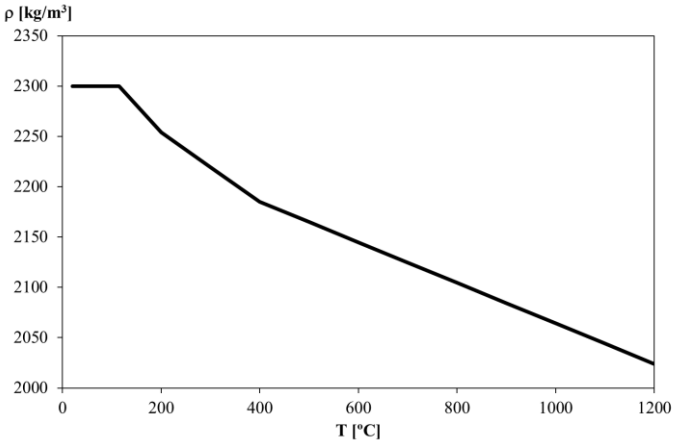

Figure 29- the density of concrete according to Eurocode EN 1992-1-2.

4.2- Temperature calculation

4.2.1- Car position

The temperature of the secondary beam is going to be analysed, based on different car positions (R=0,1,2,3,4,5 m) relative to the fire flame axis, see Figure 30.

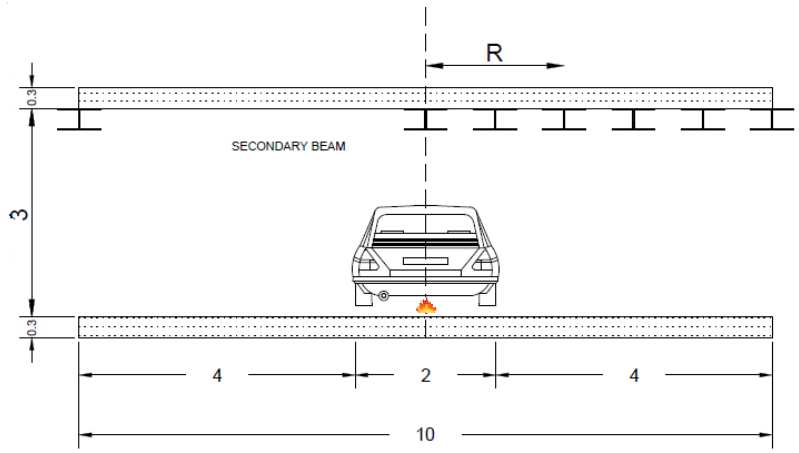

Figure 30 - The car positions.

4.2.2-Cross section

In this thesis the parametric analysis was defined: different cross sections were consider under fire by three sides, using 5 different car classes and different car position (relative distance).

Most of the cross section where defined, based on typical cross section used in open car parks. Other cross section were used to account for different section factors. It is worthy to mention that the section factor depends on the surface of the steel exposed to fire in relation to

the volume of the material. Figure 31 represents the main geometry required for the analysis of the secondary beams.

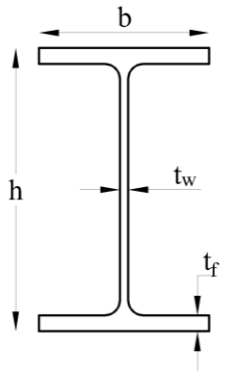

Figure 31 - The most important dimensions in a cross section.

We selected the profiles based on the variation of section factors to choose 5 different cross sections, the Profil HEAA 650 and the profil IPEA 550 are normally used in car parks, the profil HEB140 is not used but we used it just to make the comparison. Table 5 represents the main dimensions of the selected profiles to this parametric analysis.

Table 5 - Designation and dimension of cross sections.

Designation	Section factor [m^{-1}]	h [mm]	b [mm]	tf [mm]	tw [mm]
HEAA 650	118	620	300	16	12.5
IPEA 600	131	547	220	17.5	9.8
IPEA 550	111	547	210	15.7	9
IPEA 450	165	447	190	13.1	7.6
HEB 140	155	140	140	12	7

4.2.3- Steel temperature development

4.2.3.1- Unprotected internal steelwork

For an equivalent uniform temperature distribution in the cross-section, the increase of temperature $\Delta\theta_{a,t}$ in an unprotected steel member during a time interval Δt should be determined from: Eq 32. It is worth mention that this steel element is going to be submitted to fore from 3 sides, because it is assumed to be protected from the top (slab of concrete). This effect is considered when performing the calculation of the section factor.

$$\Delta\theta_{a,t} = k_{sh}\frac{A_m/V}{c_a\rho_a}\dot{h}_{net}\Delta t \qquad , \Delta t \le 5s \qquad \text{Eq 32}$$

Where : k_{sh} represents the correction factor for the shadow effect, A_m/V represents the section factor for unprotected steel members[1/m], A_m is the surface area of the member per unit length[m²/m], V is the volume of the member per unit length [m^3/m], c_a : the specific heat of steel [J/kg.k], $\dot{h}_{net}$ represents the design value of the net heat flux per unit area [W/m²], Δt is the incremental time interval [seconds] and ρ_a represents the unit mass of steel [kg/m^3].

Under nominal fire actions, the correction factor for the shadow effect may be determined from: Eq 33.

$$k_{sh} = 0.9\,[A_m/V]_b/[A_m/V] \qquad \text{Eq 33}$$

Where : $[A_m/V]_b$ is box value of the section factor [47].

The model that is considered in this thesis for simple calculation method uses a mix of Heskestad and Hasemi: For the first period $0 < t < 19$ min the Heskestad method should be applied. For the second phase $19 < t < 32$ min the Hasemi method should be applied. For the third and last period $32 < t < 70$ min the Heskestad method should be applied again.

Up to 19 min if the beam is 1 m located to the right the temperature of the beam should be 20 [℃].

4.2.3.2- Steel section HEAA 650

Figure 32 shows the temperature evolution for the secondary beam (HEAA 650) in the relative position R=0 m, for different car classes. This figure also presents the temperature of the gas near for relative position R=0.

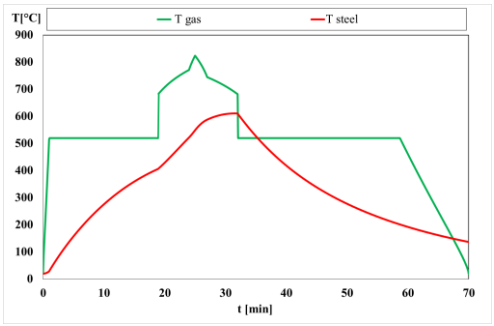

Class 1

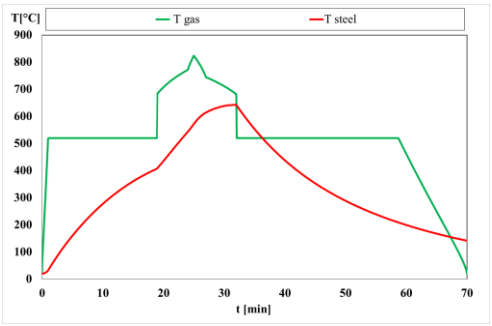

Class 2

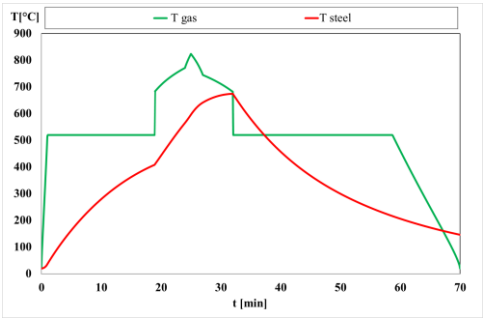

Class 3

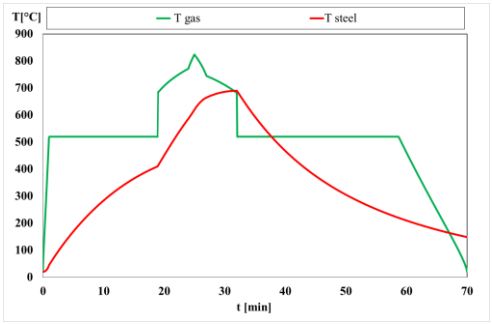

Class 4/5

Figure 32 - Flame and steel temperature for all car classes.

Figure 33 shows the gas temperature of the car class 3 fire event and the temperature of the secondary beam, for different radial relative positions to the flame axis (parameter R= 0 m, 1 m,…,5 m).

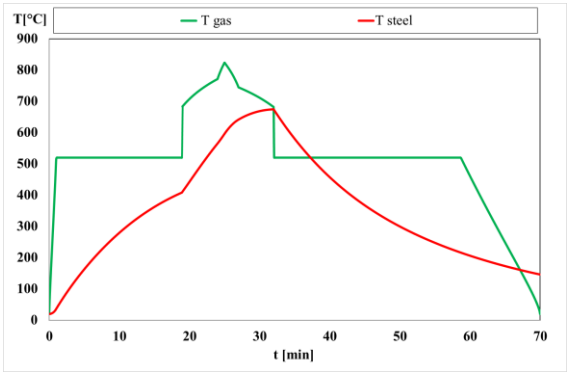

R=0 m

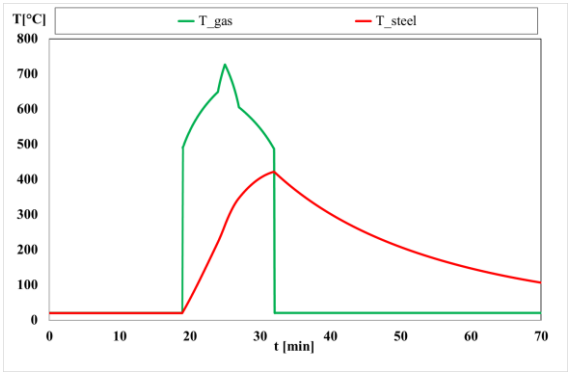

R=1 m

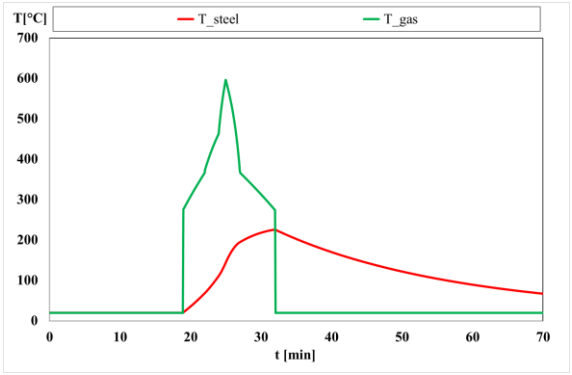

R=2 m

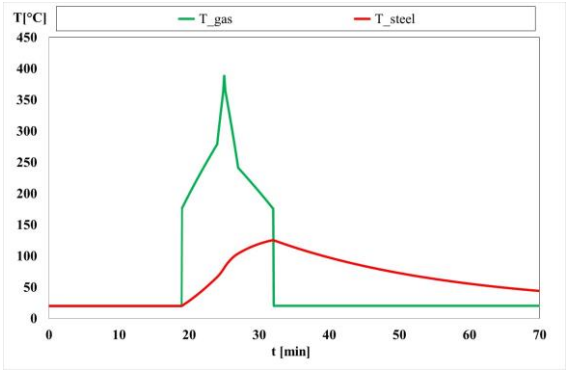

R=3 m

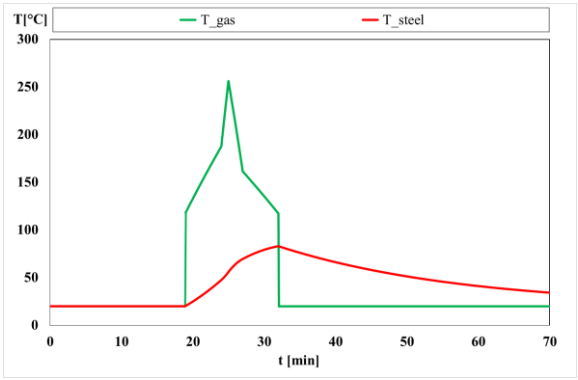

R=4 m

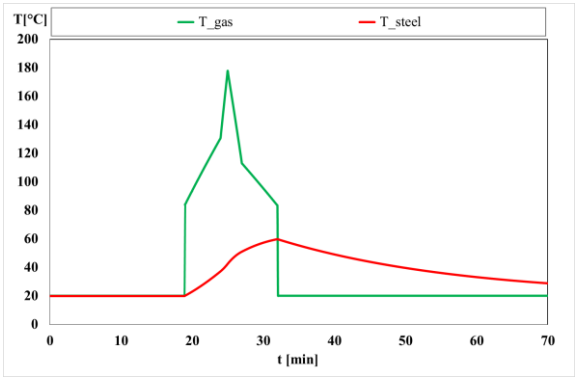

R=5 m

Figure 33 - Flame and steel temperature of different positions from the fire axis.

It can be noticed that the Heskestad method is only valid for R=0 m. This means that the heat flux for R=1,2,..,5 m should not be consider when the flame is not touching the ceiling. For the first period of fire event the Heskestad method should be applied, calculating the temperature of the gas base on Eq 3 when R=0 m, and assuming no heat effect (TGas = 20 °C) for other radial position.

When the flames are touching the ceiling, the Hasemi method is valid and the heat flux can be calculated for any radial position.

After the decreasing of the fire event, the length of the flames are decreasing and the Heskestad method should be applied again, keeping the temperature of the gas equal to 20 ºC.

Results for other cross sections are presented in **Annex A**.

5- THERMAL ANALYSIS - SIMPLE CALCULATION METHOD (ELEFIR_EN) and ADVANCED CALCULATION METHOD(ANSYS FLUENT)

5.1- The computer program Elefir-EN

Elefir-EN is a software for the evaluation of the fire resistance of carbon and stainless steel members loaded about the strong axis or about the weak axis, according to EN 1991-1-2 and EN 1993-1-2. Calculations can be performed in the time domain, resistance domain and temperature domain, Typical shapes of sections are available: HD, HE, HL, HP, IPE, UB, UC, W, L, RHS, CHS. Two options for fire exposure: three or four sides of the element. Options for section protection: no protection, contour encasement and hollow encasement. Properties of several protection materials are available: rock glass wool, gypsum and allows for the introduction of a new material defined by the user Temperature dependent thermal properties of protection material can be defined Several heating curves are available: ISO curve, external fire curve, hydrocarbon curve, localized fires, parametric fire curves and there is also the possibility of introducing an user defined curve. The following calculations can be performed Calculation of the time in which the critical temperature of the element is reached Reached temperature after the introduced critical time. Calculation of the critical temperature of the element and the critical time for members subjected to tension, compression, bending and compression, bending and shear, global plastic analysis of continuous beams, Figure 34 shows the first screen of the program.

Figure 34 - First screen of the Software Elefir_EN.

The main objective of this work is not only to check the fire resistance of a real open car park but also to validate the calculation process. This validation is performed with the comparison for the temperature evolution using software Elefir-EN which is based on Hasemi method.

5.1.1- Available thermal calculations

The program allows the user to choose the section type, the fire exposure, type of fire protection and the heating curve.

5.2- Temperatures of The Beams with Elefir-EN

5.2.1- HEAA 650

Figure 35 shows the temperature of the secondary beam (HEAA 650) in the relative position R=0 m, for different car classes. The maximum temperature reached by the gas was 880.2 ºC for the fire event of a car class 4/5. The temperature of the steel element depends on the temperature evolution of the gas.

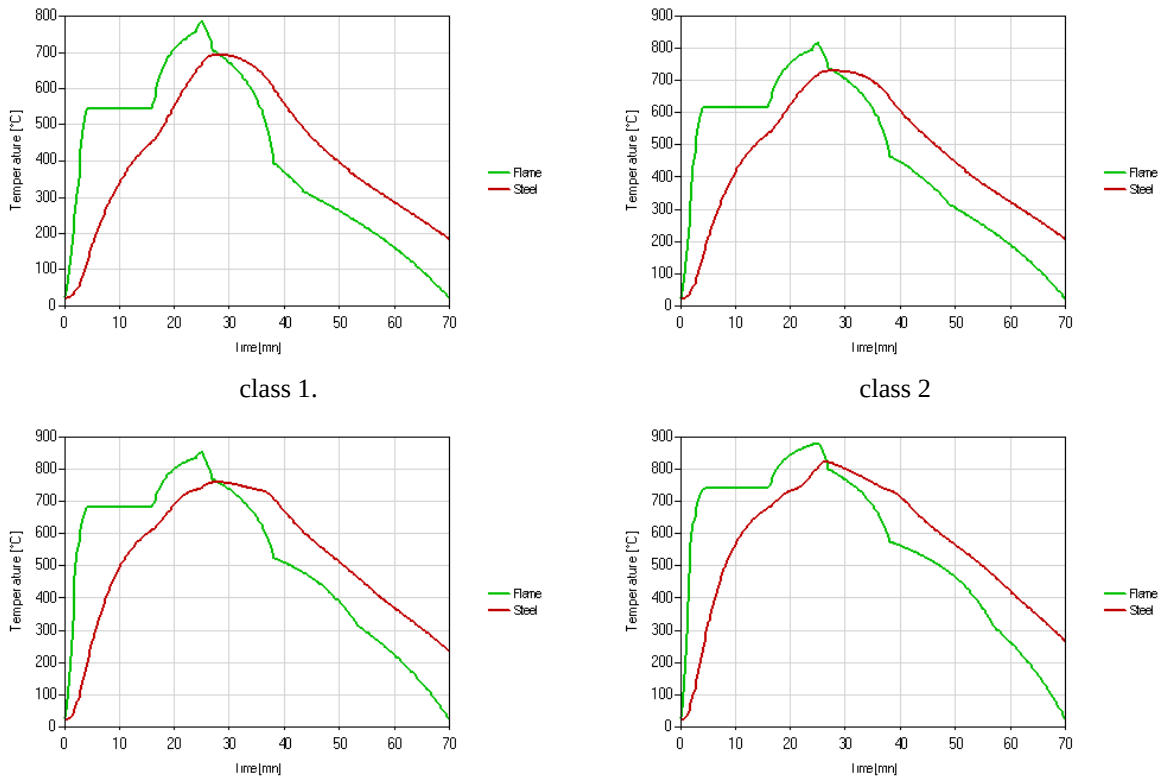

class 1. class 2

class 3 class 4/5

Figure 35 - Flame and steel temperature for car class :1,2,3 and 4/5.

The gas temperature of the fire event for a car class 3 and the temperature of the secondary beam are presented for different positions relative to the flame axis (parameter R= 0 m, 1 m,…,5 m), see Figure 36. The maximum temperature of the gas was 858.7 ºC and was achieved for the

case of the beam above the car (R=0 m). It is worth to mention that the time that corresponds to the maximum temperature of the gas is not coincident with the time achieved to the maximum temperature of the steel element.

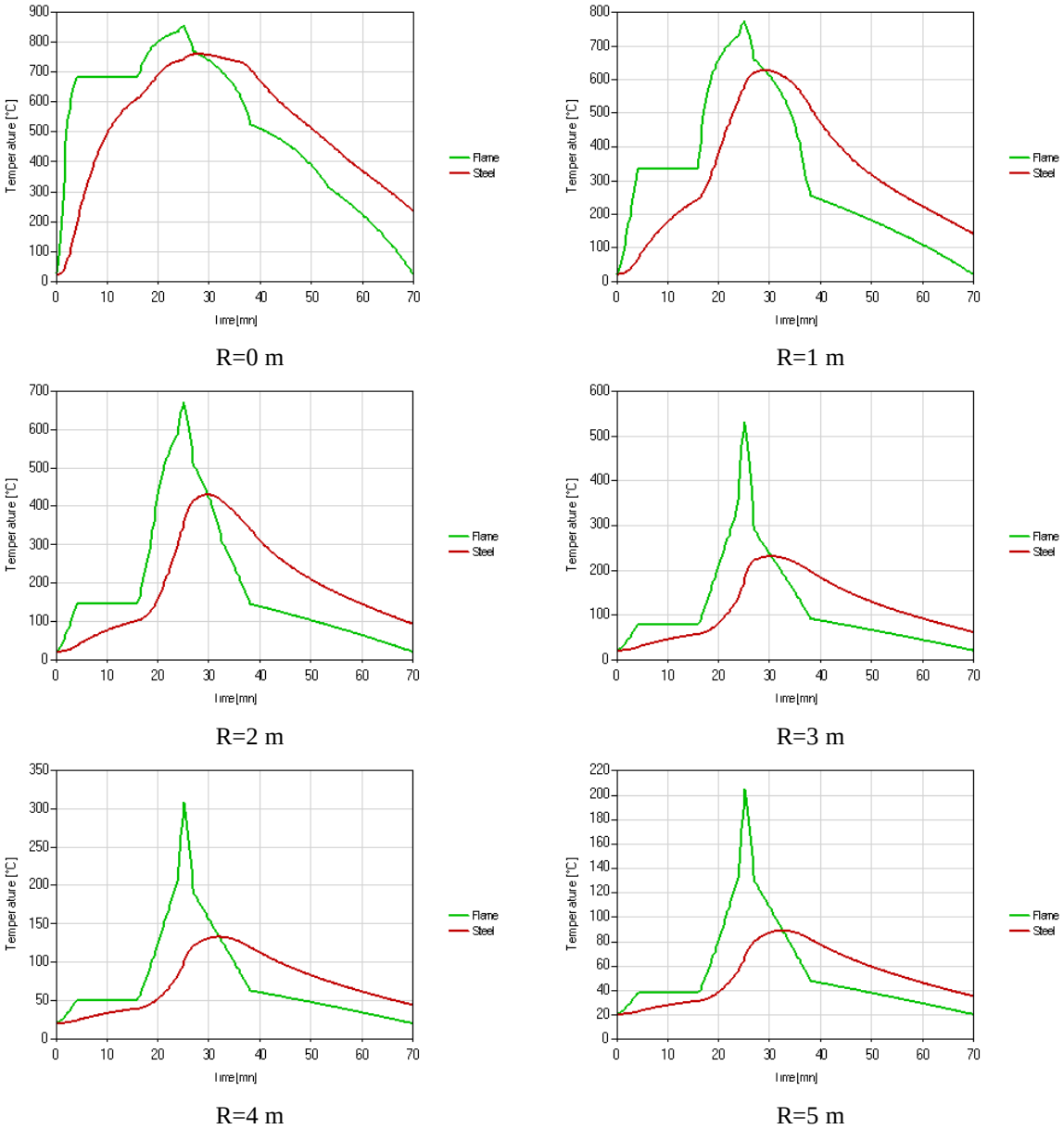

R=0 m R=1 m

R=2 m R=3 m

R=4 m R=5 m

Figure 36 - Flame and steel temperature for different positions for car class 3.

Figure 37 represents the gas temperature during the fire event for different radial positions with respect to the flame axis. The maximum temperature is expected to be achieved after the maximum HRR has been reached (25 minutes).

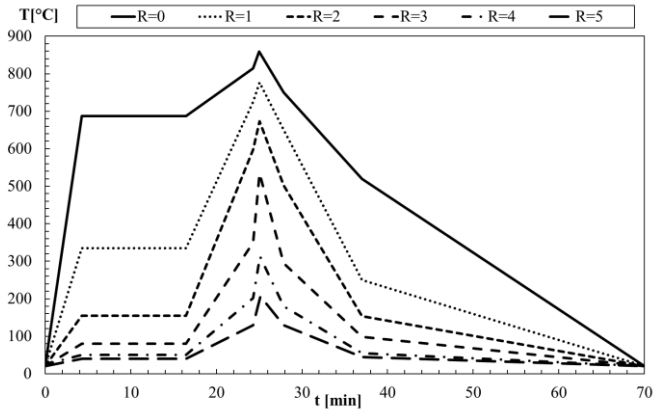

Figure 37 - The gas Temperature for car class 3 .

Figure 38 represents the steel temperature during the fire event. The maximum temperature is expected to be achieved after the maximum HRR has been reached (25 minutes).

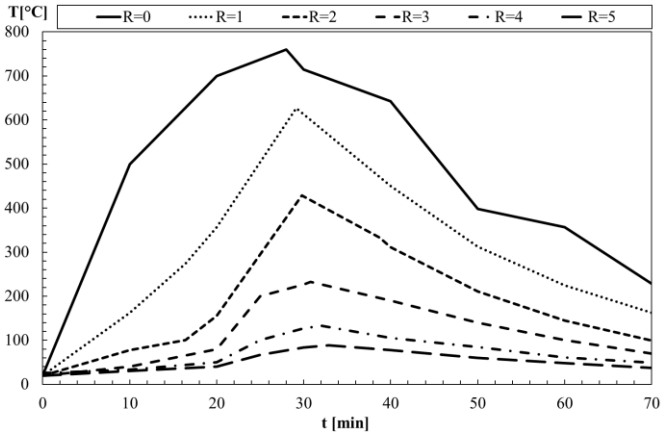

Figure 38 - The steel temperature for car class 3.

The Elefir results shows that the values of the temperature of the gas (green line) and temperature of the steel (red line) are considered as maximum when the time is equal to 25 min for gas and 32 min for steel.

Elefir is always using HASEMI method taking into consideration the length of the flame for the maximum peak of the HRR.

For the results of other cross sections see **Annex B**.

5.3- ADVANCED CALCULATION METHOD (CFD MODEL)

ANSYS, Inc. is an USA Computer-aided engineering software developer. ANSYS is a general purpose multi physics software, used to simulate interactions of all disciplines of physics, structural, vibration, fluid dynamics, heat transfer and electromagnetic for engineers.

One of its most significant products is ANSYS FLUENT, a proprietary computational fluid dynamics (CFD) program.

ANSYS FLUENT was used in this thesis to solve the thermal and fluid dynamics used to simulate the fire event.

ANSYS FLUENT is one of the most popular commercial CFD (Computational Fluid Dynamics) software packages. This program is actually included in ANSYS workbench. This integrated software allows to create the geometry of the domain (fluid and solid) and also allows to create the mesh or grid, using the finite volume method.

ANSYS FLUENT is capable of simulation fire even to determine heat in the far field. However, the use of a vent instead of a combustion process makes the near field data unreliable. Because ANSYS FLUENT is modelling a heat vent and not combustion, the air coming into the compartment is different from it should be. Combustion involves chemical reactions with the oxygen around it pulling air into the fire and releasing hot gases that travel upwards. Entrainment in a combustion model is stronger than that of a vent. In combustion, air is pulled into replacing the air that was heated or burnt in the fire. Once the fire is large enough to require more air than is in the room around it, air is pulled in from the surrounding area.

The fire simulation by ANSYS FLUENT uses a vent, and is being used to simulate the heat that would result due to combustion. Vents also cause convection, however due to the fact that air is being brought in through the fire vent whereas in actual combustion all air would be brought in through the openings of the compartment. In order to counter balance this, an artificial entrainment was created (pressure outlet) to mimic the cold airflow that would be coming in from the external of the compartment [50].

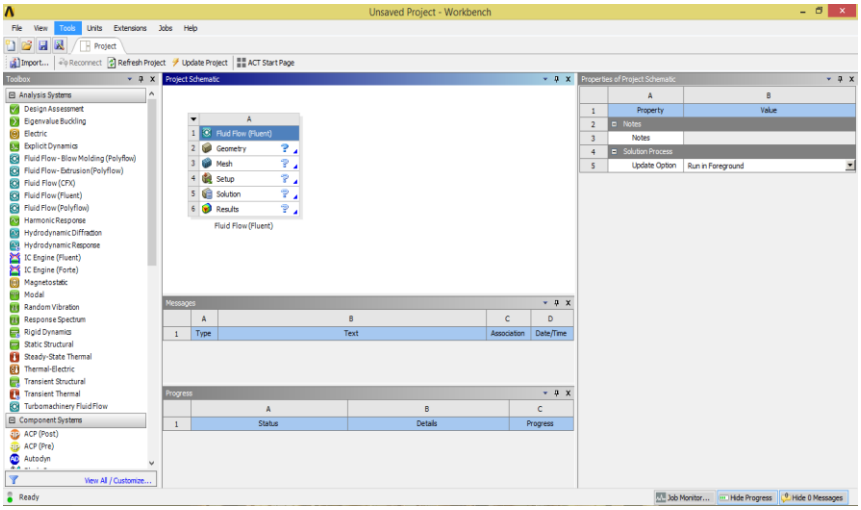

Figure 39 - ANSYS WORKBENCH running ANSYS FLUENT.

5.3.1- Equations to be solved

For systems in which there is fluid motion present, a different set of equations must be introduced that relate to the conservation principles that must be met by a system [51]. This software account for the solution of the energy equation, Navier stokes and continuity. The model also includes a turbulent model for the viscosity and a radiation model.

The equation used for the conservation of mass must be satisfied in any closed system. Mass must not be created or destroyed. The equation governing this principle is known as the continuity equation [51] and is shown below in Eq 34.

$$\frac{\partial \rho}{\partial t} + \vec{\nabla} \cdot \left(\rho \vec{V}\right) = 0 \qquad \text{Eq 34}$$

where ρ is the density, t is the time and ∇ is Del operator $\vec{\nabla} = \langle \partial/\partial x \quad \partial/\partial y \quad \partial/\partial z \rangle$, then V is the vector of velocity $\vec{V} = \langle V_x \quad V_y \quad V_z \rangle$ presents the velocity of each particle.

The Navier-Stokes equations are a collection of the 3-dimensional momentum equations for any Newtonian fluid. In fluid dynamics, a Newtonian fluid is one in which the stresses at each point in the fluid are linearly proportional to the strain rates at that point. These equations ensure that in any system, the momentum is conserved. This means that the total force generated by the momentum transfer in each direction must be balanced by the rate of change of momentum in each direction. The Navier-Stokes equations are provided below in Eq 35 [51].

$$\begin{aligned} &\frac{\partial \rho V_z}{\partial t} + \frac{\partial (\rho V_x V_z)}{\partial x} + \frac{\partial (\rho V_y V_z)}{\partial y} + \frac{\partial (\rho V_z V_z)}{\partial z} \\ &= \rho g_z - \frac{\partial p}{\partial z} + R_Z + \frac{\partial}{\partial x}(\mu_e \frac{\partial V_z}{\partial x}) + \frac{\partial}{\partial y}(\mu_e \frac{\partial V_z}{\partial y}) + \frac{\partial}{\partial z}(\mu_e \frac{\partial V_z}{\partial z}) + T_z \end{aligned} \qquad \text{Eq 35}$$

Where: g_y is the gravity acceleration component that exists in this direction. μ_e is the effective viscosity of the fluid, T_y refers to Viscous loss terms and p refers to pressure. The reference density is set on the 'Operating Conditions' panel. However careful choice the reference density will make a big difference to the rate of convergence (in some cases whether the model will even converge or not). For enclosed problems, use a value that represents a typical mean density in the flow [51].

The first law of thermodynamics requires that the energy of a system be conserved. The three-dimensional energy equation for fluid flow must also be solved, following the differential see Eq 36 [51]: This equation is going to be used in the fluid and solid regions.

$$\frac{\partial(\rho C_p T)}{\partial t}+\frac{\partial(\rho V_x C_p T)}{\partial x}+\frac{\partial(\rho V_y C_p T)}{\partial y}+\frac{\partial(\rho V_z C_p T)}{\partial z}=\frac{\partial}{\partial x}\left(\lambda_x \frac{\partial T}{\partial x}\right)+\frac{\partial}{\partial y}\left(\lambda_y \frac{\partial T}{\partial y}\right)+\frac{\partial}{\partial z}\left(\lambda_z \frac{\partial T}{\partial z}\right) \qquad \text{Eq 36}$$

Where : ρ is Density, C_p is specific heat, $V_{x;y;z}$ refers to the velocity in x, y, z directions and T represents the temperature, $\lambda_{x,y,z}$ is thermal conductivity in x, y, z directions.

5.3.2- The model

The 2D model represents the fire compartment with 3 m of height and 10 m of width. The fire event is localized in the middle of this compartment, considering a burning car with an equivalent pool fire with a diameter of 2 m as it is shown in Figure 40.

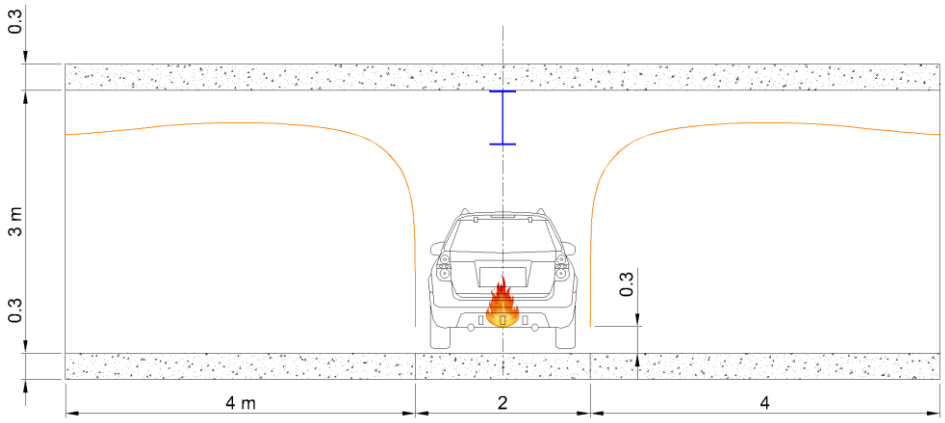

Figure 40 - The real model of an open car parking.

Figure 41 shows a fire event with a car class 3 vehicle, burning in the centre of a fire compartment and all the necessary boundary conditions. The compartment has two openings on the left side and right side, a steel cross section defined above the flame axis. This cross section is going to be consider with different relative positions with regard to the origin of the fire. The thermal load is defined by the Heat Released Rate, and is going to be equivalent to the velocity and temperature profiles of the inlet boundary condition. Four types of boundary conditions were applied: wall concrete insulation, stationary wall insulation, pressure outlet and velocity inlet which has the boundary condition of surrounding gas temperature and velocity.

The boundary conditions were retrieved based on a previous analysis of CFAST and defined in C language as: V_class1, T_class1, V_class2, T_class2, V_class3, T_class3, V_class4 and T_class4, all written in Annex C.

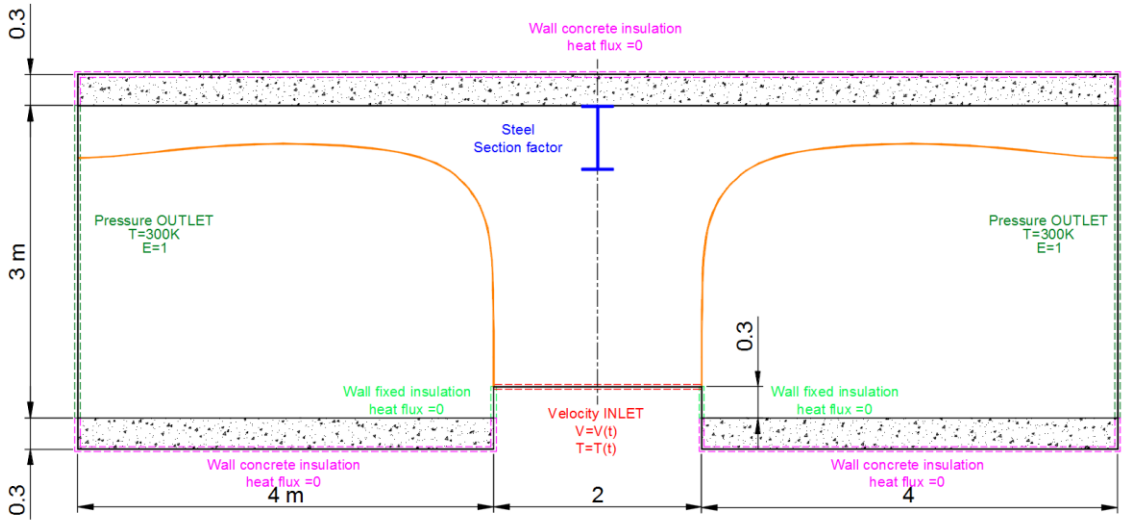

Figure 41 - The fluent model of an open car parking.

This two graphs in figures : Figure 42 and Figure 43 we putted in fluent are equivalent to the graph of heat release rate (HRR).

We used the formulas of heat release rate (HRR) in CFAST, we took this condition at the basement of the car, and we pick this boundary condition and we apply it in FLUENT.

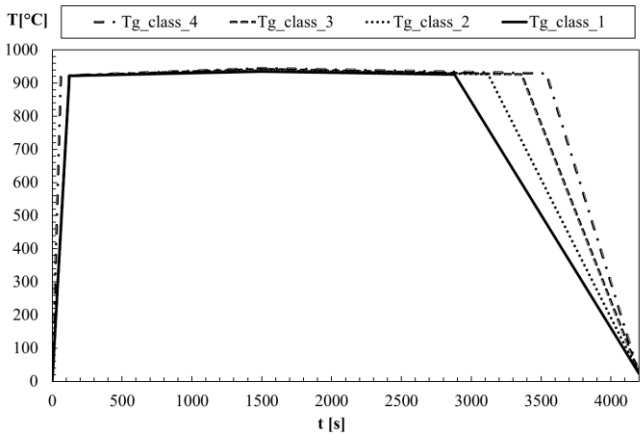

Figure 42 - Surrounding gas temperature for all car classes.

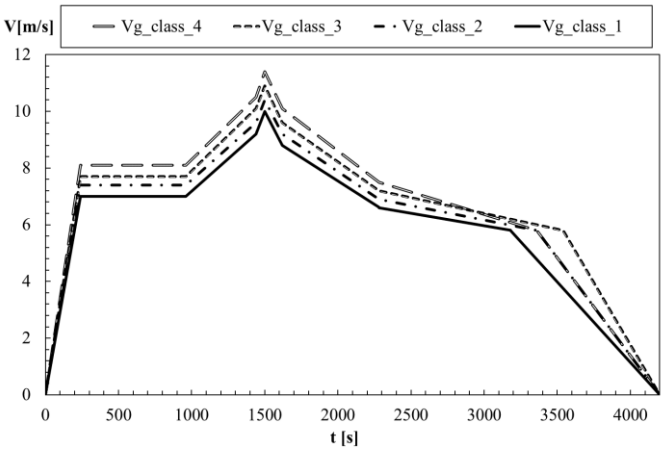

Figure 43 - Velocity for all car classes.

5.3.2.1- HEAA 650 for R=0 m

The model geometry was created by surfaces. Some of them were considered for fluid region and others for solid region, see Figure 44.

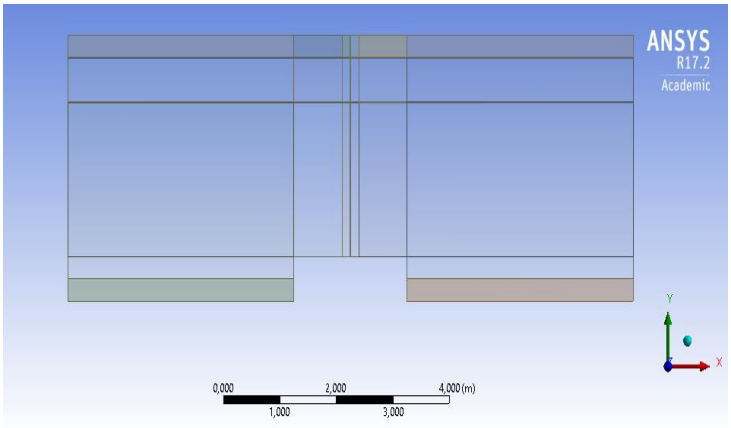

Figure 44 - The Geometry of the model using HEAA 650 cross section for R=0 m.

The grid was generated by the definition of the element size expected on the edges of the surfaces. There was no specification for the dimension of the mesh size on the surfaces. The mesh is defined by nodes and regions, see Figure 45. The name selections should be used to identify the regions where the boundary conditions are to be defined.

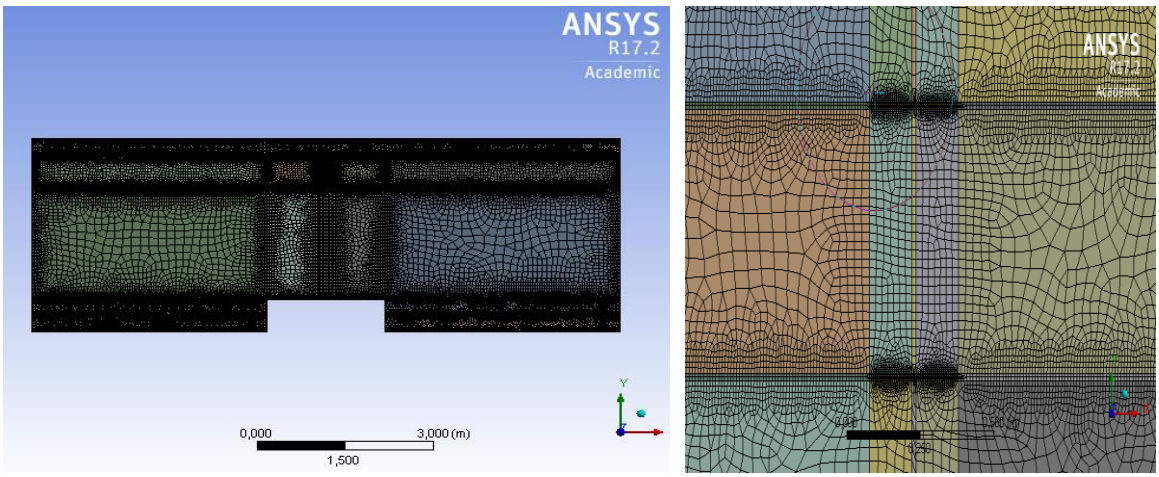

Figure 45 - The final mesh of the model using only edges with hard option for R=0.

The grid is automatically imported by ANSYS FLUENT. Here is the location to define the boundary conditions and the solution method.

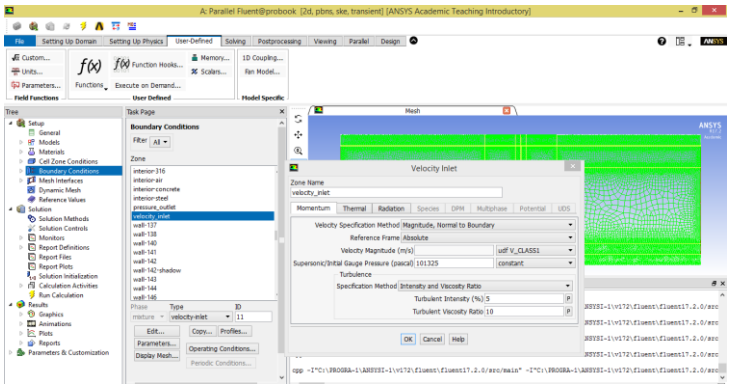

Figure 46 - Defining boundary conditions in FLUENT.

After solving the simulation, seven points were define point locations, according to the needs to get the results of temperature in the steel. This temperature is an average of temperature evolution in each single point, also two pints were define according to the needs to get results of temperature in the concrete see Figure 47 and Figure 48.

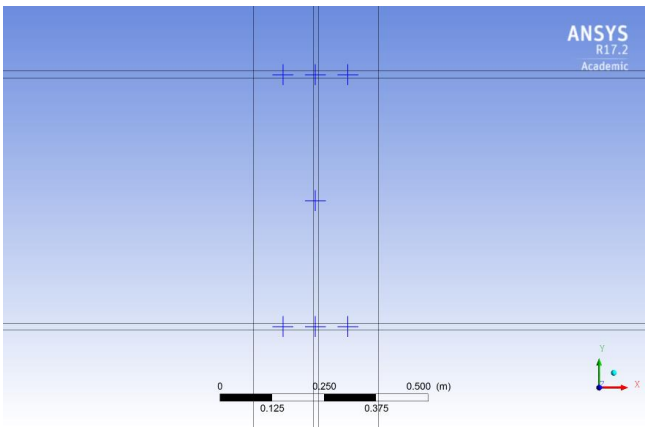

Figure 47 - Points for getting results from CFD post for temperature of the steel.

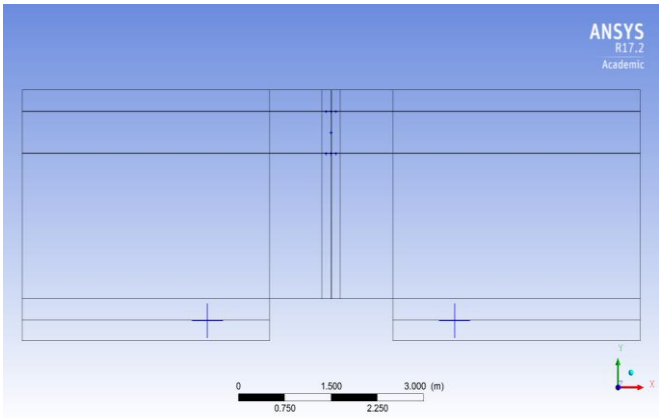

Figure 48 - Points for getting results from CFD post for temperature of the concrete.

Figure 49 represents the temperature field during the fire event. There is a clear definition of two zones (hot layer and cold layer). The temperature is increasing in accordance to the evolution of the HRR in the fluid region. The temperature of the concrete slab is also increasing. The heat flux is also affecting the steel profile.

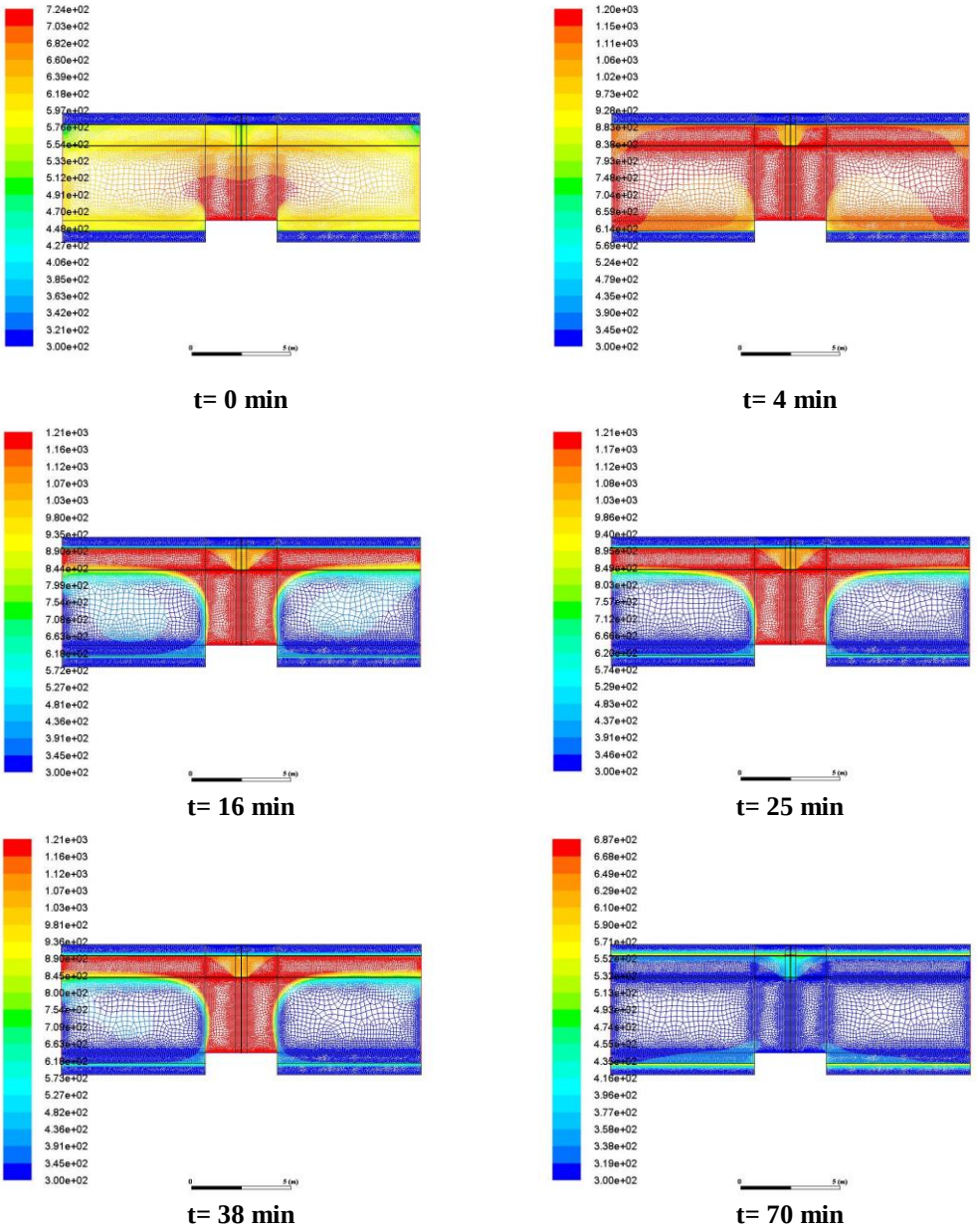

Figure 49 - Temperature [K] in different times using ANSYS FLUENT for R=0 m.

Figure 50 represents the velocity field in the fluid region. The ceiling jet is produced and the thickness of the hot layer changes with time. The motion of the hot layer is well predicted, and there is new fresh air coming from the openings from left and right.

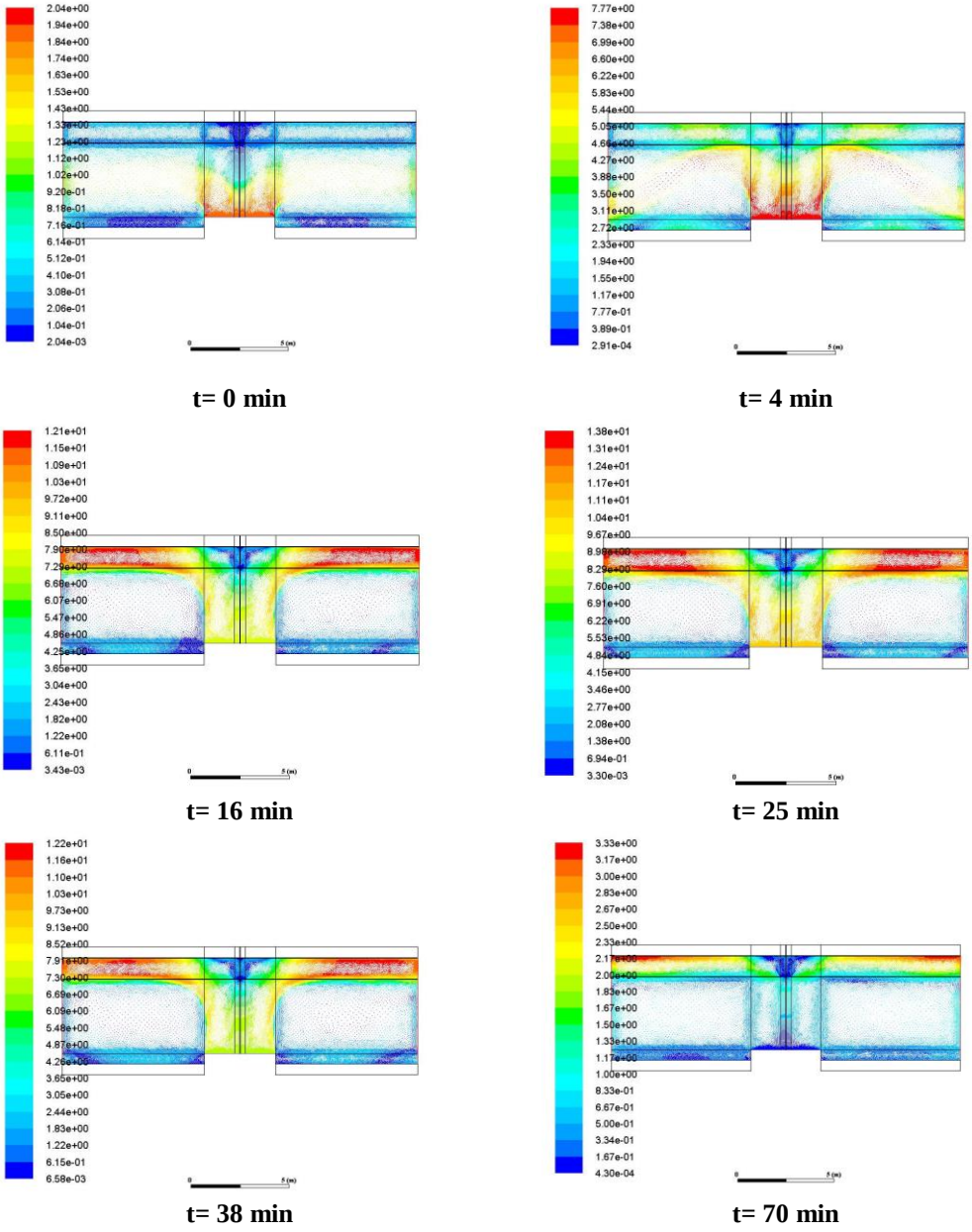

Figure 50 - Velocity [m/s] in different times for R=0 using ANSYS FLUENT for R=0 m.

Figure 51 shows the temperature of the secondary beam (HEAA 650) in the relative position R=0 m, for different car classes (car class 1,2,3 and 4/5), based on the average temperature of seven points. Figure 52 compares all the temperature evolutions.

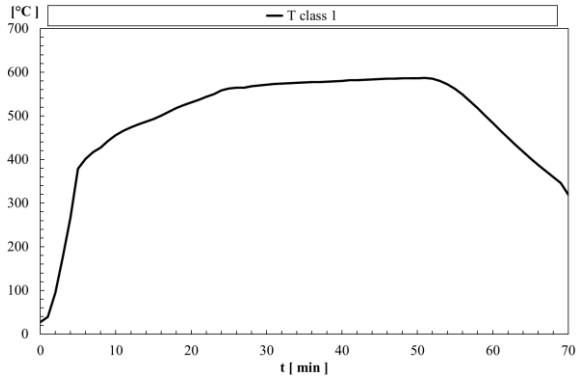

car class 1.

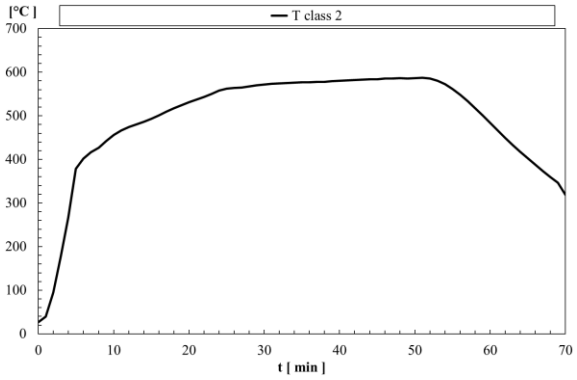

car class 2.

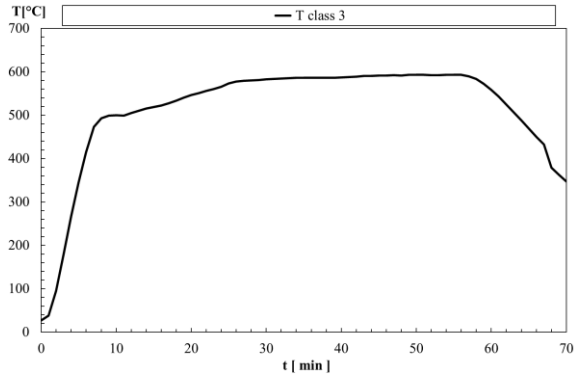

car class 3.

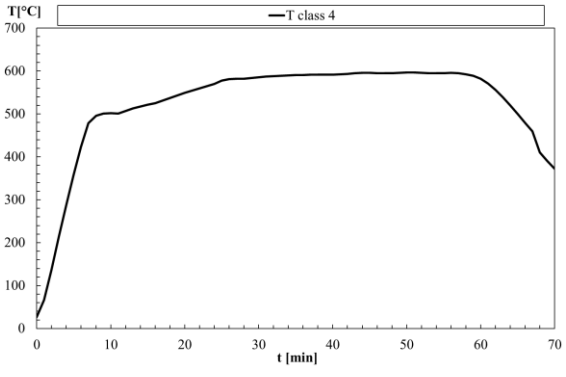

car class 4.

Figure 51 - Steel temperature for car classes.

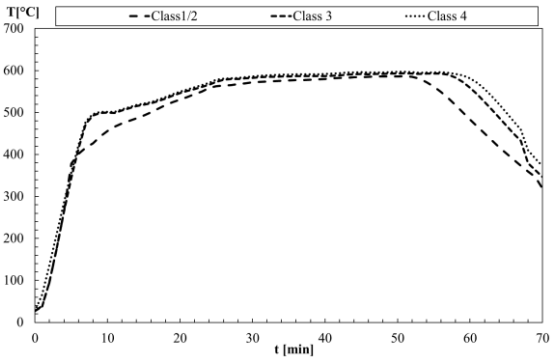

Figure 52 - The evolution of Steel temperature in R=0 m for different car class.

The temperature of the concrete is also increasing in the exposed side of the slab, near the floor, during the fire event, see Figure 53.

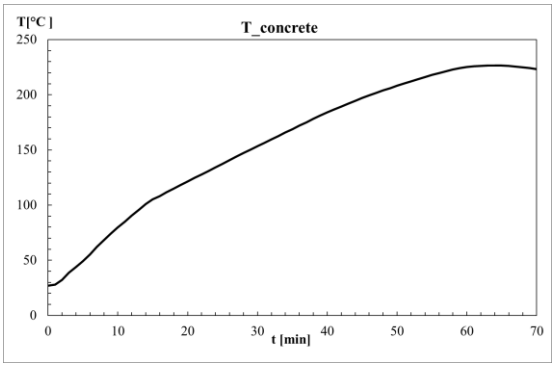

Figure 53 - Temperature of concrete.

Results for other different relative position (R=2 m) and for other cross sections HEB 140 (R=0 m) are presented in **Annex C**.

5.3.2.2- HEAA 650 for R=2 m

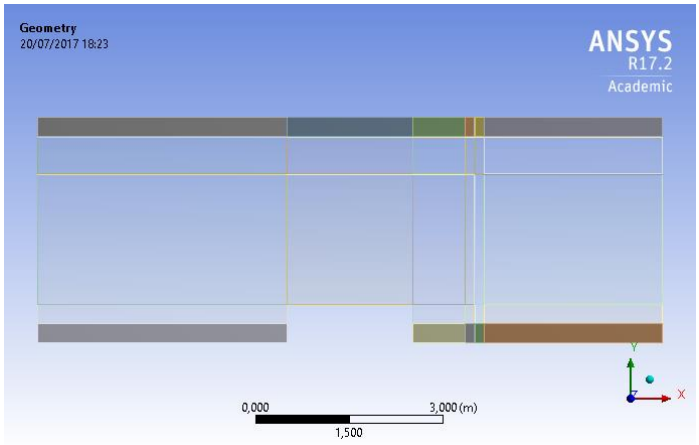

Figure 54 - The Geometry of the model using HEAA 650 cross section for R=2 m.

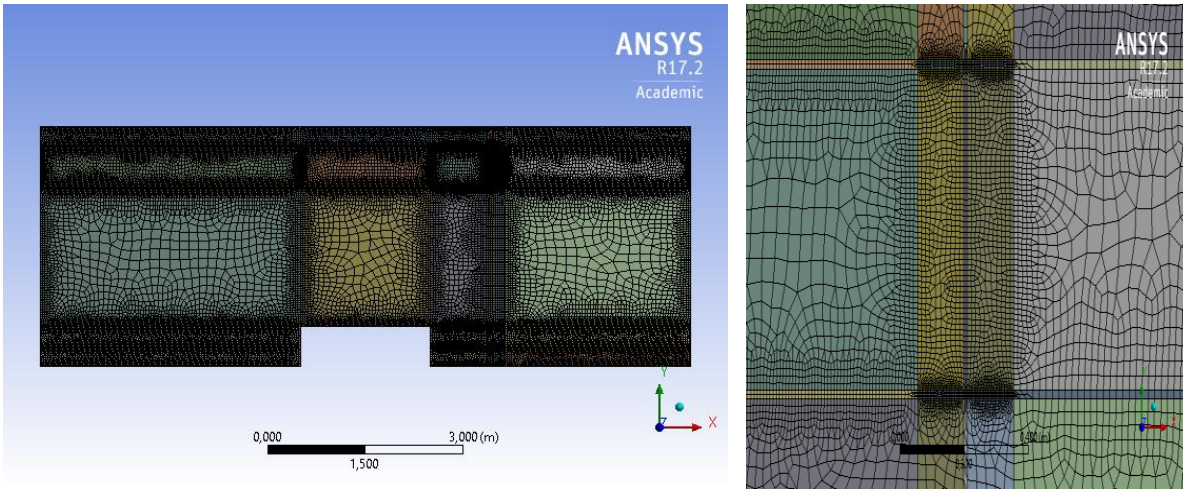

Figure 55 - The final mesh of the model using only edges with hard option for R=2 m.

5.3.2.3- HEB 140 for R=1 m

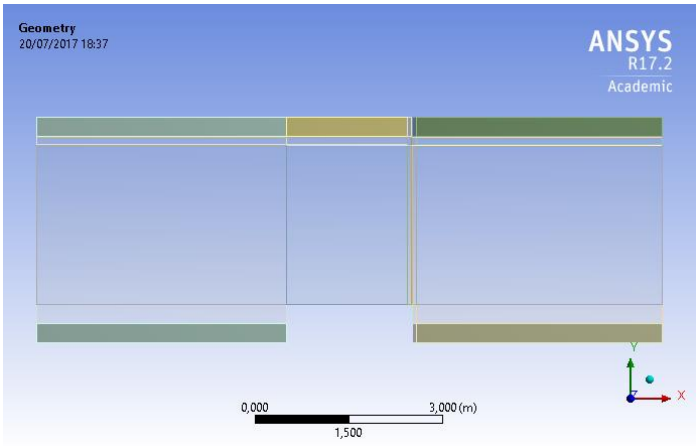

Figure 56 - The Geometry of the model using HEB 140 cross section for R=1 m.

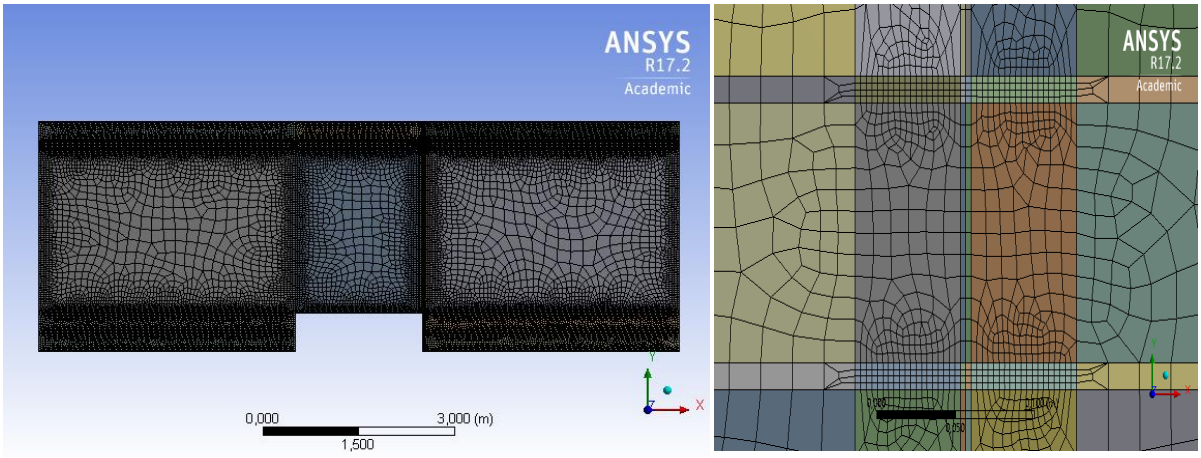

Figure 57 - The final mesh of the model using only edges with hard option for R=1 m.

5.4- Comparison of results

Figure 58 up to Figure 60 represent the comparison between both simple calculation method: Elefir and the simplified method developed using excel (Heskestad with Hasemi method)). The results are related with the fire event of a car class 3, using HEAA 650 as secondary beam, with different scenarios for different radial positions.

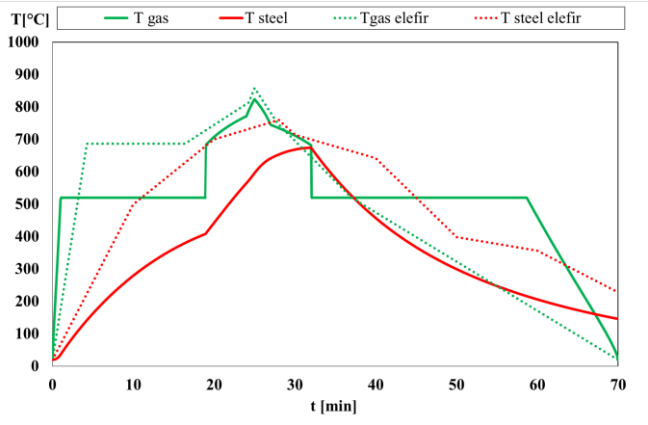

Figure 58 - Tgas and Tsteel for R=0 m.

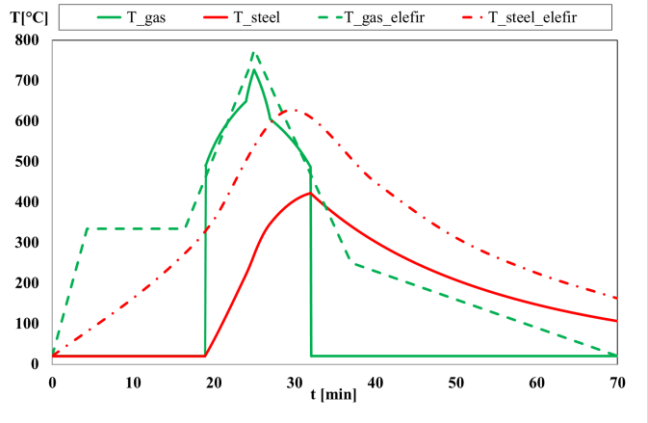

Figure 59 - Tgas and Tsteel for R=1 m.

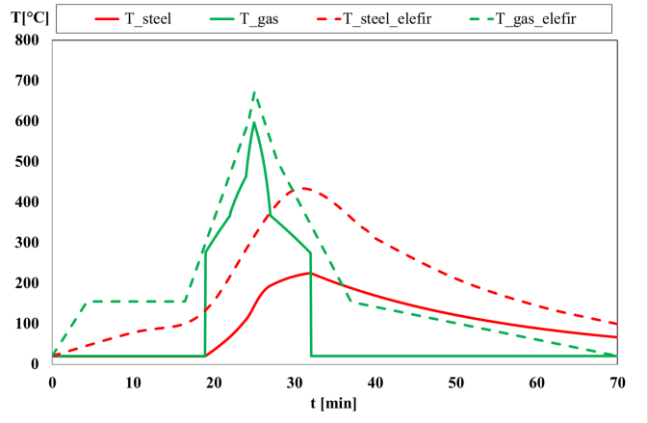

Figure 60 - Tgas and Tsteel for R=2 m.

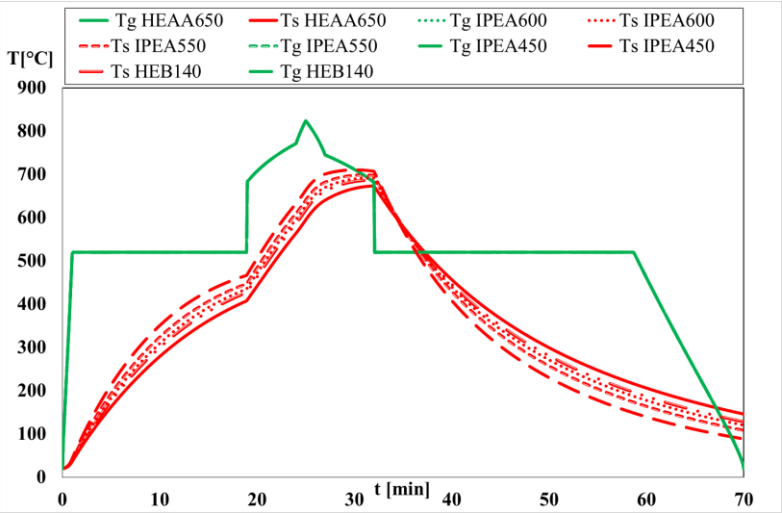

Figure 61 - Tgas and Tsteel for all cross section for R=0.

There is a good agreement between Elefir results and the simple calculation method that was developed. Differences were expected because methods are different. The ELEFIR_EN is over predicting the temperature results.

ELEFIR_EN is always using Hasemi method because he detects that for time equal to 1500 the HRR is maximum, and the length of the flame touch the ceiling.

Figure 62 and Figure 63 compares the temperature of the steel beam, using the result of the ANSYS FLUENT simulation and the results of the simple calculation method (mix of Heskestad_Hasemi_Heskestad). The results are related with a fire event of class 3, on the secondary beam HEAA 650 for two distinct radial position (R=0 and R=2). The maximum temperature agree well for the first radial position (R=0) but for the offset distance (R=2) ANSYS FLUENT is over predicting the calculation of the maximum temperature.

Figure 61 Shows that there is good agreement between the results of Tgas and Tsteel for all the cross sections, differences was expected because the cross sections are different and the section factors are different, Tsteel is always over Tgas. Tgas has the same results for all cross sections. When we increase the section factor (from 118 until 165) the increments of temperature are bigger it is expected that the biggest one will be IPEA 450.

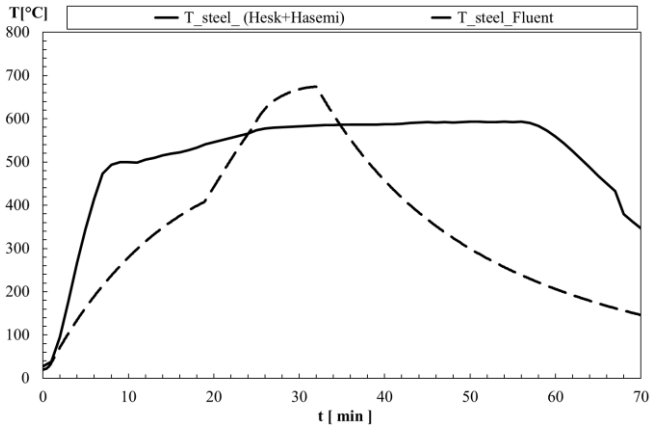

Figure 62 - TSteel comparison for R=0 m.

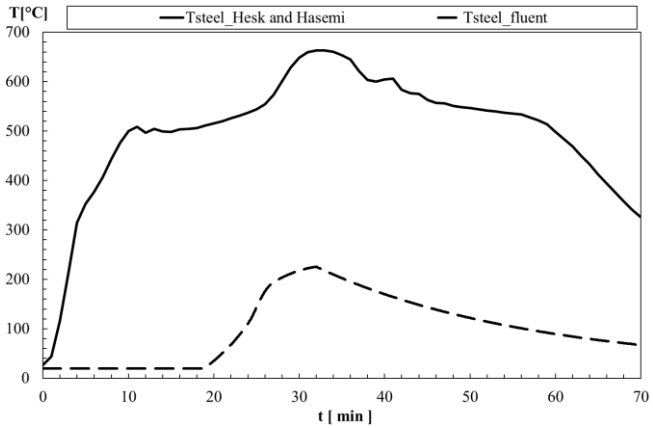

Figure 63 - TSteel comparison for R=2 m.

6- CONCLUSIONS AND FUTURE DEVELOPMENTS

This thesis was developed to evaluate the temperature of elements of the structure of an open car park due to the fire event of a localize fire induced by a car fire. The main target is to determine the temperature of the steel profiles using three different methods (two simplify method and one advanced calculation method which is Ansys Fluent).

The study was developed for an open car park of 3 m height, different car classes and different fire scenarios.

The simplified method was implemented to calculate the temperature of the gas and the temperature of the steel beam element, using different relative positions between the fire source and the position of the steel element.

According to the car localization with respect to the fire source, the present procedure allows for a suitable positioning of the beam regarding its thermal conditions, as well as a possible modification of the entire car park design.

The examples showed the advantage of using the design methodology based on fire scenarios against the use of standard fire curves (ISO curve).

Finally, the results showed in this thesis, reveal extreme importance because they give great information for designers, more details about the behaviour of the Steel and Concrete, in fire situations. This knowledge can be taken into account for the building construction to minimize the failure and increasing the safety of the people.

Considering the works carried out in this thesis, some future developments will be presented, as the following:

- Propose a numerical model under coupled mechanical and thermal analysis. The thermo-mechanical analysis could give different results to compare with the previous investigations;
- Perform different experimental tests for both mechanical and the thermal behaviour to correlate the results with the numerical analysis;
- Carry out different experimental and numerical tests with other type of simple calculation method or advanced calculation method to account for the effect of fire dynamics on this kind of events. An experimental study can be performed in a small scale to validate the numerical simulation that we found.

REFERENCES

[1] R. Craign, Schrol, Industrial Fire Protection Handbook, Second ed.

[2] Terry Buis, Owner Sun Valley Automotive, Sun Valley Automotive Repair - Las Vegas Nevada - Since 1988, [Online]. Available: http://www.sun-valley-automotive.com/car-fires.html.

[3] The University of Waikato, "SCI," Science Learing Hub, 2007-2009. [Online]. Available: https://www.sciencelearn.org.nz/images/831-the-fire-triangle..

[4] Votruba, Joe, "New Jersey 101.5," 9 January 2013. [Online].

[5] Mike, kirby, "Fire Rescue," 02 01 2012. [Online]. Available: http://www.firerescuemagazine.com/articles/print/volume-7/issue-2/strategy-and-tactics/fighting-vehicle-fires-in-parking-garages.html.

[6] Ales Jug, Stojan Petelin and Peter Bukovec, Designing an Underground Car Park Fire Scenarios on a Probabilistic Basis, Slov: Acta Chim,57, 136–143, 2010.

[7] Li, Y, "Assessment of Vehicle Fires in New Zealand Parking Buildings. Master's thesis," 2004.

[8] Noordijk, L. and Lemaire, T, "Modeling of Fire Spread in Car Parks," HERON, (2005).

[9] B. Merci and M.Shipp, "Smoke and Heat Control for Fires in Large Car Parks: Lessons Learnt from Research," 2013.

[10] De Feijter MP, Breunese MP, "Efectis-R0894(E)– Investigation of Fire in the Lloydstraat Car Park,," Rotterdam, 2007.

[11] BRE Research Project, "Fires in Enclosed Car Parks," on Behalf of the UK, oct 2009.

[12] Building Research Establishment,, "Fire Spread in Car Parks. Building Research Establishment (BRE)," Eland House Bressenden Place London SW1E 5DU United Kingdom, 2010.

[13] Van der Heijden, M. G. M, "Heat and Smoke Removal in Semi-open Car Parks," Eindhoven, Netherlands, 2010.

[14] Collier, P. C. R, "Car parks - Fires Involving Modern Cars and Stacking Systems," 2011.

[15] Shipp M. P, Spearpoint M. J., "Measurements of the Severity of Fires Involving Private Motor Vehicles." Fire and Materials., 19, 143-151. ed., 1995.

[16] W, Stroup D., ""Experimental Investigation of Burning and Fire Jumping Behavior of Automobiles."," *VFDB Journal*, no. 172, p. 163, 4 2000.

[17] Stroup D. W., DeLauter L., Lee J., Roadarmel, G., "Passenger Minivan Fire Tests.", M. Gaithersburg, Ed., National Institute of Standards and Technology, 2001.

[18] Ohlemiller, T. J. and Shields, J. R, "Burning Behavior of Selected Automotive Parts From a Sports Coupe," 2001.

[19] "Reaction-to-fire tests — Heat release smoke production and mass loss rate," 15-12-2002.

[20] Butcher E.G et al, "Fire Car Park Buildings", HMSO: Fire note 10, July 1968.

[21] R.G., Gewain, ""Fire Experience and Fire Tests in Automobile Parking Structures"," *Fire Journal,* vol. (4), no. 50-54, p. 67, 1973.

[22] Bilal, Fettah, "FIRE ANALYSIS OF CAR PARK BUILDING STRUCTURES. Master thesis," july 2016.

[23] E. Annerel, L.Taerwe , B.Merci , D.Jansen , P.Bamonte , R.Felicetti, "Thermo-Mechanical Analysis of an Underground Car Park Structure Exposed to Fire," *International Association for Fire Safety Science Fire Safety Journal,* pp. 97-98, 2013.

[24] M.P, Feijter, "Kort Verslag Brandonderzoek Parkeergarage Ruitersweg 77," Efectis Nederland, 2007.

[25] RTS INFO, 14 december 2010. [Online]. Available: http://www.rts.ch/info/suisse/2796979-drame-de-gretzenbach-le-verdict-tombe.html.

[26] Heidsvoorzieningen, brand veilig, "Brand in parkeergarages De Brandweeracademie is Onderdeel Van Het Instituut Fysieke Veiligheid".

[27] ECCS, "Fire Safety in Open Car Parks", Modern Fire Engineering, Technical Committee 3,, Belgium: nº75, European Convention for Constructional Steelwork: Brussels, 1993, p. page 90.

[28] Haremza, Cécile, ROBUSTNESS OF OPEN CAR PARKS UNDER LOCALISED FIRE, 2014.

[29] Cwiklinski, C, ""Parcs de Stationnement en Superstructure Large Ment ventilés – Avis D'expert sur les scénarios d'incendie"," 2001.

[30] According to Ae-letter from Mr. R.HASS, and to: Garagenbau, Verordnung Nordrhein, Westfalen., 5 August 1992.

[31] Mr.GRUBITS, According to the letter from, The Building Code of Austrália 1990., CSIRO, 30 April 1991 and to Australia's model bulding code.

[32] According to the letter from Mr.VANDEVELD, Laboratorium voor aanwending der Brandstoffen en waimte-overdracht, Gent, 12 April 1991 and to the N.B.N. S21-201/S21-202..

[33] According to Mr.LODCKANEN, 3 meetings and to thie National Building Code of Finland: Fire Safety ofcar shelters instructions 1990, VTT , T.W.G. 3.

[34] According to Mr.BOUELLETTE, Sécurité contre l'incendie , Bâtiments d'habitadon , Texte règlementaire and to :, Edition 1987 ed.T. VI, Ed.

[35] Gazzetta Ufficiale delia Repubblica Italiana, Serie generais n° 38, February 1986.

[36] Garagenbau, According to :, Verordnung Nordrhein, Westfalen.

[37] Portaria nº1532/2008", Diário da República, 1ª série, N.º 250, 29 de Dezembro, 2008, pp. page 9050-9127.

[38] Decreto-Lei n º 220/2008, Diário da República, 1ª série, N.º 220, 2008, pp. 7903-7922.

[39] Esch, ArcelorMittal R&D, Open Steel Car Parks Design for the Polish Market, B. R. I. (ITB), Ed., Poznan University of Technology, 2011.

[40] C. Haremza, A.Santiago, L. Simões da Silva, "Design of Steel and Composite Open Car Parks Under Fire, Advanced Steel Construction.," vol. 9, pp. 321-339, 2013.

[41] "A New Temperature–time curve for Fire-resistance Analysis of Structures.," *Fire Safety.*

[42] Olov Sundström, Sarah Gustavsson, Simple Temperature Calculation Models for Compartment Fires..

[43] Joyeux, D., Kruppa J., Cajot L.G., Schleich J.B., van de Leur P., Twilt L., ""Demonstration of Real Fire Tests in Car Parks and High Buildings"," 2002.

[44] C. Haremza, A. Santiago and L. Simões da Silva, "DESIGN OF STEEL AND COMPOSITE OPEN CAR PARKS UNDER FIRE," January 2013.

[45] EN 1991-1-2, Eurocode 1: Actions on structures - Part 1-2: General actions -Actions on structures exposed to fire, November 2002.

[46] Quintiere, James G., Compartment Fires-Fundamentals of Fire Phenomena, 2006 John Wiley & Sons, Ltd ISBN.

[47] in *CEN - EN 1993-1-2 ;"Eurocode 3: Design of Steel Structures - Part 1-2: General Rules - Structural Fire Design"standards*, Brussels, April 2005.

[48] Dr.Deepa A Sinha, "Thermal Properties of Concrete," *PARIPEX - INDIAN JOURNAL OF RESEARCH,* vol. 3, no. 2, Feb 2014.

[49] CEN - EN 1992-1-2; “Eurocode 2: Design of Concrete Structures - Part 1-2: General Rules Structural Fire Design., Brussels: European standards, 2004.

[50] Viall, Robert, "FIRE MODELING IN FLUENT," April 24, 2008.

[51] Knop, Nathaniel Michael, "Thermal Analysis of a Fireplace using ANSYS," 2009.

ANNEX A : RESULTS FROM HESKESTAD AND HASEMI METHOD

1- HEB 140 (class 3)

Figure 64 shows the temperature of the secondary beam (HEB 140) in different radial positions R=0,1,...,5 m, for car class 3.

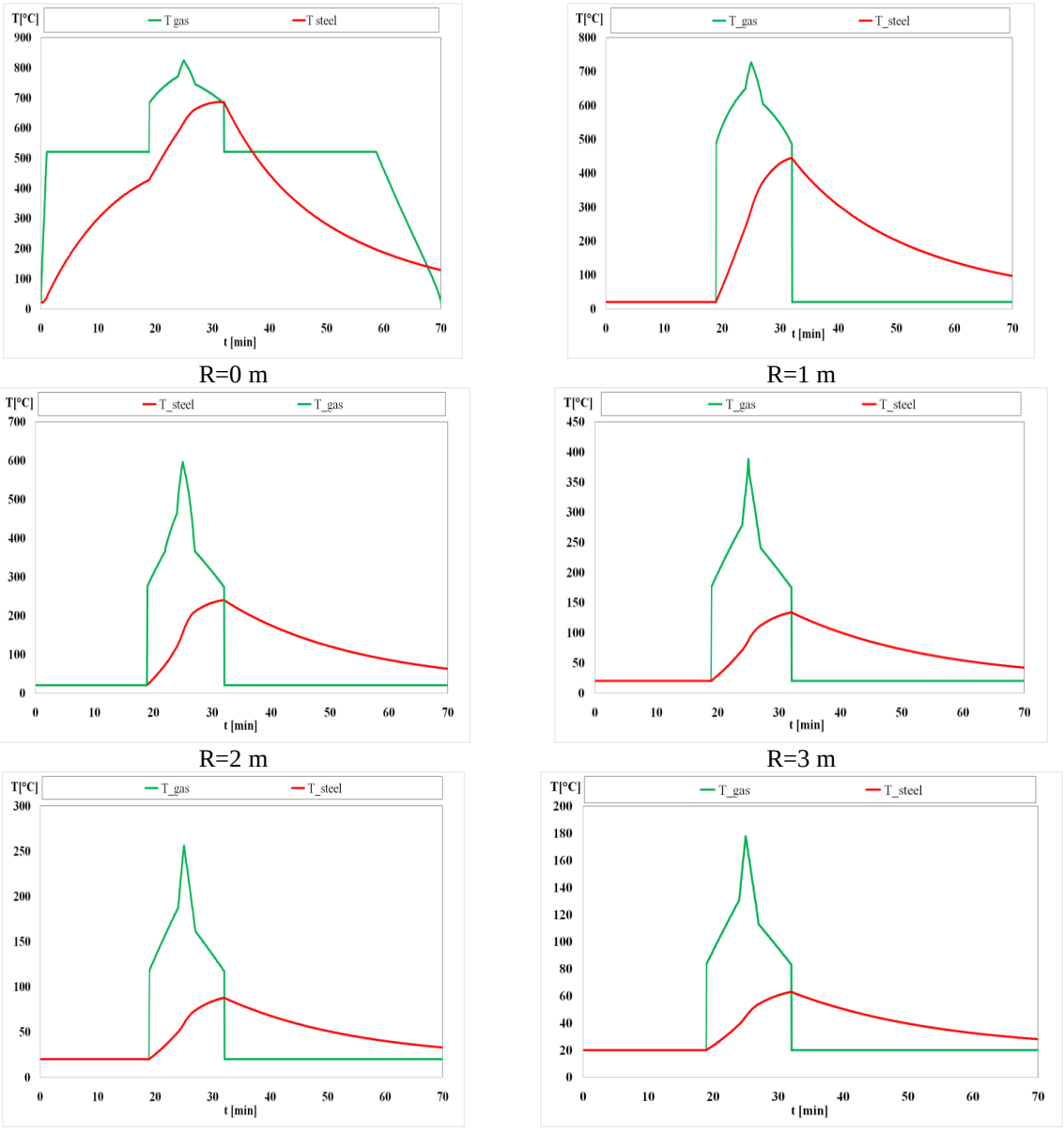

Figure 64 - Flame and steel temperature of different positions from the fire axis.

2- IPEA 600

Figure 65 shows the temperature of the secondary beam (IPEA 600) in different radial positions R=0,1,...,5 m, for car class 3.

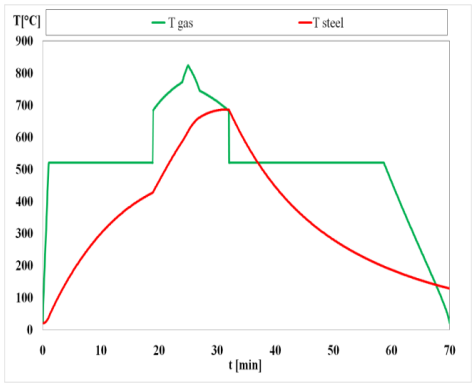

R=0 m

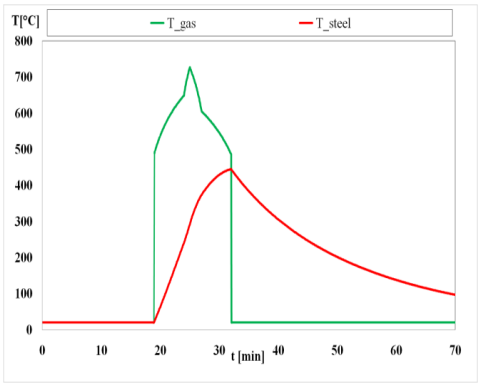

R=1 m

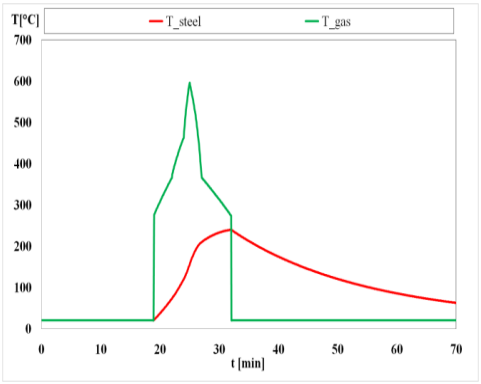

R=2 m

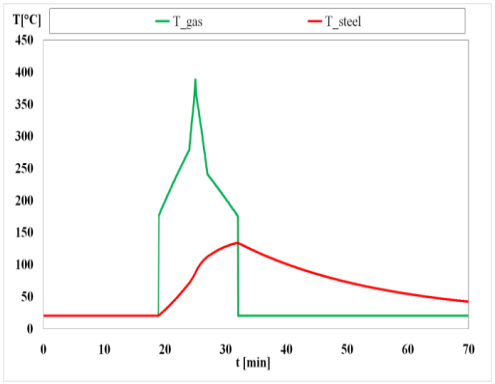

R=3 m

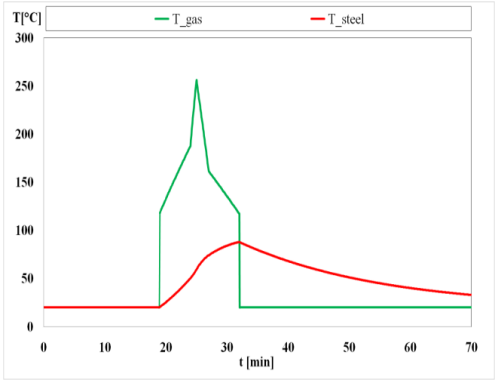

R=4 m

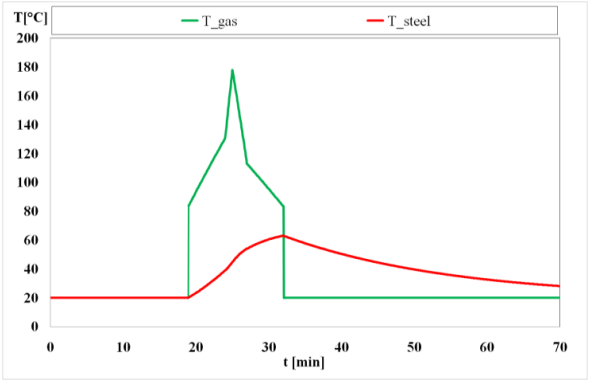

R=5 m

Figure 65 - Flame and steel temperature of different positions from the fire axis.

3- IPEA 550

Figure 66 shows the temperature of the secondary beam (IPEA 550) in different radial positions R=0,1,...,5 m, for car class 3.

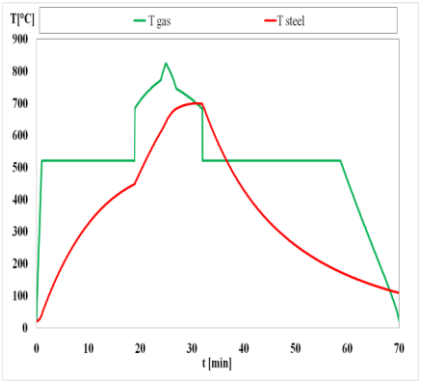

R=0 m

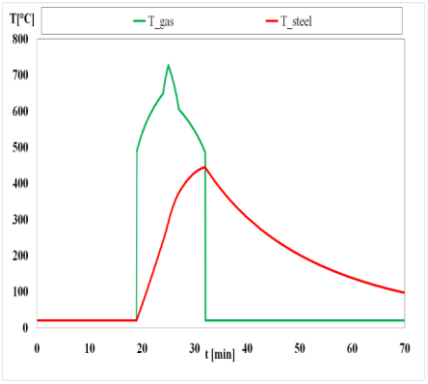

R=1 m

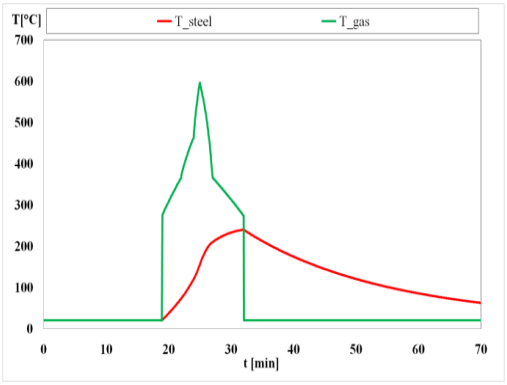

R=2 m

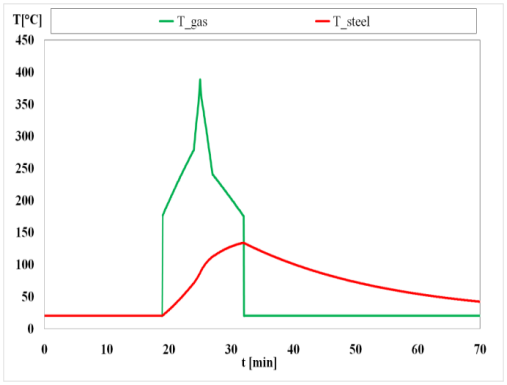

R=3 m

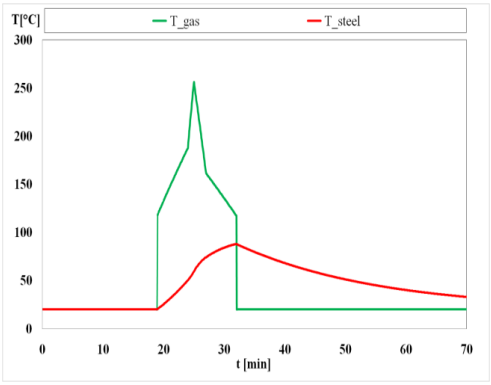

R=4 m

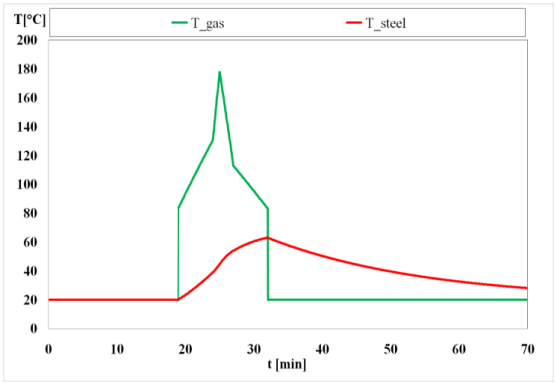

R=5 m

Figure 66 - Flame and steel temperature of different positions from the fire axis.

4- IPEA 450

Figure 67 shows the temperature of the secondary beam (IPEA 450) in different radial positions R=0,1,...,5 m, for car class 3.

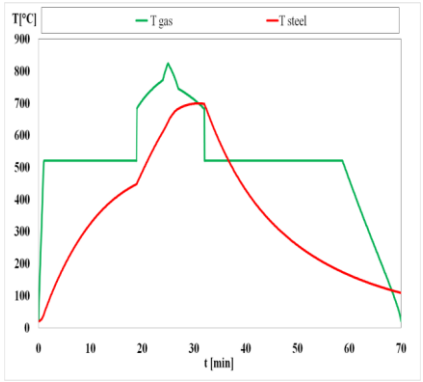

R=0 m

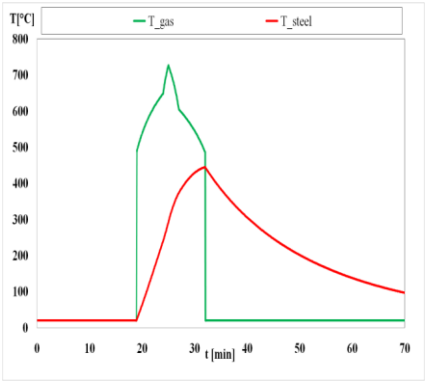

R=1 m

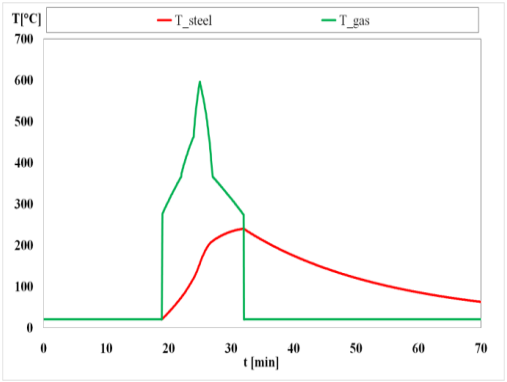

R=2 m

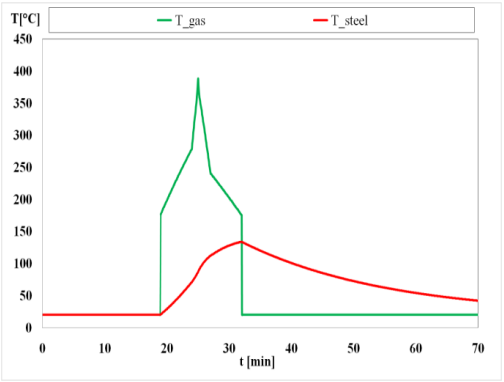

R=3 m

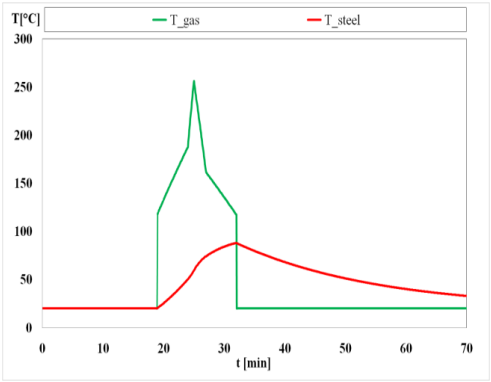

R=4 m

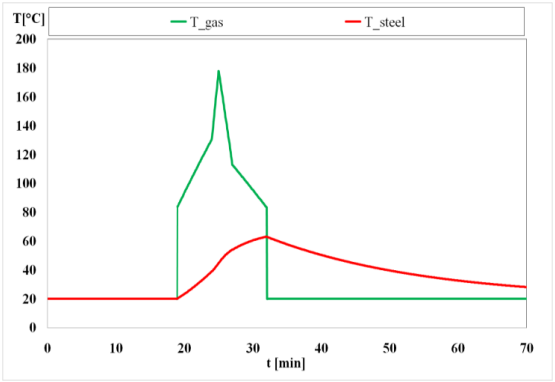

R=5 m

Figure 67 - Flame and steel temperature of different positions from the fire axis.

ANNEX B : RESULTS FROM ELEFIR_EN

The program allows the user to choose the section type, the fire exposure, type of fire protection and the heating curve. All of these options are explained below. Typical cross sectional shapes include: HD, HE HL, HP, IPE, UB, UC, W, L, RHS and CHS from a database or user-defined dimensions can be included.

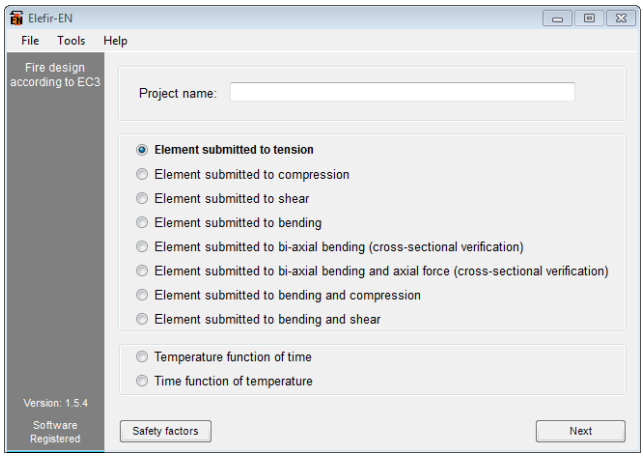

Figure 68 - Elefir-EN main menu of mechanical response.

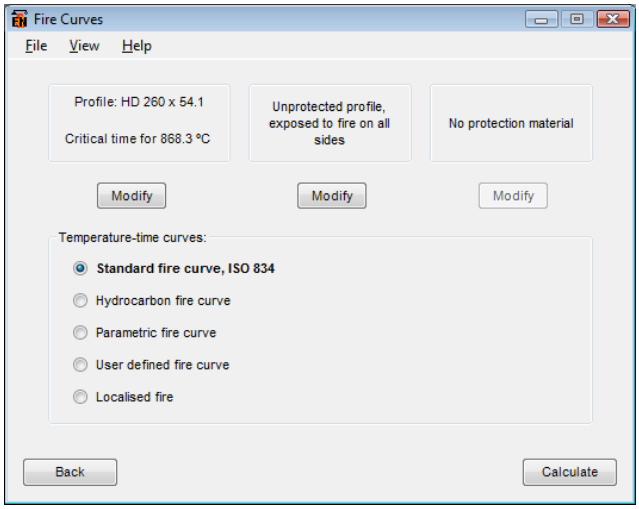

Figure 69 - Elefir-EN main menu of thermal response.

1- HEB 140

Figure 70 shows the temperature of the secondary beam HEB 140) in the relative position R=0 m, for different car classes, the maximum temperature is 880.20 ºC .

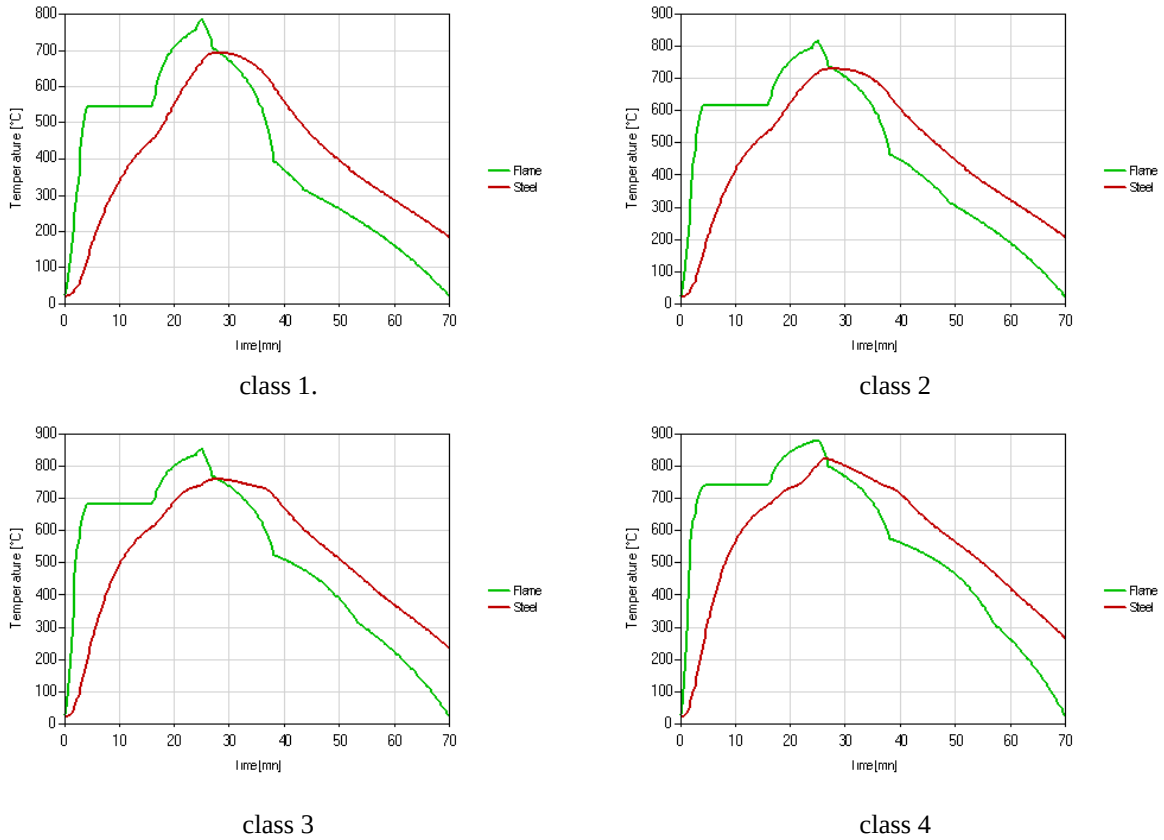

class 1. class 2

class 3 class 4

Figure 70 - Flame and steel temperature for all car classes.

Figure 71 the gas temperature of the fire event for burning a car class 3 and the temperature of the secondary beam are presented for different positions relative to the flame axis (parameter R= 0 m, 1 m,…,5 m), the maximum temperature is : 858.7 ºC.

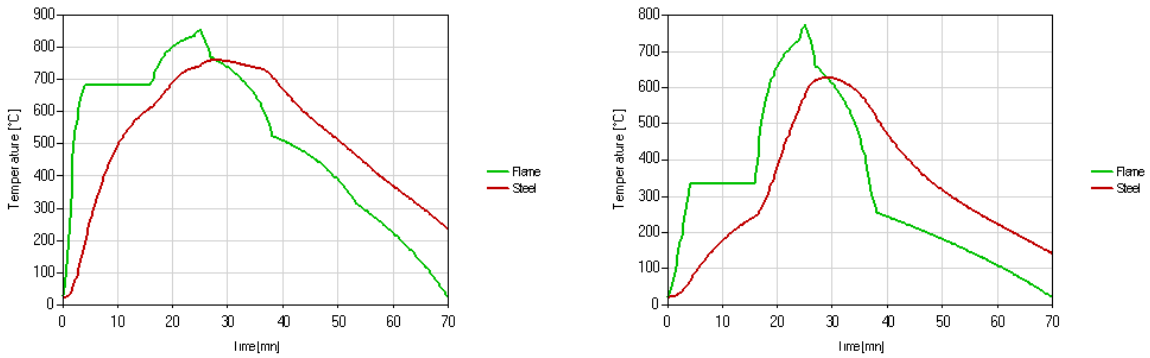

R=0 m

R=1 m

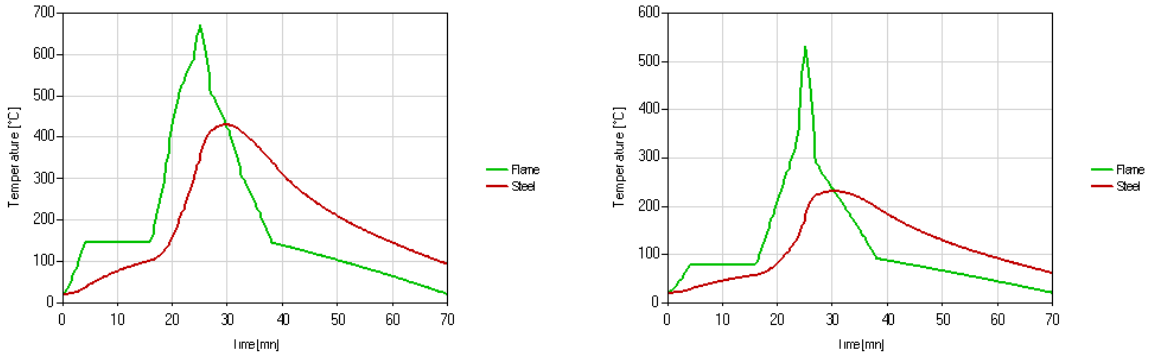

R=2 m

R=3 m

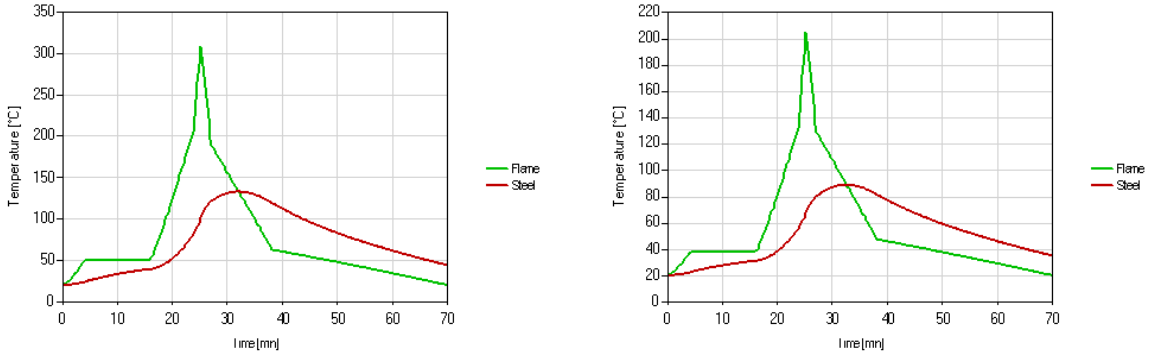

R=4 m

R=5 m

Figure 71 - Flame and steel temperature of different radial positions.

Figure 72 represents the gas temperature during the fire event for different position to the fire axis . The maximum temperature is expected to be achieved after the maximum HRR has been reached (25 minutes).

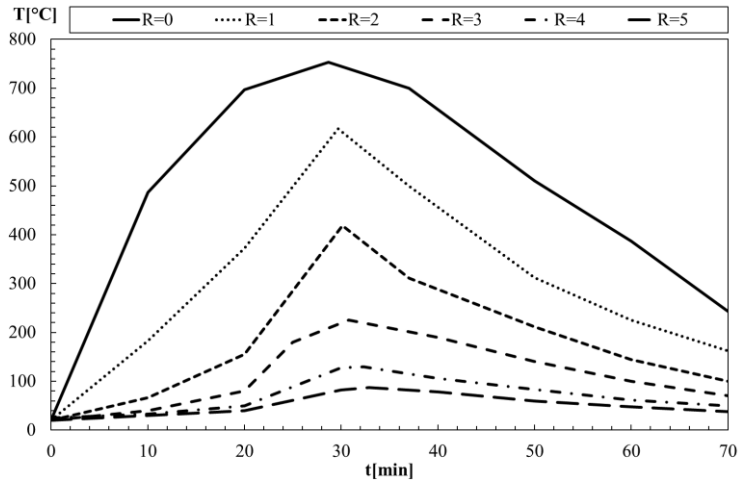

Figure 72 - The gas Temperature for car class 3 .

Figure 73 represents the steel temperature during the fire event. The maximum temperature is expected to be achieved after the maximum HRR has been reached (25 minutes).

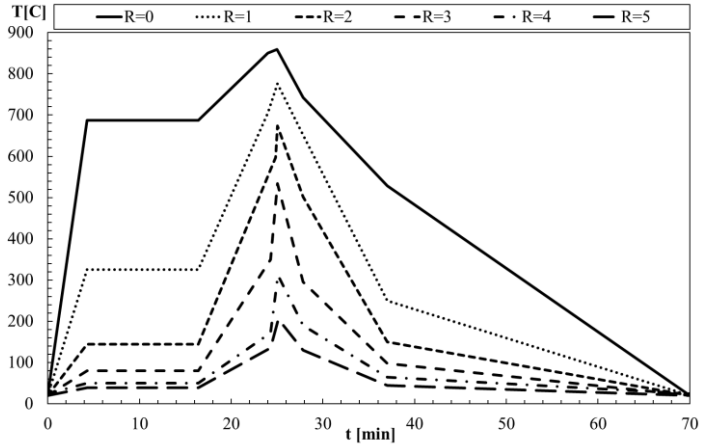

Figure 73 - The steel temperature for car class 3 .

2- IPE A 600

Figure 74 shows the temperature of the secondary beam (IPE A 600) in the relative position R=0 m, for different car classes, the maximum temperature is 880.20 ºC .

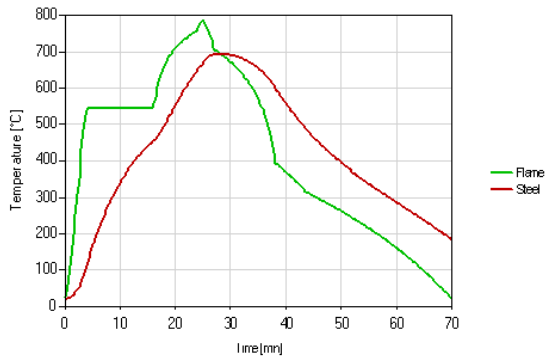

class 1.

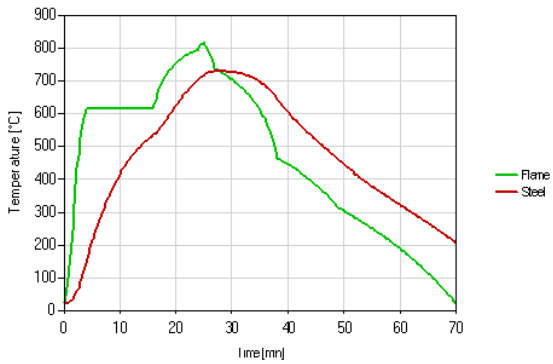

class 2

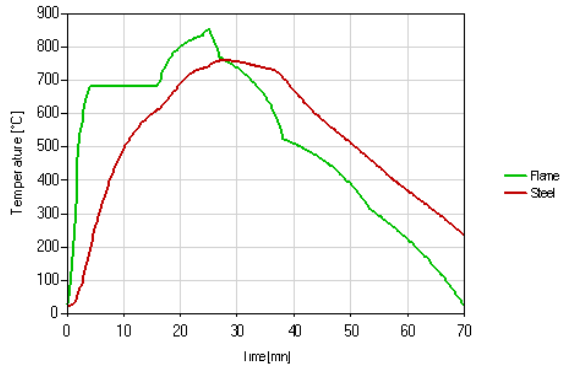

class 3

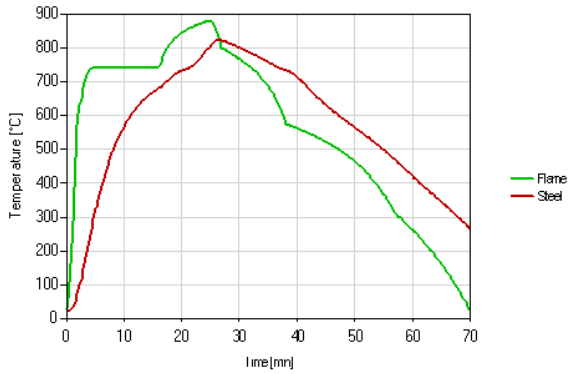

class 4

Figure 74 - Flame and steel temperature for all car classes.

Figure 75 the gas temperature of the fire event for burning a car class 3 and the temperature of the secondary beam are presented for different positions relative to the flame axis (parameter R= 0 m, 1 m,…,5 m), the maximum temperature is : 858.7 ºC.

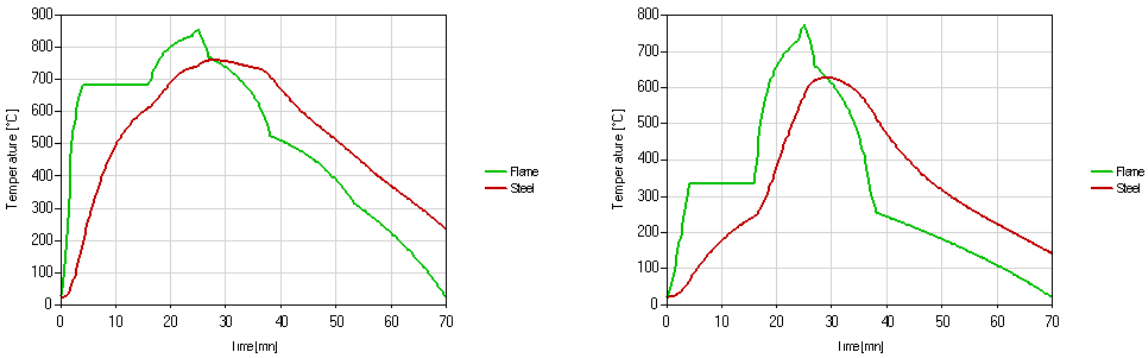

R=0 m

R=1 m

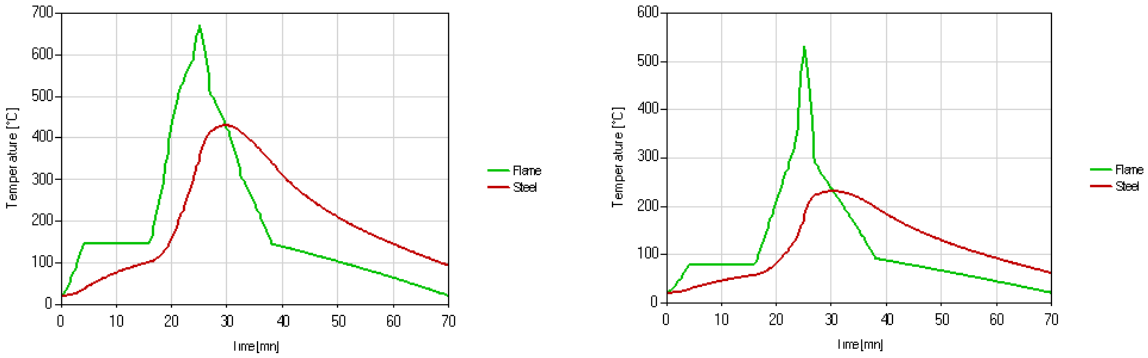

R=2 m

R=3 m

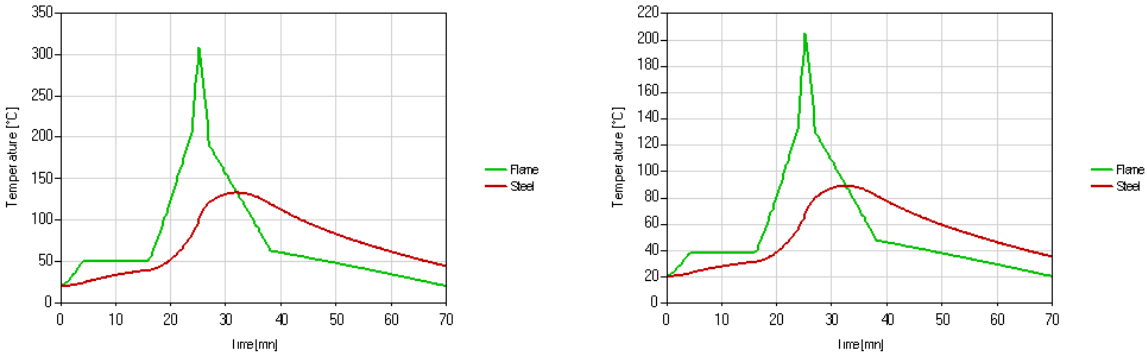

R=4 m

R=5 m

Figure 75 - Flame and steel temperature of different radial positions from the fire axis.

Figure 76 represents the gas temperature during the fire event for different position to the fire axis . The maximum temperature is expected to be achieved after the maximum HRR has been reached (25 minutes).

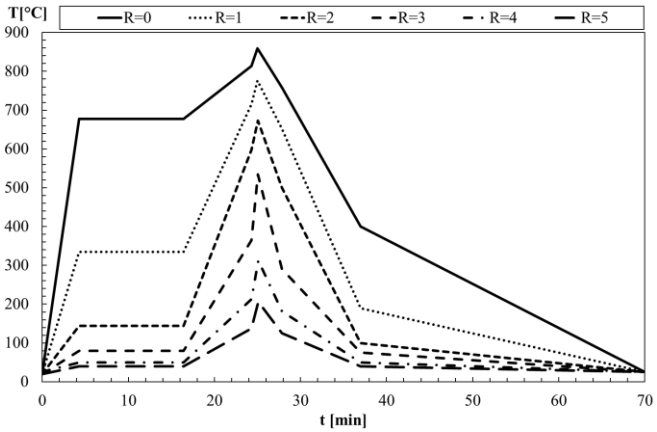

Figure 76 - The gas Temperature for car class 3 .

Figure 77 represents the steel temperature during the fire event. The maximum temperature is expected to be achieved after the maximum HRR has been reached (25 minutes).

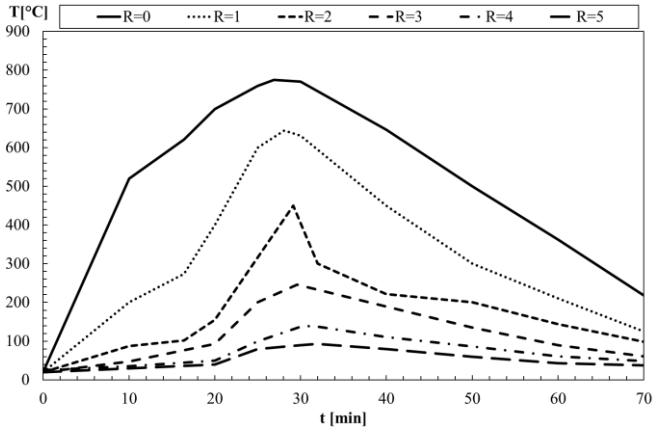

Figure 77 - The steel temperature for car class 3 .

3- IPE A 550

Figure 78 shows the temperature of the secondary beam (IPE A 550) in the relative position R=0 m, for different car classes, the maximum temperature is 880.20 ºC .

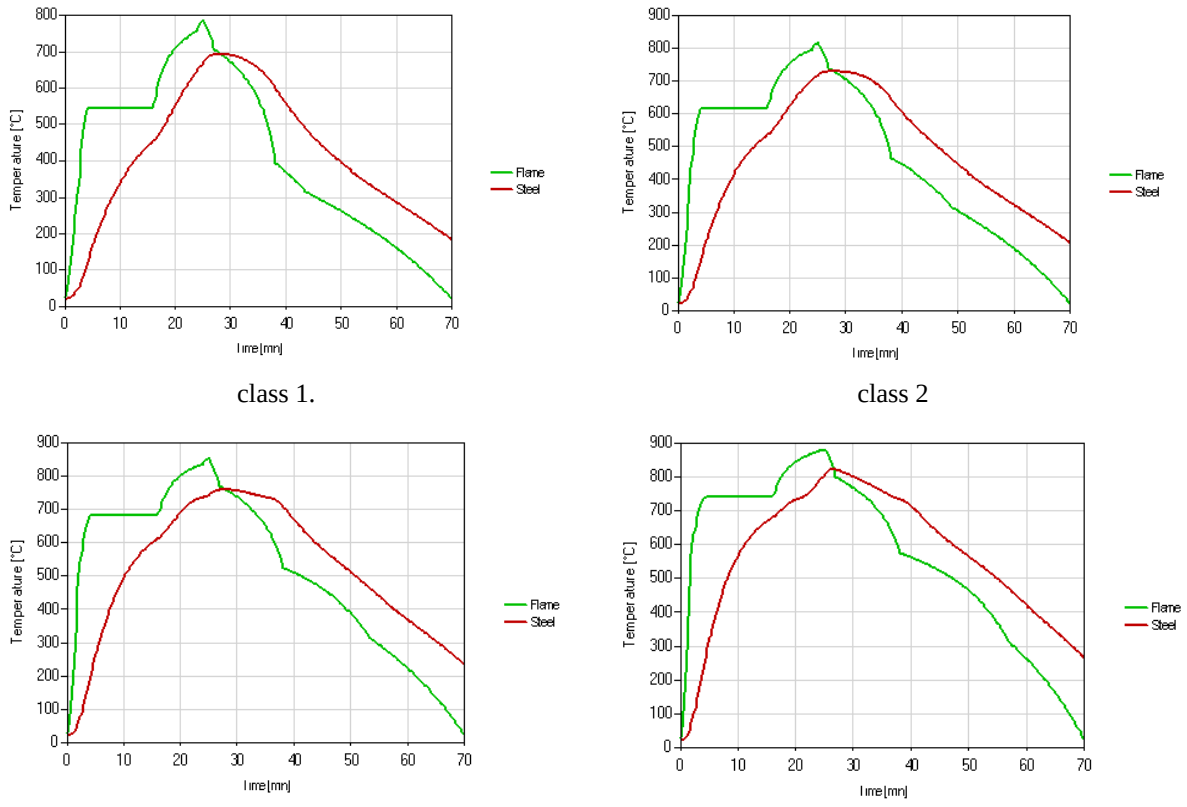

class 1. class 2

class 3 class 4

Figure 78 - Flame and steel temperature for all car classes.

Figure 79 shows the gas temperature of the fire event for burning a car class 3 and the temperature of the secondary beam are presented for different positions relative to the flame axis (parameter R= 0 m, 1 m,…,5 m), the maximum temperature is : 858.7 ºC.

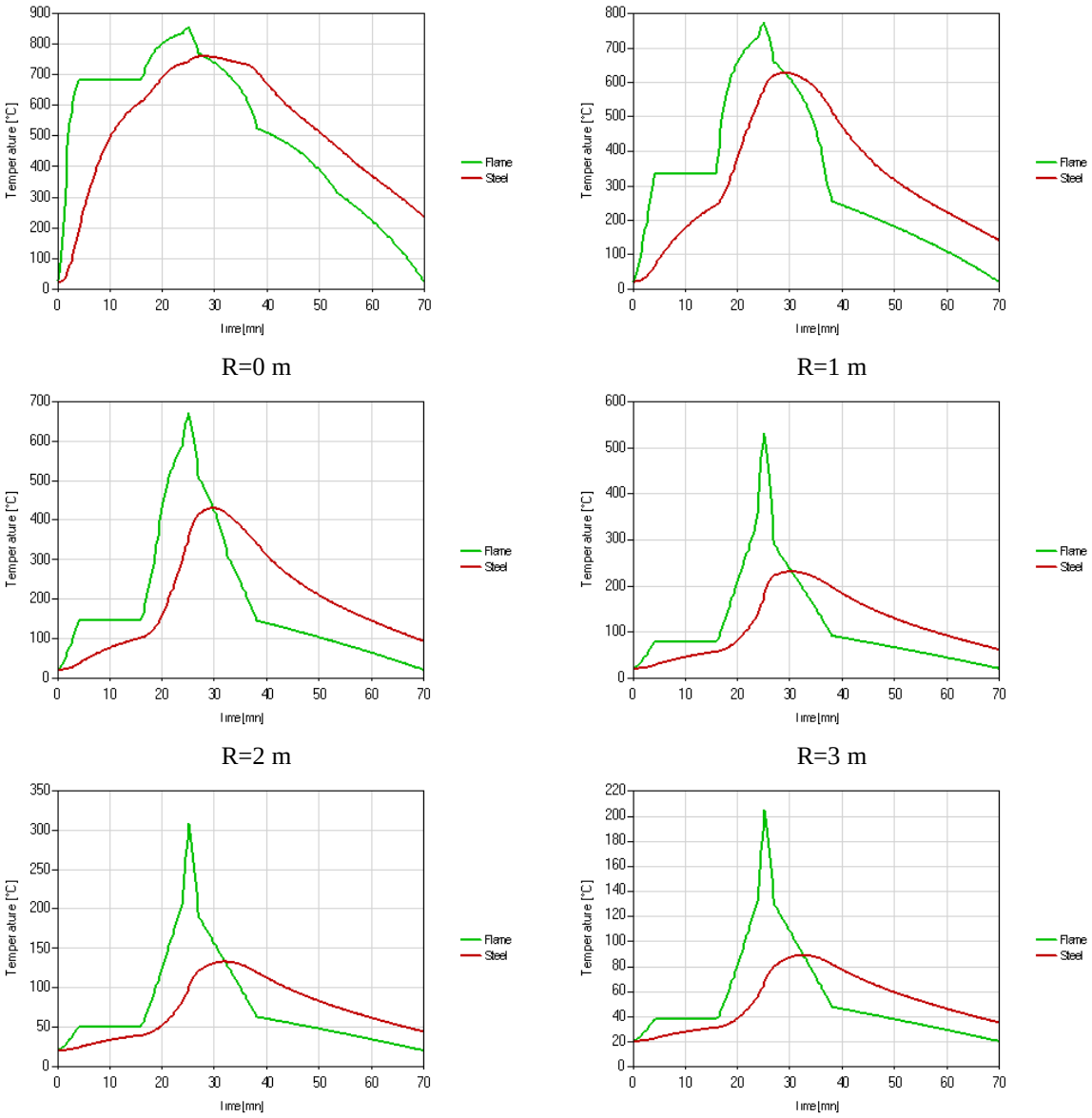

Figure 79 - Flame and steel temperature of different radial positions from the fire axis.

Figure 80 represents the gas temperature during the fire event for different position to the fire axis . The maximum temperature is expected to be achieved after the maximum HRR has been reached (25 minutes).

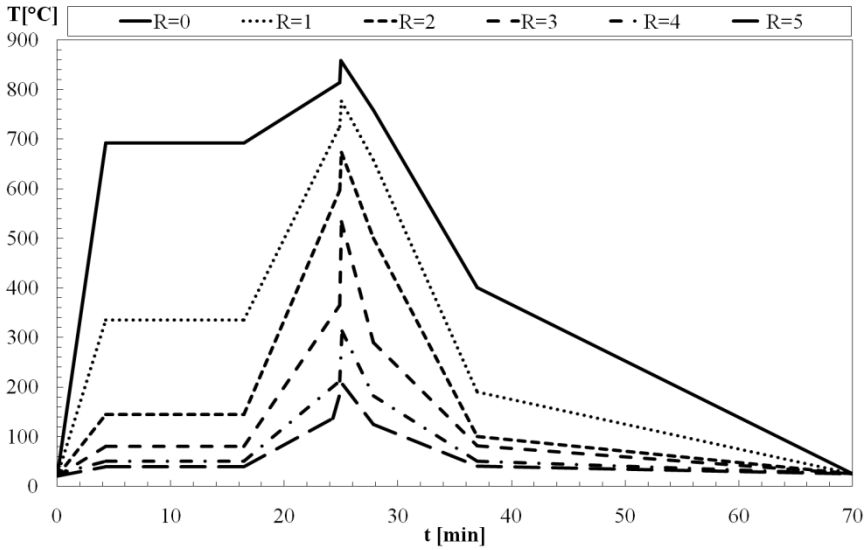

Figure 80 - The gas Temperature for car class 3 .

Figure 81 represents the steel temperature during the fire event. The maximum temperature is expected to be achieved after the maximum HRR has been reached (25 minutes).

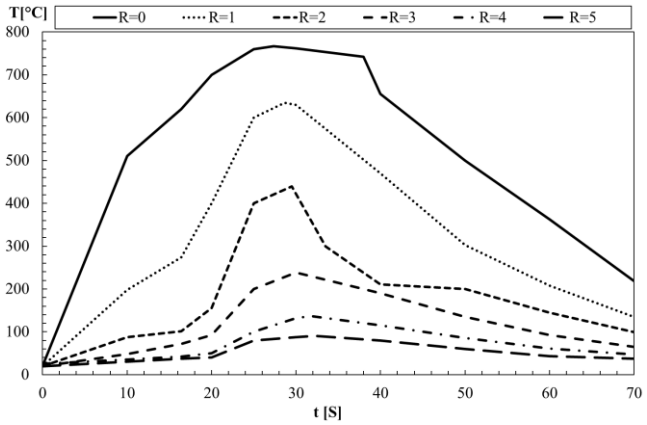

Figure 81 - The steel temperature for car class 3 .

4- IPE A 450

Figure 82 shows the temperature of the secondary beam (IPE A 450) in the relative position R=0 m, for different car classes, the maximum temperature is 880.20 ºC .

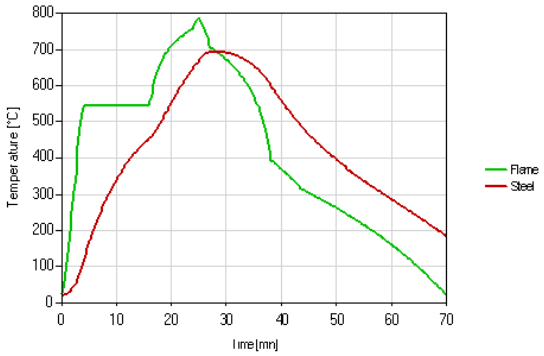

class 1.

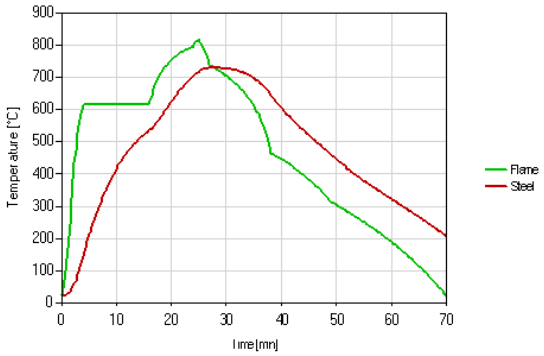

class 2

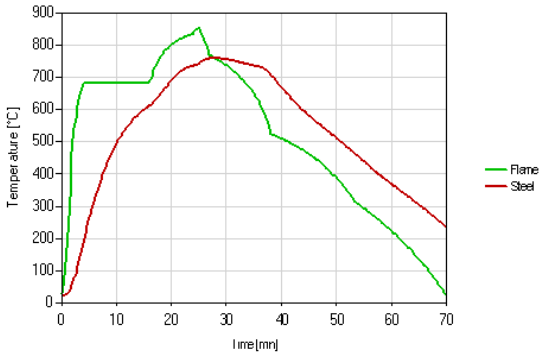

class 3

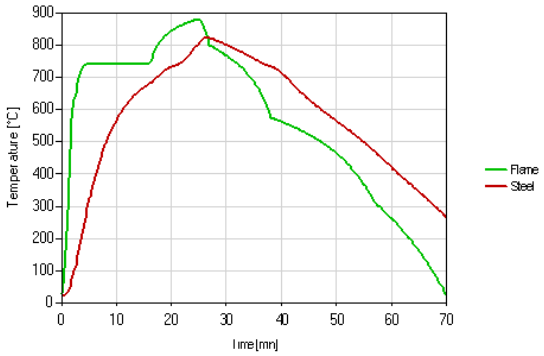

class 4

Figure 82 - Flame and steel temperature for all car classes.

The gas temperature of the fire event for burning a car class 3 and the temperature of the secondary beam are presented in Figure 83 for different positions relative to the flame axis (parameter R= 0 m, 1 m,…,5 m), the maximum temperature is : 858.7 ºC.

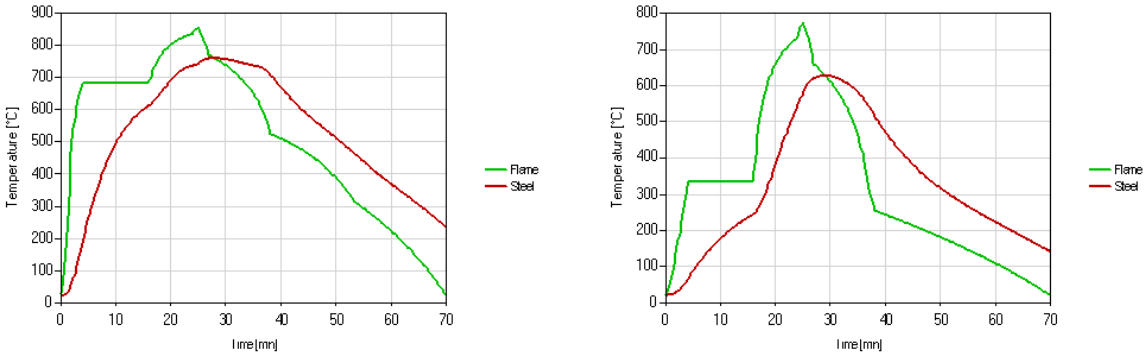

R=0 m R=1 m

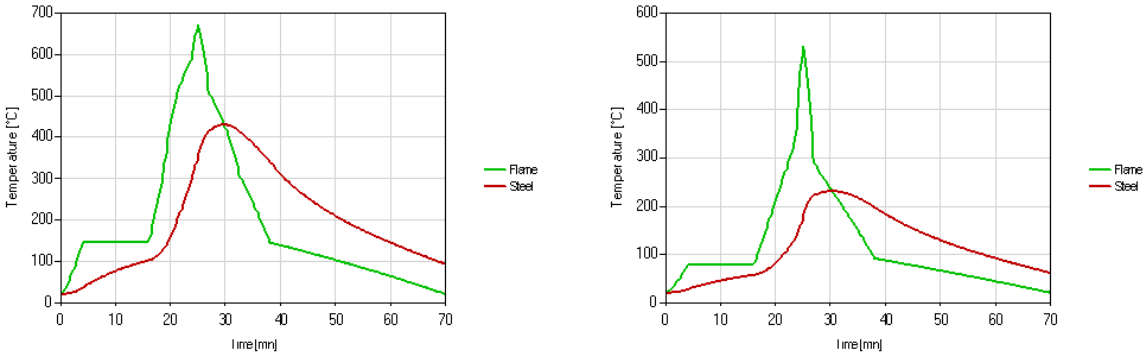

R=2 m R=3 m

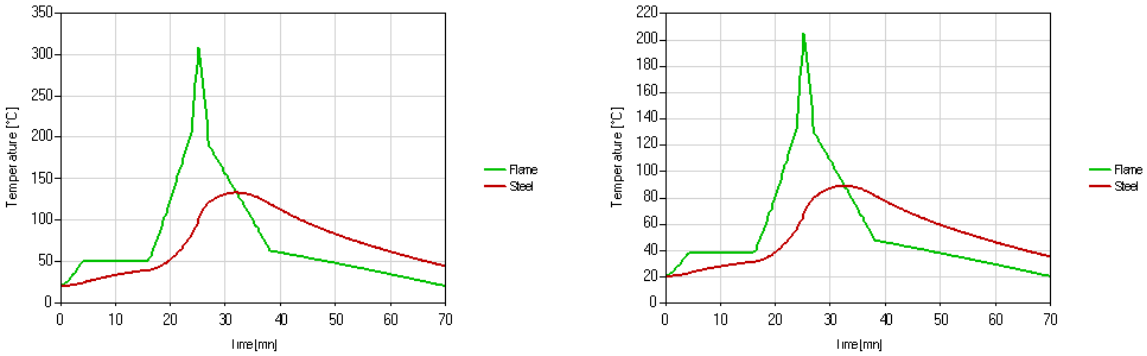

R=4 m R=5 m

Figure 83 - Flame and steel temperature of different radial positions .

Figure 83 represents the gas temperature during the fire event for different position to the fire axis . The maximum temperature is expected to be achieved after the maximum HRR has been reached (25 minutes).

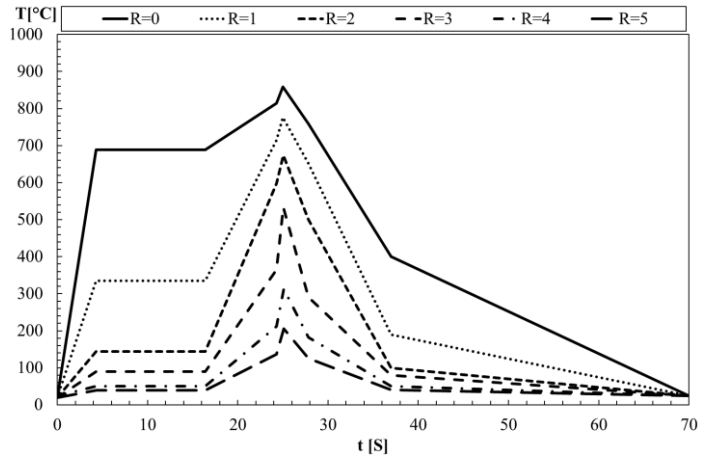

Figure 84 - The gas Temperature for car class 3 .

Figure 85 represents the steel temperature during the fire event. The maximum temperature is expected to be achieved after the maximum HRR has been reached (25 minutes).

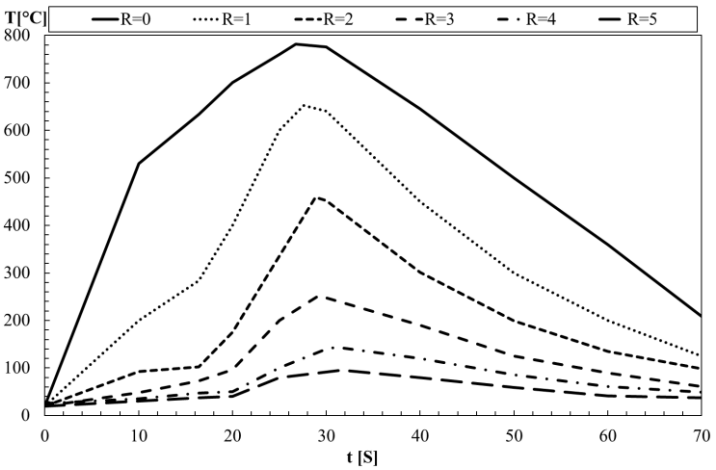

Figure 85 - The steel temperature for car class 3 .

ANNEX C : RESULTS FROM ANSYS FLUENT

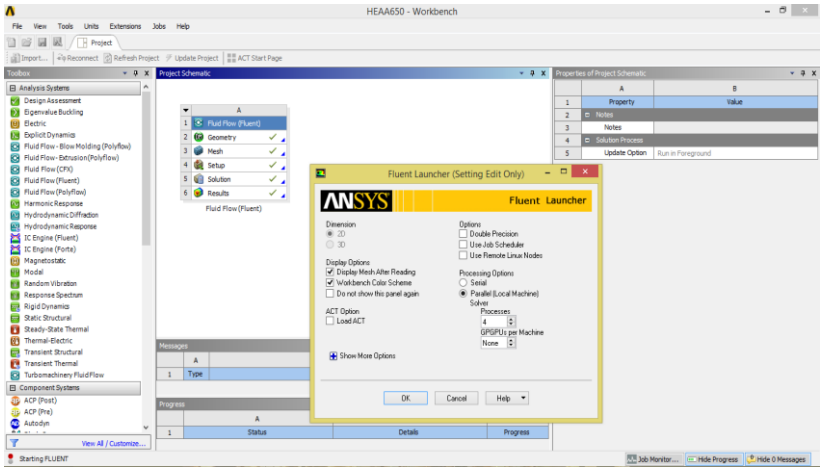

Figure 86 - Starting FLUENT simulation.

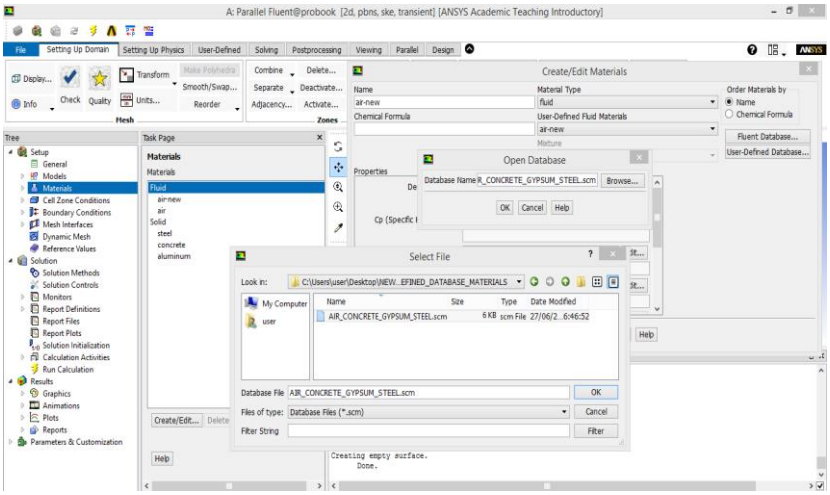

Figure 87 - Uploading of the material properties (thermal and fluid).

Table 6 presents the thermal and fluid properties of the air. This data is included in the local data base, using piecewise approximation data previously defined, based on the number of data points that are representative of the variation of the material property.

Table 6 - Air properties.

Data Points	[ºC] Temp	[K] Temp	[W/mK] Thermal conductivity	[kg/m^3] density	[kg/ms] viscosity	[J/kgK] Specific heat
1	20	293	0.025	1.2050	0.0000181	1.006
2	30	303	0.026	1.1650	0.0000186	1.006
3	60	333	0.028	1.0600	0.0000200	1.008
4	100	373	0.032	0.9460	0.0000217	1.011
5	200	473	0.039	0.7460	0.0000257	1.025
6	300	573	0.045	0.6160	0.0000293	1.045
7	500	773	0.056	0.4560	0.0000355	1.093
8	1000	1273	0.076	0.2770	0.0000479	1.185
9	1200	1473	0.076	0.2770	0.0000521	1.185

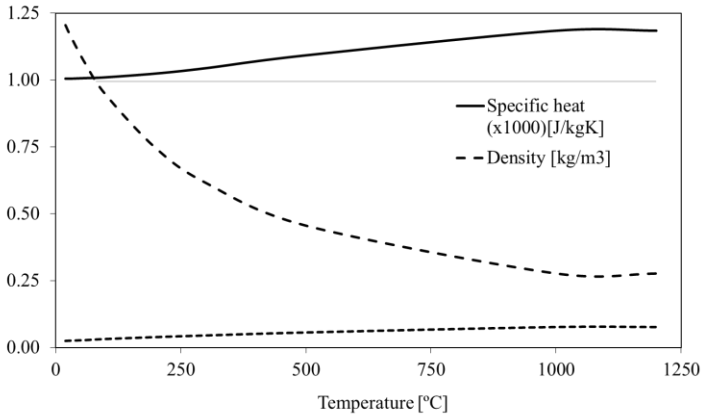

Figure 88 - Thermal properties for the fluid material (Air).

Table 7 presents the thermal properties for the solid region identified by: Concrete.

Table 7 - Concrete thermal properties .

Data Points	[ºC] Temp	[K] Temp	[J/kgK] Specific heat	[W/mK] Thermal conductivity	[kg/m^3] Specific mass
1	20	293	900	1.95	2300
2	100	333	900	1.77	2300
3	101	358	2020	1.76	2300
4	115	370	2020	1.73	2300
5	200	373	1000	1.55	2254
6	300	396.5	1050	1.36	2220
7	400	413	1100	1.19	2185
8	500	421	1100	1.04	2165
9	600	673	1100	0.91	2145
10	700	882	1100	0.81	2125
11	800	933	1100	0.72	2105
12	900	942.5	1100	0.66	2084
13	1000	958	1100	0.62	2064
14	1100	1072	1100	0.60	2044
15	1200	1473	1100	0.60	2024

Table 8 presents the thermal properties for the solid region identified by : Steel .

This data is included in the local data base, using piecewise approximation data previously defined, based on the number of data points that are representative of the variation of this material property.

Table 8 - Steel properties .

Data Points	[ºC] Temp	[K] Temp	[W/mK] Thermal conductivity (upper)	[J/kgK] Specific heat	[kg/m^3] Specific mass
1	20	293	53.33	440	7850
2	100	373	50.67	488	7850
3	200	473	47.34	530	7850
4	300	573	44.01	565	7850
5	400	673	40.68	606	7850
6	500	773	37.35	667	7850
7	600	873	34.02	760	7850
8	650	923	32.36	814	7850
9	700	973	30.69	1008	7850
10	730	1003	29.69	2291	7850
11	735	1008	29.52	5000	7850
12	750	1023	29.03	1483	7850
13	800	1073	27.30	803	7850
14	900	1173	27.30	650	7850
15	1000	1273	27.30	650	7850
16	1100	1373	27.3	650	7850
17	1200	1473	27.3	650	7850

1- HEAA 650 (R=2 m)

The temperature of the secondary beam (HEAA 650) in the relative position R=2 m, for different car classes(car class 1,2,3 and 4/5) as it shown in Figure 89.

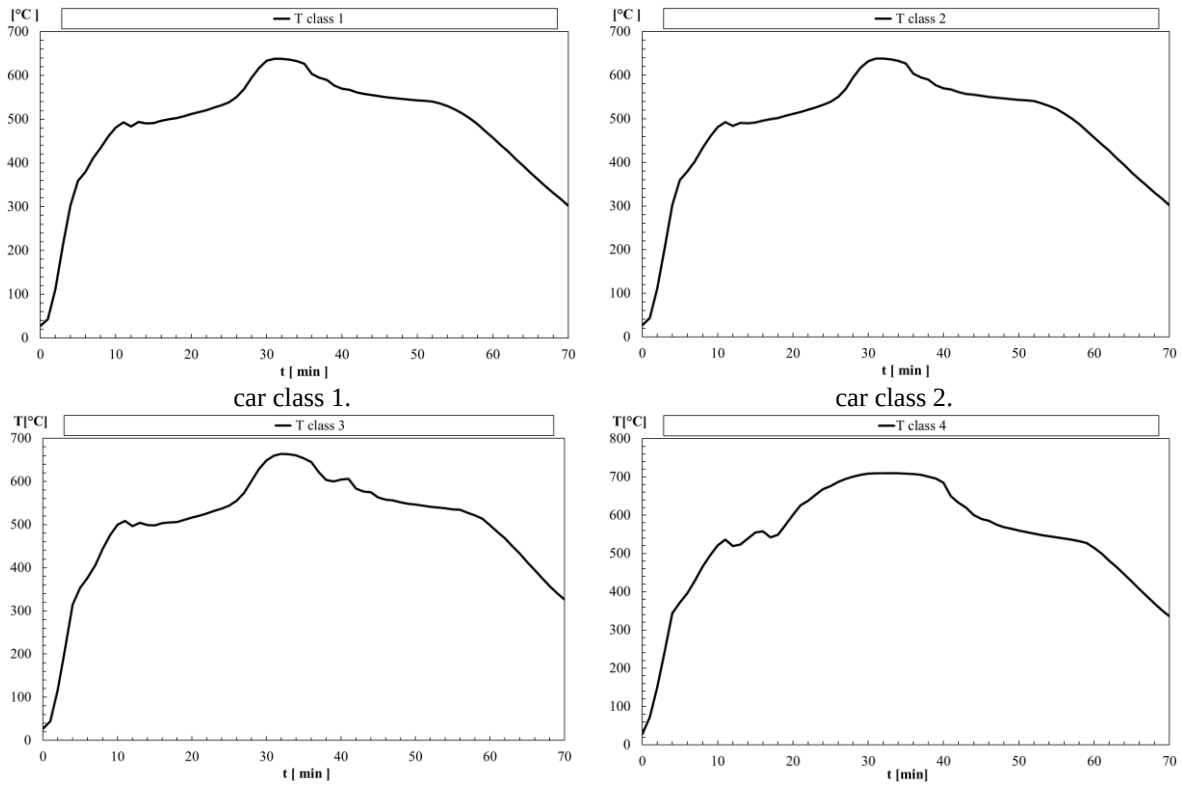

car class 1. car class 2.

car class 3. car class 4/5.

Figure 89 - Steel temperature for car class 1,2,3 and 4/5.

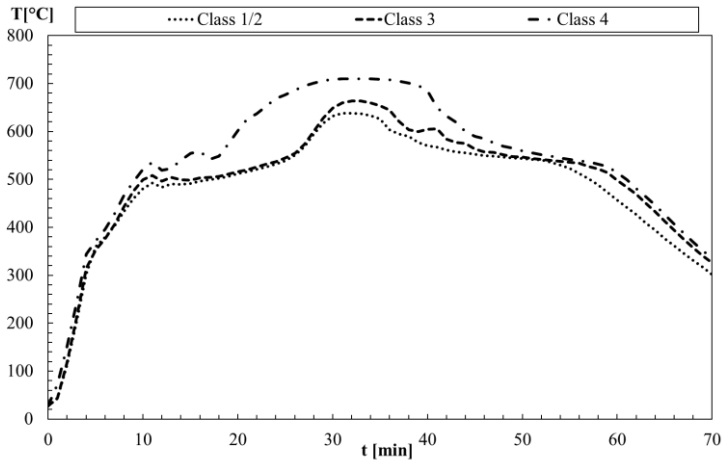

Figure 90 - The evolution of Steel temperature in R=2 m for different car class.

2- HEB 140 (R=0 m)

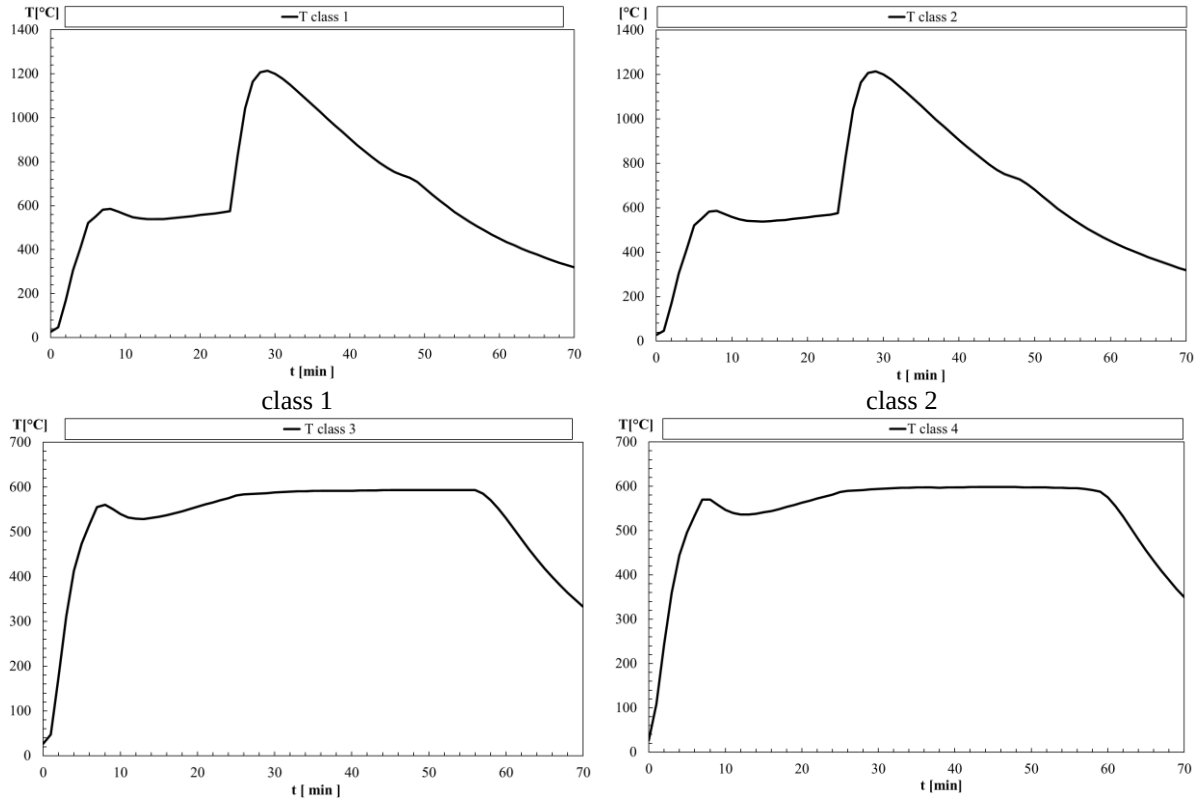

class 1 class 2

class 3 class 4/5.

Figure 91 - Steel temperature for different car classes.

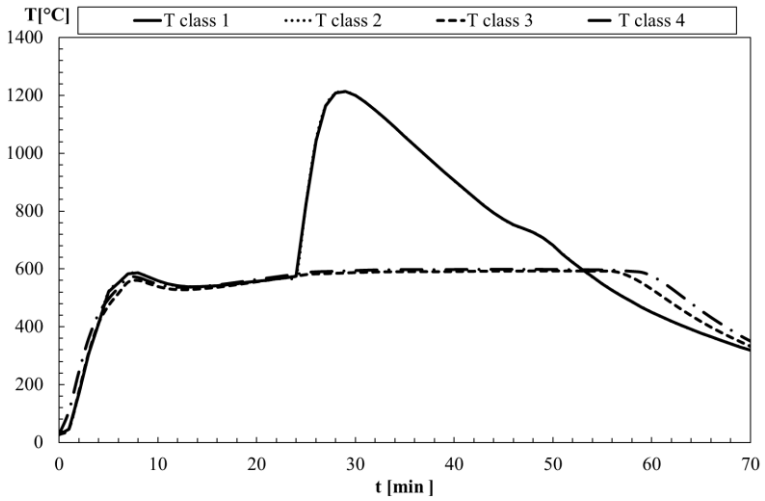

Figure 92 - The evolution of Steel temperature in R=0 for different car class.

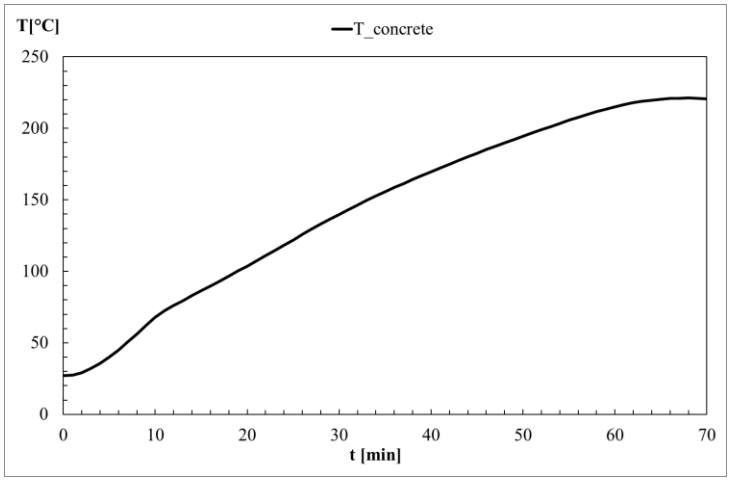

Figure 93 - Concrete temperature for car class 3.

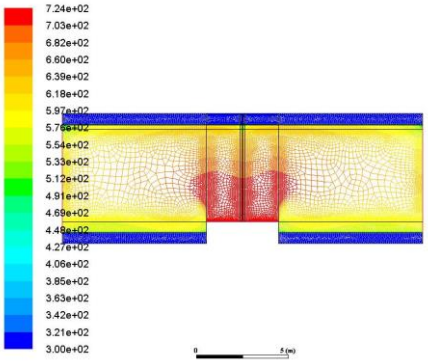

t= 0 min

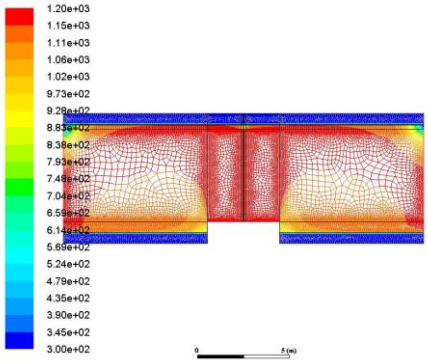

t= 4 min

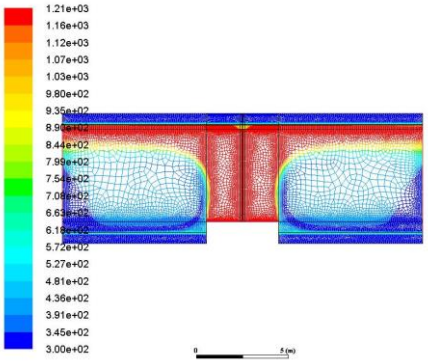

t= 16 min

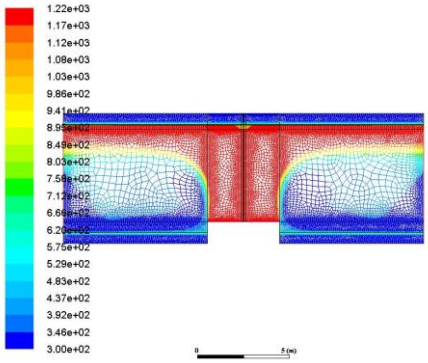

t= 25 min

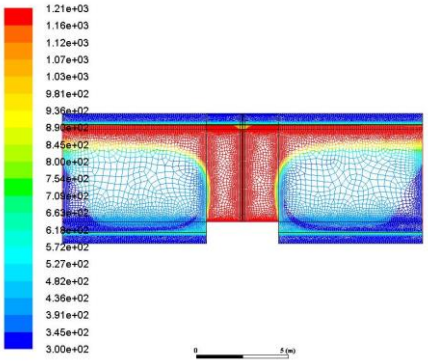

t= 38 min

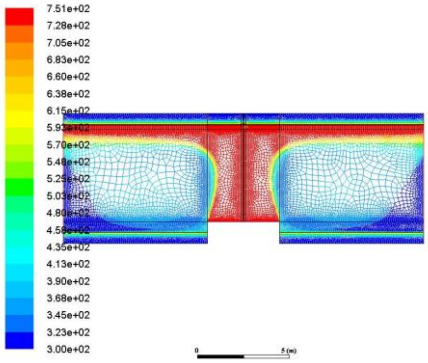

t= 70 min

Figure 94 - Temperature in different times using FLUENT, R=0.

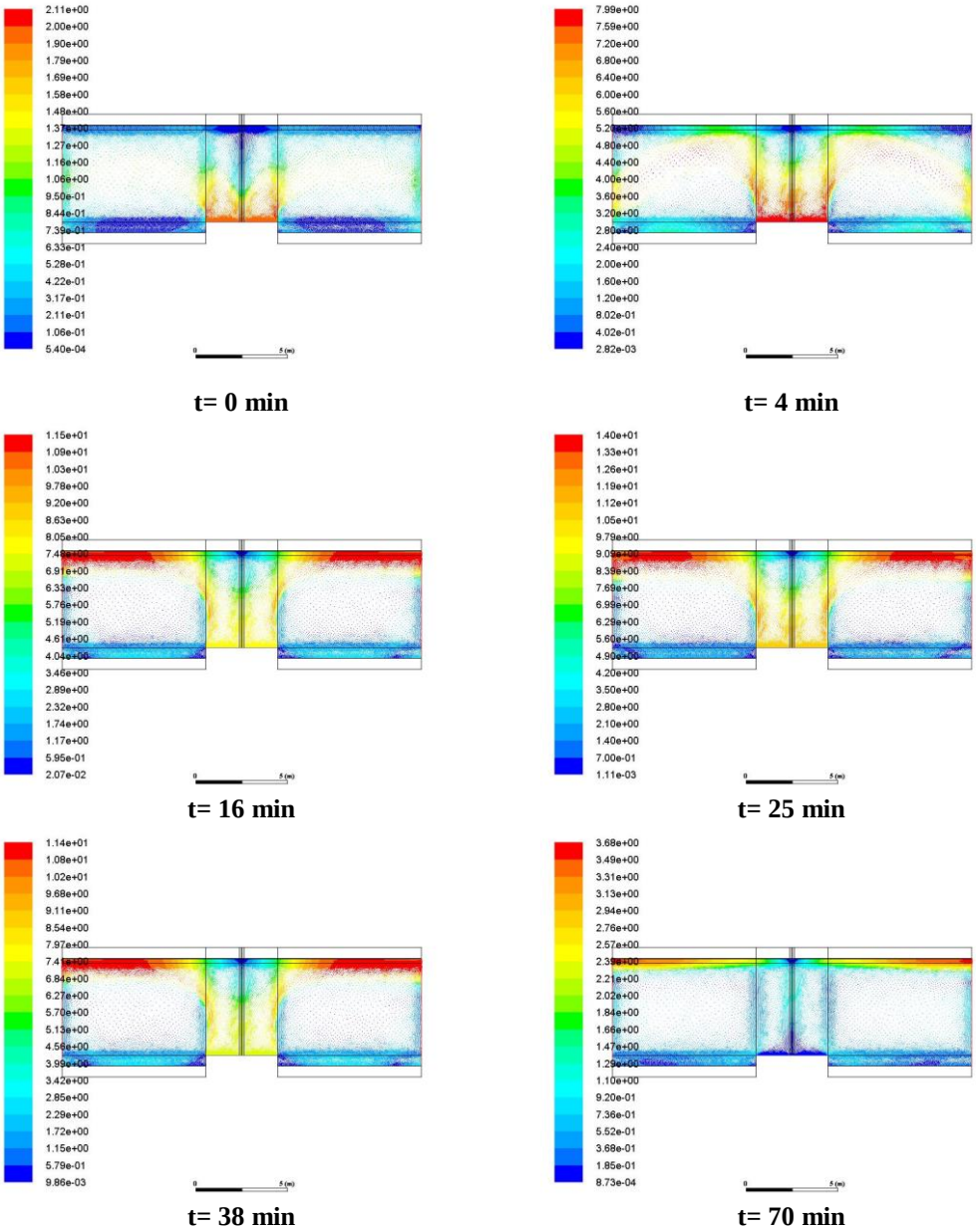

Figure 95 - Velocity in different times for R=0 m using Fluent.

3- Boundary conditions used in ANSYS FLUENT

We used the formulas of HRR in CFAST, we took this condition at the basement of the car, and we pick this boundary condition and we apply it in FLUENT.

3.1- Car class 1

3.1.1- Surrounding gas temperature

$0 \leq tim \leq 120$ [°C]	$T = 273{,}15 + (7{,}5166 \times tim)$	Eq 37
$12 < tim \leq 1500$ [°C]	$T = 273{,}15 + (922 + 0{,}00942 \times (tim - 120))$	Eq 38
$1500 < tim \leq 2880$ [°C]	$T = 273{,}15 + (935 - 0{,}00652 \times (tim - 1500))$	Eq 39
$2880 < tim \leq 4200$ [°C]	$T = 273{,}15 + (926 - 0{,}6833 \times (tim - 2880))$	Eq 40

3.1.2- Surrounding gas velocity

$0 \leq tim \leq 240$ [°C]	$V = 0{,}02916 \times tim$	Eq 41
$240 < tim \leq 960$ [°C]	$V = 7$	Eq 42
$960 < tim \leq 1440$ [°C]	$V = 7 + 0{,}00458 \times (tim - 960)$	Eq 43
$1440 < tim \leq 1500$ [°C]	$V = 9{,}2 + 0{,}0133 \times (tim - 1440)$	Eq 44
$1500 < tim \leq 1620$ [°C]	$V = 10 - 0.01 \times (tim - 1500)$	Eq 45
$1620 < tim \leq 2280$ [°C]	$V = 8{,}8 - 0{,}0033 \times (tim - 1620)$	Eq 46
$2280 < tim \leq 3180$ [°C]	$V = 6{,}6 - 0{,}0008 \times (tim - 2280)$	Eq 47
$3180 < tim \leq 4200$ [°C]	$V = 5{,}8 –{,}00568 \times (tim - 3180)$	Eq 48

3.2- Car class 2

3.2.1- Surrounding gas temperature

$0 \leq tim \leq 120$ [°C]	$T = 273{,}15 + (7{,}516 \times tim)$	Eq 49
$120 < tim \leq 1500$ [°C]	$T = 273{,}15 + (922 + 0{,}001159 \times (tim - 12))$	Eq 50
$1500 < tim \leq 3120$ [°C]	$T = 273{,}15 + (938 - 0{,}00679 \times (tim - 1500))$	Eq 51
$3120 < tim \leq 4200$ [°C]	$T = 273{,}15 + (927 - 0{,}83518 \times (tim - 3120))$	Eq 52

3.2.2- Surrounding gas velocity

$0 \leq tim \leq 240$ [°C]	$V = 0{,}03083 \times tim$	Eq 53
$240 < tim \leq 960$ [°C]	$V = 7{,}4$	Eq 54
$960 < tim \leq 1440$ [°C]	$V = 7{,}4 + 0{,}00458 \times (tim - 960)$	Eq 55

$1440 < tim \leq 1500$ [°C]	$V = 9{,}6 + 0{,}01333 \times (tim - 1440)$	Eq 56
$1500 < tim \leq 1620$ [°C]	$V = 10{,}4 - 0{,}01 \times (tim - 1500)$	Eq 57
$1620 < tim \leq 2280$ [°C]	$V = 9{,}2 - 0{,}00348 \times (tim - 1620)$	Eq 58
$2280 < tim \leq 3360$ [°C]	$V = 6{,}9 - 0{,}001018 \times (tim - 2280)$	Eq 59
$3180 < tim \leq 4200$ [°C]	$V = 5{,}8 - 0{,}0069 \times (tim - 3360)$	Eq 60

3.3- Car class 3

3.3.1- Surrounding gas temperature

$0 \leq tim \leq 120$ [°C]	$T = 273{,}15 + (7{,}5166 \times tim)$	Eq 61
$120 < tim \leq 1500$ [°C]	$T = 273{,}15 + (922 + 0{,}01449 \times (tim - 120))$	Eq 62
$1500 < tim \leq 3360$ [°C]	$T = 273{,}15 + (94 - 0{,}0086 \times (tim - 1500))$	Eq 63
$3360 < tim \leq 4200$ [°C]	$T = 273{,}15 + (926 - 1{,}071 \times (tim - 3360))$	Eq 64

3.3.2- Surrounding gas velocity

$0 \leq tim \leq 240$ [°C]	$V = 0{,}03083 \times tim$	Eq 65
$240 < tim \leq 960$ [°C]	$V = 7{,}7$	Eq 66
$960 < tim \leq 1440$ [°C]	$V = 7{,}7 + 0{,}005 \times (tim - 960)$	Eq 67
$1440 < tim \leq 1500$ [°C]	$V = 10{,}1 + 0{,}01333 \times (tim - 1440)$	Eq 68
$1500 < tim \leq 1620$ [°C]	$V = 10{,}9 - 0{,}01083 \times (tim - 1500)$	Eq 69
$1620 < tim \leq 2280$ [°C]	$V = 9{,}6 - 0{,}00363 \times (tim - 1620)$	Eq 70
$2280 < tim \leq 3540$ [°C]	$V = 7{,}2 - 0{,}001111 \times (tim - 2280)$	Eq 71
$3540 < tim \leq 4200$ [°C]	$V = 5{,}8 - 0{,}00878 \times (tim - 3540)$	Eq 72

3.4- Car class 4/5

3.4.1- Surrounding gas temperature

$0 \leq tim \leq 60$ [°C]	$T = 273{,}15 + (15{,}03 \times tim)$	Eq 73
$60 < tim \leq 1500$ [°C]	$T = 273{,}15 + (922 + 0{,}01597 \times (tim - 60))$	Eq 74
$1500 < tim \leq 3540$ [°C]	$T = 273{,}15 + (945 - 0{,}0078 \times (tim - 1500))$	Eq 75
$3540 < tim \leq 4200$ [°C]	$T = 273{,}15 + (926 - 1{,}366 \times (tim - 3540))$	Eq 76

3.4.2- Surrounding gas velocity

$0 \leq tim \leq 240$ [°C]	$V = 0{,}03375 \times tim$	Eq 77
$240 < tim \leq 960$ [°C]	$V = 8{,}1$	Eq 78
$960 < tim \leq 1440$ [°C]	$V = 8{,}1 + 0{,}005 \times (tim - 960)$	Eq 79
$1440 < tim \leq 1500$ [°C]	$V = 10{,}5 + 0{,}015 \times (tim - 1440)$	Eq 80
$1500 < tim \leq 1620$ [°C]	$V = 11{,}4 - 0{,}01083 \times (tim - 1500)$	Eq 81
$1620 < tim \leq 2280$ [°C]	$V = 10{,}1 - 0{,}00393 \times (tim - 1620)$	Eq 82
$2280 < tim \leq 3600$ [°C]	$V = 7{,}5 - 0{,}001574 \times (tim - 2280)$	Eq 83
$3600 < tim \leq 4200$ [°C]	$V = 5{,}8 - 0{,}0069 \times (tim - 3360)$	Eq 84